Identification of factors involved in processing of mRNA
in a fimbrial operon of *Escherichia coli*

Jovanka Tepavcevic Koo

A dissertation submitted in partial fulfillment of the
requirements for the degree of

Doctor of Philosophy

University of Washington

2004

Program Authorized to Offer Degree: Microbiology

University of Washington
Graduate School

This is to certify that I have examined this copy of a doctoral dissertation by

Jovanka Tepavcevic Koo

and have found that it is complete and satisfactory in all respects,
and that any and all revisions required by the final
examining committee have been made.
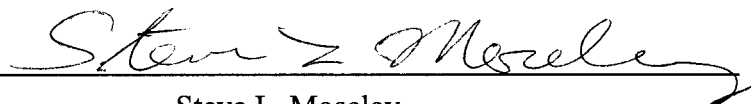
Chair of Supervisory Committee:

_____
Steve L. Moseley

Reading Committee:

_____
Michael G. Katze

_____
Adam P. Geballe

_____
Steve L. Moseley

Date: _____2.25.04_____

In presenting this dissertation in partial fulfillment of the requirements for the Doctoral degree at the University of Washington, I agree that the Library shall make its copies freely available for inspection. I further agree that extensive copying of the dissertation is allowable only for scholarly purposes, consistent with "fair use" as prescribed in the U.S. Copyright Law. Requests for copying or reproduction of this dissertation may be referred to Proquest Information and Learning, 300 North Zeeb Road, Ann Arbor, MI 48106-1346, to whom the author has granted "the right to reproduce and sell (a) copies of the manuscript in microform and/or (b) printed copies of the manuscript made from microform."
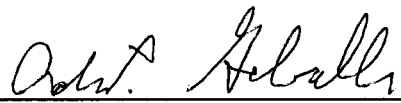
Signature _____

Date_____ 2.25.04 _____

University of Washington

Abstract

Identification of factors involved in processing of mRNA
in a fimbrial operon of *Escherichia coli*

by Jovanka Tepavcevic Koo

Chairperson of the Supervisory Committee: Associate Professor Steve L. Moseley
Department of Microbiology

Endonucleolytic cleavage of mRNA in the *daa* operon of *Escherichia coli* is responsible for coordinate regulation of genes involved in F1845 fimbrial biogenesis. Cleavage occurs by an unidentified endoribonuclease and involves translation of *daaP* which spans the processing site. It was previously determined that the amino acid sequence of DaaP downstream of the processing site is required for mRNA processing. Here, we show by alanine scanning mutagenesis of the final ten codons of *daaP* that the important amino acids for processing are G49, P50 and P51. When these codons were changed to an alanine processing of the mRNA was abolished, while synonymous substitutions in these codons had no effect on processing. This suggested the hypothesis that the DaaP peptide interacts with a ribosome or an associated component and facilitates cleavage of the *daa* mRNA in the ribosome.

Here we also present results of a genetic strategy used to identify factors involved in *daa* mRNA processing. We utilized a reporter construct consisting of the *daa* mRNA processing region fused to the gene encoding green fluorescent protein (GFP). A mutant defective in *daa* mRNA processing and expressing high levels of GFP was isolated by

flow cytometry. Hfr crosses and P1 transductions were employed to locate the relevant mutation, and the mutation responsible for the processing defect was mapped to the 32 min region on *E. coli* chromosome. A putative DEAH-box RNA helicase-encoding gene at this position, *hrpA*, was able to restore *in trans* the ability of the mutant to cleave *daa* mRNA. Site-directed mutagenesis of the *hrpA* regions predicted to encode nucleotide triphosphate binding and hydrolysis functions abolished the ability of the gene to restore processing in the mutant.

We have also identified ribosome associated factor SsrA as being involved in processing of *daa* mRNA. Mutant deficient in SsrA results in defective *daa* mRNA processing. The processing defect in this strains could be complemented by providing a wild type copy of *ssrA* on a plasmid. The cleavage defect in SsrA deficient strain is augmented by a mutation in *hrpA*, providing further evidence that SsrA is required for efficient processing of *daa* mRNA.

TABLE OF CONTENTS

LIST OF FIGURES

LIST OF TABLES

ACKNOWLEDGEMENTS

DEDICATION

To my family. Without you I would not be who I am.

CHAPTER 1: INTRODUCTION

DEGRADATION OF mRNA IN BACTERIA

In addition to efficiency of transcription of DNA into mRNA and of mRNA translation into proteins, stability of mRNA is an important determinant of the control of gene expression. The evidence for decay rate of mRNA in control of gene expression comes from the observation that there is great variability in mRNA stability among genes of prokaryotes and eukaryotes. While the half-life of transcripts in eukaryotic cells ranges from 25 minutes (min) in yeast (213) to 16 hours in mammalian cells (187), 80% of *Escherichia coli* mRNA half-lives are between three and eight minutes (26). The exceptionally stable transcripts in *E. coli* include *ompA* with a half-life of ~15 min (20). The short mRNA half-lives in bacteria are a result of the short cell division times, and they facilitate adaptation of metabolic changes for growth and division in new environments and conditions.

It is important to note that in bacteria genes that encode proteins of related functions are often organized into polycistronic mRNAs, also known as operons. This is advantageous in that the expression of genes within an operon can be coordinated. Apart from disparate translation efficiencies (93, 113), secondary promoters (19, 199) and transcript attenuation (15, 18, 221), mRNA processing and differential stabilities of cleavage products are an additional mechanism for regulating gene expression from polycistsronic transcripts (96, 133, 137, 159, 221). Examples of these include the Pap, CFA/I, Sfa and F1845 adhesin determinants of *E. coli* (14, 27, 86, 131).

Factors involved in transcriptional and translational regulatory mechanisms have long been appreciated, while the importance of mRNA processing and decay in the regulation of bacterial gene expression has been under intense scrutiny only in the last decade. These studies have resulted in the elucidation of a number of mechanisms that determine the stability of mRNAs in bacteria and have been a topic of recent reviews (6, 50, 98, 166, 193). It has become apparent that the pathway of mRNA decay in bacteria is far more complex than originally predicted (3) and that it plays an important role in regulation of gene expression. In this section, I will give an overview of major ribonucleases involved in mRNA decay in bacteria, as well as of higher order structures in the RNA that control the accessibility of sites to degradation.

The degradation machinery

Endonucleases (which cleave within an RNA sequence, between internal phosphodiesters) and exonucleases (which remove terminal nucleotides) are involved in mRNA degradation in bacteria. It is noteworthy that ribonucleases that participate in mRNA decay are also important for processing and maturation of stable ribosomal RNAs (rRNA) and transfer RNAs (tRNA). In this way bacteria can utilize a limited number of ribonucleases to accomplish all RNA cleavages and presumably save the energy that would be required to synthesize a large set of specific enzymes.

RNase III

RNase III is an endonuclease that specifically cleaves double-stranded RNA molecules (170). This protein *in vivo* degrades stem-loop structures and especially those

present in the intercistronic regions (64, 159). Although stem-loop structures are present in almost all RNA molecules, RNase III does not cleave most. The specific structural motif in double-stranded RNA recognized by RNase III is thought to be complex and remains unpredictable (169). RNase III plays a major role in processing of the 30S rRNA precursor to 16S and 23S rRNAs (64). In addition, the enzyme modulates the stability of several bacterial and phage transcripts and the expression of corresponding genes, including polynucleotide phosphorylase (PNPase) (159) and autoregulation of its own transcript (17). In some cases RNase III is involved in degradation of mRNAs whose ribosome binding sites (RBS) are sequestered by antisense RNAs, such as the transposase mRNA of the IS*10* transposon (44). In other cases RNase III can induce structural changes in the mRNA that do not affect the stability of the transcript but improve the efficiency of translation, as in the case of T7 phage 1.1 and 1.2 genes (174). However, since the null mutants in the RNase III structural gene (*rnc*) show only a mild phenotype (12), it has been suggested that this enzyme does not play a major role in mRNA degradation in bacteria.

RNase P

RNase P is an essential enzyme in *E. coli* (153). It is composed of a protein component C5 and an RNA component, M1 RNA, which is the catalytic moiety of the enzyme, which is therefore a ribozyme. This enzyme plays a major role in processing of the 5' ends of precursors to tRNAs and other naturally occurring stable RNAs in *E. coli* (153). It is an endoribonuclease and the classic model for the RNase P recognition site includes a stretch of duplex RNA followed downstream by the consensus sequence, CCA

(195). RNase P cleaves at the 5' base of the stem-loop structure resulting in the stabilization of the downstream RNA. Until recently, the only example of an RNase P role in mRNA decay was the *his* operon in *Salmonella typhimurium* (2), a system which also requires cleavage by RNase E just upstream of the RNase P site and translation of the downstream gene *hisB*. However, it now appears that RNase P cleavage in the intercistronic regions of the *tna, secG, rbs*, and *his* operons in *E. coli* affects gene expression for regions downstream of its site of cleavage (102). High-density DNA microarray experiments have demonstrated that mRNA levels of the above mentioned operons were increased at restrictive temperatures in an *E. coli* strain mutant in the protein subunit of RNAse P (103). *In vitro* RNase P cleavage assays determined that indeed the enzyme can cleave all of the above transcripts (102), however additional experiments are required to determine how RNase P regulates gene control in these operons.

RNase E and the degradosome

RNase E, thought to be the major enzyme of mRNA decay in bacteria, is required for viability, since mutations at codons 66 and 68 confer temperature sensitivity (121). RNase E is required for maturation of 9S rRNA into 5S form (126), in processing of the 5' end of 16S rRNA (105), the maturation of the RNA subunit of RNase P (112), the degradation of the antisense inhibitor of plasmid colE1 DNA replication (204), and the processing of tRNAs (104, 150, 164). In addition, RNase E is implicated in the decay of total pulse-labeled RNA (7, 149) as well as a number of specific transcripts (7, 78, 115, 132, 133). The cleavages by RNase E have been mapped to the 5' or 3' UTRs in coding

sequences or in intercistronic regions of polycistronic transcripts. Originally it was thought that RNase E cleaves within a 10-nucleotide (nt) region (ACAGA/UAUUUG) (204), however subsequent analysis demonstrated that RNase E prefers single-stranded sequences that are typically, but not always, A-U rich (50). More recently it was shown that RNase E is a 5' end-dependent enzyme (114), and that it more efficiently processes 5' monophosphorylated ends of transcripts than triphosphorylated primary transcripts (114). The enzyme activity is also affected by secondary structures in the RNA (see below, (116)).

RNase E is a large polypeptide of ~118 kDa (43). The structure of the protein can be divided into two regions: the essential N-terminal region that harbors the ribonucleolytic activity (120), and the non-essential C-terminal region which harbors the potential RNA binding domain (homologous to ribosomal protein S1) (198) and a 'scaffold' domain for binding of exoribonuclease PNPase, a glycolytic enzyme enolase, and a putative DEAD-box RNA helicase RhlB (205). The discovery of the association of RNase E with the above- mentioned proteins into a high molecular weight complex, now termed the degradosome, was one of the most exciting findings in the field of mRNA degradation in bacteria in the past decade (160). This finding suggested that the complex might coordinate the endo- and exonucleolytic digestion and unwinding of RNA structures and that the RNase E-based degradosome is the primary mechanism for mRNA degradation in *E. coli* (163). Recent studies, however, have questioned this hypothesis. First, although the N-terminal region of RNase E is highly conserved in prokaryotes, the C-terminal region that serves as the scaffold for the degradosome is not (88). More

significantly, the deletion mutants of RNase E that lack the degradosome scaffolding

region exhibit wild type mRNA decay properties (151). Therefore, the relevant role of

the degradosome in mRNA decay in bacteria still remains to be determined.

RNase G

Very recently a homologue of RNase E was identified and designated RNase G.

The gene encoding RNase G was originally discovered as the product of *cafA*

(cytoplasmic axial filament), because overproduction of CafA protein induced

morphological changes in which the bacteria formed anucleated chained cells with long

axial filaments (147). The RNase G protein shares significant amino acid sequence

identity (34.1%) to the first 469 amino acids of the N-terminus of RNase E (121). The

functional homology of the two proteins was suggested by the observations that

conditional lethality associated with the *rne-1* mutation was partially suppressed by

multiple copies of the *cafA* gene, and that mutations in *cafA* lower the temperature at

which the temperature-sensitive *rne-1* mutant can grow (208). Additional studies

demonstrated that RNase G is in fact an endoribonuclease and is involved in the

maturation of the 5'end of the 16S rRNA (105, 209). Experiments with purified RNase

G showed that, like RNase E, *in vitro* this enzyme is 5'-end dependent and that it prefers

5' monophosphorylated versus triphosphorylated substrates (203). Moreover, RNase G

can cleave *in vitro* RNA I and the 5' UTR of *ompA*, which are the substrates for RNase E,

but at different sequences (203). Despite the sequence homology and some similarity of

function *in vitro*, RNAse E and RNase G share very limited functional overlap *in vivo*

(152). The distinction between the two enzymes apparently comes from the inability of

RNase G to cleave tRNA precursors (152). With regard to the mRNA decay, it was recently reported that mutations which inactivate RNase G result in increased half-lives of the *adhE* and *eno* mRNAs (89, 207). However, it appears that RNase G plays a secondary role in mRNA decay, since its participation in mRNA decay was generally only manifested when RNase E was absent from the cell (152).

PNPase and RNase II

Unlike in eukaryotic cells, there are no 5'- 3' exonucleases in bacteria, thus oligoribonucleotides generated by endonucleolytic cleavages are exclusively degraded in the 3'- 5' direction. The two major exonucleases involved in 3'- 5' degradation of mRNA in *E. coli* are RNase II and PNPase. Single null mutants of either RNase II or PNPase are viable, but the double mutant is not, suggesting that the two enzymes can substitute for each other (62). RNase II appears to be the primary enzyme responsible for the bulk of mRNA decay, since it uses a hydrolytic mechanism (190) and at least 90% of the degradative capacity in *E. coli* is hydrolytic in nature (59). PNPase, on the other hand, uses a phosphorolytic mechanism to generate dipohsphate oligoribonucleotides (72). A significant recent finding with respect to the role of PNPase in the mRNA decay is the activation of the enzyme by polyadenylation of potential substrates (see below, (128)). The common feature of RNase II and PNPase is that their 3'- 5' progressive removal of nucleotides is slowed, and even arrested, by the stabilizing stem-loop structures present in most transcripts.

mRNA structural motifs

The nature and distribution of stabilizing and destabilizing structural elements in mRNA determines sensitivities of mRNA to ribonuclease attack. The standard repertoire of secondary structure elements, such as stem-loops, bulges and single stranded regions that vary in thermodynamic stability, have been shown to control the lifetime of mRNAs.

5' stabilizing structures

A number of *cis*-acting elements in the 5'-terminal segments of slowly degraded mRNAs can enhance the stability of heterologous labile mRNAs when fused downstream. The secondary structure present in the 5' UTR of *ompA* transcript can stabilize labile mRNAs, i.e. *lacZ* and *bla* (21), if fused at their 5' extremities. It appears that a single stranded 5' end allows better access to mRNA by ribonucleases. Mackie and colleagues have demonstrated that oligonucleotides complementary to the 5' ends of labile mRNAs can protect them against the cleavage by RNase E (32, 117). It was also reported that circularization of mRNA that is normally a substrate for RNase E activity decreases its sensitivity to RNase E (114). Additionally, as mentioned previously, since RNase E requires 5' monophosphates for activity, the triphosphates at 5' ends of transcripts protect them from degradation. These observations support the premise that RNase E, as the major enzyme of mRNA decay in bacteria, primarily interacts with 5' ends and that the decay of possibly most bacterial mRNAs is initiated by endonucleolytic cleavage at the 5' end. The processed mRNA molecules that then have a 5' monophosphate can be progressively degraded from their 5' ends toward 3' ends. This suggests a hypothesis that the net 5'- 3' directionality of mRNA decay in bacteria is a

result of successive 5' end cleavages that generate 3' ends for exonucleolytic attack by RNase II and PNPase.

3' stabilizing structures

Stem-loop structures located at the 3' ends of transcription units, including rho-independent terminators and REP (repetitive extragenic palindromic) sequences, protect the upstream mRNA from degradation by 3'- 5' exonucleases (20, 138). There are examples of mRNAs for which the rate-limiting step in decay is the endonculeolytic cleavage at the 3' end that then serve as substrates for exonucleolytic degradation. For instance, the *int* mRNA of λ phage can be inactivated by an RNase III cleavage at the stabilizing hairpin of transcription terminator at the 3' end of transcript (177). Also, the decay of *rpsO* mRNA is initiated by RNase E cleavage between the termination codon and the 3' hairpin (167) and is followed by rapid degradation by PNPase. It was proposed that unpaired nucleotides located 3' to the 3' stabilizing structures could be used as a toehold for exonucleases and initiation of decay of mRNAs with 3' protective elements (50). Additionally it was suggested that polyadenylation downstream of the secondary structures facilitates access to a transcript by 3'- 5' exonucleases (31).

Polyadenylation

Although the enzyme that adds poly(A) tails to bacterial transcripts, poly(A) polymerase (PAP I), was first purified in the 1960s (10), the role of relatively short poly(A) tails in bacteria was not taken seriously until recently (35). Polyadenylation can occur on mature mRNAs as well as on RNA fragments resulting from endo- and exonucleolytic degradation and on stable RNAs and their precursors. It affects the

degradation of nontranslated RNAs such as RNA I (220), as well as a number of specific transcripts (51, 79). The poly(A) tails in *E. coli* are usually 5-40 nt in length and are extended up to 30-400 nt in strains deficient in PNPase or RNase II (79). It thus appears that PNPase and RNase II are the primary enzymes involved in the removal of the poly(A) tails from mRNAs.

A model was proposed for degradation of transcripts with stabilizing secondary structures at the 3' end in which successive rounds of poly(A)-addition and progressive degradation by PAP I and PNPase progressively shorten the RNA and weaken the . hairpins, generating RNAs that can be degraded by PNPase (166). RNase II, like PNPase is inhibited by secondary structures at the 3' end. It can, however, very efficiently remove oligo(A) tails that can be used as binding sites by PNPase (52). In this way RNase II can protect mRNAs that end in a stable hairpin from degradation by PNPase.

It was not clear whether poly(A) tails contribute significantly to the degradation of primary transcripts since the decay of many full length mRNAs is initiated by endonucleoleolytic cleavages of RNAse E, and exonucleases and PAP I mostly contribute to the degradation of fragments lacking RNase E sites. Regnier and colleagues recently reported preferential mRNA decay of the *E. coli rpsO* transcript by a poly(A)-dependent pathway when RNase E-dependent decay is inactivated by *rne* mutations or by removal of RNase E cleavage sites (119). Also, it was determined that an increase in polyadenylation leads to stabilization of the *pnp* and *rne* transcripts, which in turn leads to increased levels of PNPase and RNase E (a consequence of alterations in autoregulation of the respective genes) (127). Therefore, it is now clear that

polyadenylation not only serves to promote RNA decay, but also as a sensing mechanism by which cells adjust the levels of both RNase E and PNPase.

Proposed mechanism for mRNA decay

The most favored model of mRNA decay in bacteria proposes that RNase E initiates transcript decay by binding to the 5' terminus and then cleaving at a distance (Figure 1.1). Since the enzyme prefers 5' monophosphate to a 5' triphosphate, which is usually present at the 5' end of primary transcripts, it suggests that the initial cleavage to generate the 5' monophosphate is rate limiting. In this model, highly structured 5' UTR regions, such as the *ompA* leader, impart increased stability to transcripts since they inhibit RNase E binding. Once RNase E binds to the 5' end, it can presumably work its way processively in the 5'- 3' direction, degrading the mRNA into a series of smaller fragments that are susceptible to degradation by exonucleases. Since exonucleases are inhibited by secondary structures, the poly(A) tails added to the 3' end by PAP I would provide additional binding sites for the exonucleases. The final step in the mRNA decay would be the degradation of oligonucleotides generated by exonucleases to mononucleotides by an enzyme termed oligoribonuclease (since oligonucleotides 4 to 7nt in length are resistant to exoribonucleases (70)).

Figure 1.1 – Model of mRNA decay in *Escherichia coli*

The decay of a hypothetical polycistronic transcript is shown. In this model, upon

binding to the 5' end of the transcript RNase E makes initial endonucleolytic cleavages

(shown as scissors). This enzyme can move processively in 5' to 3' direction. The

smaller breakdown products are subsequently degraded by exonucleases RNase II and

PNPase (in 3' to 5' direction). Secondary structures that inhibit progression of

exonucleases are removed by addition of poly(A) tails generated by the poly(A)

polymerase (PAP I). The final step in the decay involves degradation of oligonucleotides

to mononucleotides by oligoribonuclease.

5'   3'

RNase E

PAP I   RNase II
             PNPase

AAAA   AAAA

Oligoribonuclease

Mononucleotides
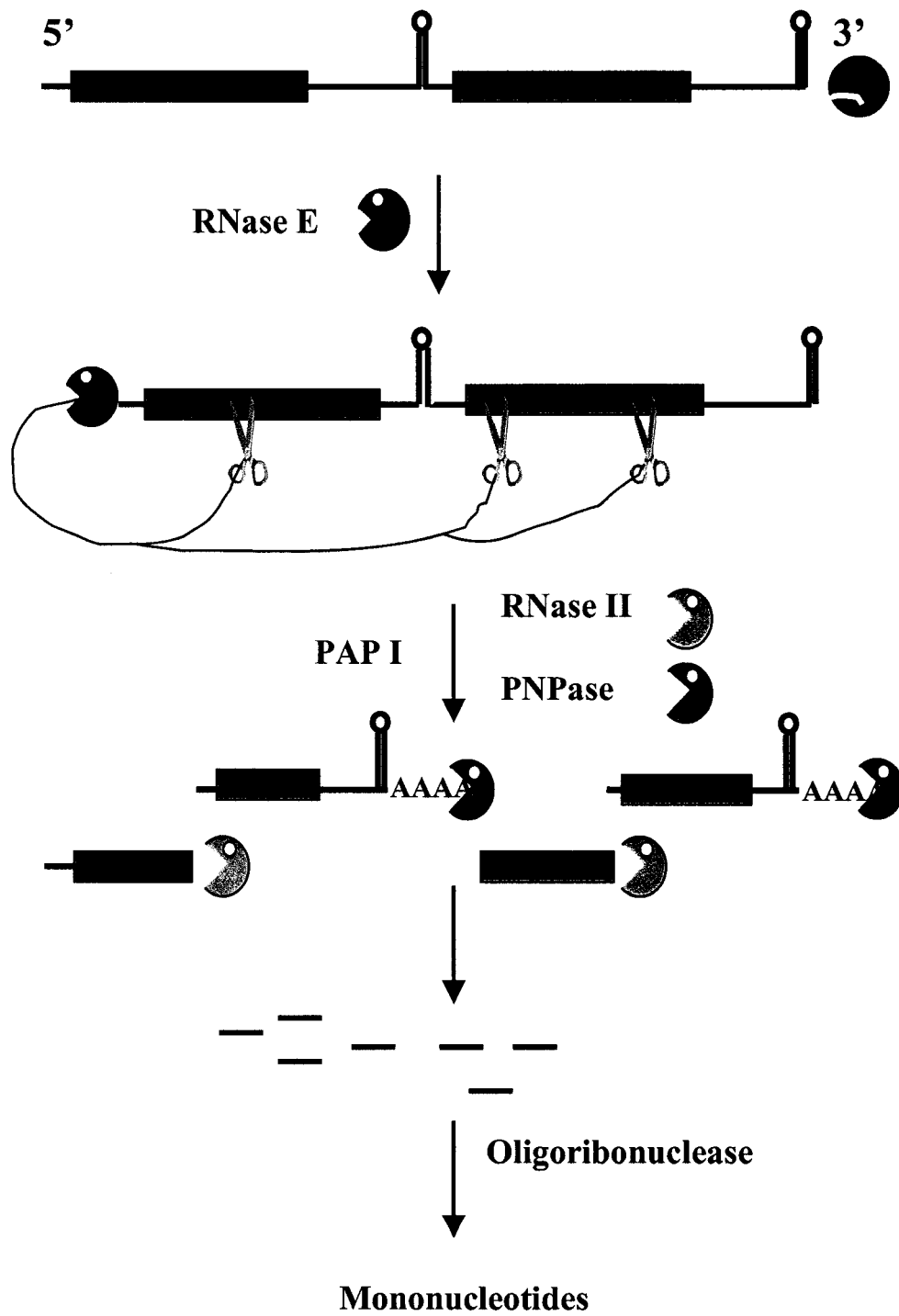
Although there is evidence to support all of the steps in this model, there are still a number of interesting questions remaining. First, what is the importance of the degradosome in mRNA decay? It could be argued that since all the components necessary for degradation of mRNA are present in a complex with RNase E that the degradosome could bind to both ends of the transcript simultaneously and lead to a more rapid decay. RNase E could make the initial cleavages of the mRNA, generate oligonucleotides for degradation by PNPase, and the helicase RhlB could unwind the secondary structures that block PNPase activity. However, in strains in which degradosome formation was blocked, the mRNA decay proceeded normally (151), suggesting that the degradosome may be involved in another pathway of RNA metabolism. The other question is concerned with the ability of RNase E to initiate decay of most mRNAs. The 5' ends of many oligoribonucleotides contain hydroxyl groups that are incogruous with the RNase E cleavage. This raises the possibility that another enzyme accounts for this activity. While much progress has been made in the field of mRNA decay in the last thirty years, many important features of this process remain to be uncovered.

NASCENT-PEPTIDE MEDIATED CONTROL OF GENE EXPRESSION

In addition to mechanisms of mRNA degradation and decay, gene expression can be regulated at the level of translation of mRNA into proteins. This type of regulation has been established for many bacterial, eukaryotic and viral genes (110, 130, 200). In a number of cases the ribosome has been identified as the target of translational control by

the nascent peptide as the effector molecule. Recent publications of crystal structures of the 50S and 30S ribosomal subunits as well as the intact 70S ribosome have transformed our understanding of protein synthesis (reviewed in (162)), therefore before describing details of some translational control mechanisms I will briefly discuss the translation in bacteria.

Overview of translation in prokaryotes

Initiation of translation in bacteria requires interaction of the 30S ribosomal subunit (in particular, the 3' end of 16S rRNA) with a complementary sequence in the mRNA, known as the Shine-Dalgarno sequence or ribosome binding site (RBS). It also involves three initiation factors, which aid in recruitment of initiator tRNA (fMet-tRNA^{fMet}) and formation of the initiation complex (mRNA-initiator tRNA-30S subunit). Next, the 50S subunit associates with the initiation complex, the initiator tRNA is in the P-site, and the A-site is available for the incoming charged tRNA.

It has been understood for a long time that proper interactions between the mRNA and the ribosome are essential for many steps of translation. Yusupova and colleagues (225) recently reported the path of mRNA through the ribosome using X-ray crystallography. This work has confirmed previous observations that about 30 nt of mRNA wraps around the neck of the 30S subunit (65). The immediate molecular environment of mRNA is mainly composed of 16S rRNA, except at the ends of its binding site where it is in proximity to ribosomal proteins S3, S4 and S5 (225). The intriguing question that remains is: how does the ribosome unwind the hairpins present

in most mRNAs, which, based on crystal structures, would be too large to pass through the narrow tunnels of the ribosome? One possibility that has been proposed is that an mRNA helicase is present at the position where mRNA starts its path through the ribosome and that it would be involved in physical disruption of the secondary structures (225). This proposed mRNA helicase has not yet been identified.

The elongation cycle of translation starts with an aminoacylated tRNA brought to the A-site of the ribosome by the elongation factor EF-Tu and GTP. The correct base pairing between the codon on the mRNA and the anticodon on tRNA is the basis for selection of the correct tRNA for addition of the next amino acid to the polypeptide chain. Ogle *et al.* have determined that the ribosome monitors base pairing between the codon and the anticodon at the first two positions of the codon (allows for the wobble in the third position) through conformational changes that result from interactions of residues A1492, A1493 and G530 of the 16S rRNA with the minor groove of the codon-anticodon base pair (146). The correct interaction between the codon in the mRNA and the anticodon of tRNA triggers a conformational change in the ribosome that results in GTP hydrolysis by EF-Tu. The aminoacyl end of the A-site tRNA is then released into the peptidyl transferase center of the 50S subunit where peptide bond formation takes place. The reaction of peptide bond formation involves a nucleophilic attack of the alpha amino group of the aminoacyl tRNA onto the carboxyl group of the amino acid bound to the peptidyl tRNA. This process in which P-site tRNA is deacylated and the extended peptide is transferred to the A-site tRNA is thought to occur spontaneously. The high-resolution crystal structures of the 50S ribosomal subunit revealed that the peptidyl

transferase center is completely devoid of ribosomal proteins (16). This suggested that the ribosomal RNA could catalyze the peptidyl transfer and that the ribosome is a ribozyme (141). Based on the structure of the 50S subunit with the Yarus inhibitor (a potent inhibitor of peptidyl transfer), it was suggested that the rRNA acts in catalysis of peptide bond formation through a charge relay that requires residues A2451 and G2447 of 23S rRNA (141). However, recent experiments have questioned the role of these residues in peptidyl transfer and the exact catalytic mechanism of peptide bond formation continues to be debated.

Following peptide bond formation, the ribosome contains a deacylated tRNA in the P-site and the nascent peptide chain attached to the A-site tRNA. The next round of peptidyl transfer requires translocation of the tRNAs and mRNA and is facilitated by the elongation factor EF-G, which is also a GTPase.

Translation termination ensues once a stop codon on the mRNA is reached by the A-site of the ribosome. Release factors RF-1 and RF-2 are involved in recognition of stop codons in bacteria (95, 189). They both recognize UAA, while RF-1 recognizes UAG and RF-2 recognizes UGA. Binding of the appropriate release factors to the stop codon results in the hydrolysis and release of the peptide chain from tRNA in the P-site of the ribosome. Recent crystallographic studies suggested that the eukaryotic release factor (eRF) 1, the bacterial RF2, and the ribosomal recycling factor (RRF) all mimic the structure and shape of tRNA (189). From these structures it was proposed that release factors contain a tripeptide 'anticodon' that recognizes the sopt codon in the mRNA. Biochemical and genetic evidence, on the other hand, do not support this model. The

specificity of bacterial RF1 and RF2 can be swapped if the domains responsible for stop

codon recognition are exchanged between the two proteins (134). The stop codon

specificity domain, however, is located far away from the proposed 'anticodon' tripeptide

on the RF2 crystal structure. To complicate this issue, cryo-electron microscopy studies

of RF2 within the ribosome suggest that this protein assumes a different conformation

than what was observed in the crystal structure (206). Therefore, the simple concept of

molecular mimicry between tRNA and release factors needs to be further examined.

Nascent peptides and translational control of gene expression

During the elongation step of protein synthesis the nascent peptides emerge out of

the ribosome through an exit tunnel. This tunnel was originally observed in the 1980s

(125, 224) and was thought to be firmly built and passive to allow through many different

types of peptide sequences. It starts near the peptidyl transfearse center in the 50S

subunit, goes through the large subunit and finally emerges on the opposite side (141).

Recently reported structures of the ribosome suggest that the diameter of the tunnel is too

small to allow folding of proteins in its interior. The tunnel is mainly composed of

rRNA, but the ribosomal proteins L22 and L4 form the narrowest part. Mutations in

these proteins that resulted in changes in the diameter of the tunnel were correlated with

different functional states of the ribosome and suggested that the exit tunnel may be

dynamic in its interactions with nascent peptides (66). Analysis of the crystal structure of

the 50S ribosome with the antibiotic troleandomycin (TAO) revealed that this macrolide

blocks the ribosomal tunnel by inducing a conformational rearrangement in protein L22

(24). It appears that the tip of the highly conserved β-hairpin of L22 is flipped across the tunnel in the presence of TAO. This study implies that this portion of the tunnel may similarly interact with the nascent peptides and be involved in sequence discrimination and gating (24).

In line with the data that the exit tunnel of the ribosome is probably not neutral with regard to protein sequences are the observations obtained in the recent years that suggest that a nascent peptide can be an effector molecule in translational control by targeting the ribosome. The nascent peptides in these systems contain particular sequence motifs that when positioned correctly in the ribosome (either near the peptidyl transferase center or the adjacent exit channel) can dramatically affect protein elongation and termination of translation (110, 130, 200). Comparison of the effector motifs present in the nascent peptides that regulate gene expression does not reveal any sequence similarities (110). This presents difficulties in ascribing functional homologies to these nascent peptides and suggests that the different effectors interact with different components of the ribosome. One common sequence characteristic of all the effector motifs is that they are devoid of acidic residues, and this leads to the hypothesis that a basic peptide might perturb the function of the ribosome by causing conformational changes in the rRNA (110). Despite the sequence divergence, there are some mechanistic features that all of the active nascent peptides share. First, these nascent peptides act *in cis* and affect only the ribosome that is involved in their own synthesis. Second, most effector motifs cause the ribosome to stall either during elongation or termination steps of protein synthesis. Third, some nascent peptides require another

cellular component (the co-effector) to exert their function on the translating ribosomes. Examples of nascent peptides that play active roles in translational mechanisms have been identified in bacteria, eukaryotes and viruses, and the details of the mechanisms for a selected number of them are presented below.

cmlA/cat86

In bacteria the most extensively studied example of nascent peptide-mediated control of gene expression is the translational attenuation of chloramphenicol (Cm) resistance genes *cat86* (from Gram$^+$ bacteria) and *cmlA* (from Gram$^-$ bacteria) (110). This system is characterized by a sequestered RBS in a secondary stem loop structure and a short translated ORF upstream of the stem loop. In the presence of the inducer Cm, the ribosome stalls in the leader and causes destabilization of the downstream stem-loop structure. This in turn exposes the RBS and allows translation initiation of the downstream resistance genes (110). The leader for the *cat86* encodes a peptide MVKTD that stalls the ribosome by inhibiting peptidyltransferase and translation termination (110). In the case of *cmlA*, the activation of translation also requires ribosome stalling, but the peptide encoded by the leader is the 8-mer MSTSKNAD that inhibits the peptidyltransferase activity of the ribosome (110).

secM/A

The *secM* (secretion monitor) gene in *E. coli* is a more recently described example of a peptide with an effector motif (135). This gene encodes a unique secretory protein that regulates the translation of the downstream gene *secA* (translocation ATPase) (148). SecM is secreted into the periplasm via the export signal in the N-terminus, where it acts

as a substrate for degradation by proteases (136). While in the cytoplasm, though, the functional form of the nascent peptide stalls the ribosomal complex through the effector motif in its C-terminus (136). Ribosome stalling in this system is dependent on the concentration of SecA (the co-effector) in the cell. When there is a SecA deficiency in the cell, the signal sequence in the N-terminus of SecM cannot initiate the translocation of SecM into the periplasm. The stalling of the ribosome at the C-terminus of SecM results in a conformational change in the mRNA that normally sequesters the RBS of *secA* in a secondary stem-loop structure. The rearrangement of mRNA exposes the *secA* RBS and promotes efficient translation of SecA (122, 136, 148). When, on the other hand, the concentration of SecA in the cell is high, it can promote the secretion of SecM across the membrane so that the effector motif of SecM is unable to induce ribosome stalling/mRNA rearrangement and thus the translation of *secA* is blocked. This system constitutes a feedback loop for controlling the amount of SecA protein required for protein export.

The sequence motif of SecM that induces elongation arrest by the ribosomes was identified to be FXXXXWIXXXXGIRAGP. A particular proline residue (Pro166) in this motif of SecM causes ribosome stalling. Mutations were identified in rRNA and a ribosomal protein that resulted in SecM translation beyond Pro166. The nascent peptide motif in SecM seemingly interacts with the ribosomal protein L22, located at the entrance to the exit tunnel, and a 23S rRNA residue A2058 that faces the inner wall of the tunnel (135). Based on these observations, a model of SecM-dependent regulation proposes that

the narrowest part of the exit channel in the ribosome acts as a discrimination gate by interaction with nascent peptides and blocks further translation by stalling the ribosome.

β-tubulin

Regulation of synthesis of tubulin (the principal component of microtubules) in eukaryotic cells occurs at the post-transcriptional level (201). In this system, an autoregulatory mechanism acts to increase the intracellular concentration of tubulin subunits and leads to specific degradation of tubulin mRNA (67, 154). It was determined that the sequence necessary and sufficient for the selective degradation of β-tubulin mRNA is located within the first 13nt of the β-tubulin coding sequence (222). A fusion of this sequence to thymidine kinase conferred the tubulin subunit-induced instability upon the hybrid mRNA (68). Additionally, it was observed that only transcripts that are actively translated are subject to this kind of regulation and that translation beyond codon 41 was required for mRNA instability to be detected. Nucleotide substitutions that changed the N-terminal four amino acids of β-tubulin, Met-Arg-Glu-Ile (MREI) abolished the regulation of mRNA stability (223). These data led to the hypothesis that the regulation of β-tubulin mRNA stability is mediated through binding of tubulin to the nascent amino-terminal tubulin peptide. However, no meaningful binding was ever detected between the tubulin subunits and the MREI peptide (201). A monoclonal antibody that binds to the β-tubulin nascent peptide selectively disrupts the regulation of β-tubulin, suggesting a new hypothesis that one or more cellular factors are involved in the cotranslational β-tubulin mRNA degradation (201). The cellular component(s) that control the gene expression in this system have not yet been reported.

gpUL4

An example of a viral active nascent peptide in translational control of gene expression is found in the cytomegalovirus (CMV) gpUL4 gene that encodes a structural glycoprotein of the virion (46). This gene is preceded by short upstream ORFs (uORFs), and it was determined that uORF2 influences translation of the downstream gene (46). uORF2 encodes a peptide of 22 amino acids and missense mutation analysis determined that amino acid 22 (Pro) of the uORF is essential for the function of uORF in translational control (58).

gpUL4 uORF is thought to exert its regulatory role by impeding translation termination. Using the toeprinting technique (which detects stalled ribosomes on a transcript), it was determined that uORF2 causes ribosome stalling on the mRNA when the termination codon of uORF2 is very close to the A-site of the ribosome (36). When the termination codon of uORF2 was deleted, no effect on downstream translation was observed, further suggesting that this nascent peptide interferes with termination and not with the elongation step of translation (39). Furthermore, experiments in cell-free extracts demonstrated that the final sense codon of uORF2 links the nascent peptide to the tRNA responsible for the decoding of this terminal codon (37, 38). These data further supports the model in which gpUL4 uORF mediates translational control during termination.

In conclusion, numerous examples of effector motifs in nascent peptides have been reported and additional ones await discovery. It is apparent that the mechanisms of

these active nascent peptides in translational control of gene expression are diverse,

which frustrates their identification, but it opens up a rich area for further

experimentation.

TRANSLATIONAL CONTROL OF F1845 FIMBRIAL EXPRESSION IN E. COLI

F1845 is a fimbrial adhesin of *E. coli* strain C1845 which was isolated from a

child with persistent diarrhea (29). It is a member of the Dr family of adhesins that

includes AFA/I and the Dr hemagluttinin (143, 158). Members of this family of *E. coli*

adhesins are associated with urinary tract infections, in particular with cystitis and

pyelonephritis linked with pregnancy, as well as with diarrheal disease (8, 71, 84, 101,

144, 192). They recognize the Dr^a blood-group antigen present on a complement

regulatory and signaling molecule, decay-accelerating factor (DAF; CD55) (111, 145).

The F1845 adhesin is characterized by its ability to mediate diffuse adherence of bacterial

cells to HEp-2 cells in culture (29).

The F1845 fimbriae are encoded in a gene cluster consisting of seven genes

designated *daa* (Figure 1.2). Six of these genes, *daaABCDPE* are organized into a single

transcriptional unit (28). In the promoter region upstream of *daaA* potential regulatory

sequences were identified: two consensus leucine-responsive regulatory protein (Lrp)-

binding sites that contain differentially methylated GATC sequences, a cAMP-CRP-

binding site, and an integration host factor (IHF)-binding site (28). Work in our

laboratory demonstrated that *lrp*, a gene that encodes a global regulatory DNA-binding

protein, is important for the expression of F1845 fimbriae (28). Additionally, the *daa*

24

Figure 1.2 – Transcriptional organization of the *daa* operon and biogenesis of F1845 fimbriae.

The two promoters identified upstream of *daaA* and *daaF* are designated with P. Large arrows indicate the two transcripts generated from these promoters. The bold arrow represents the stable portion of the transcript, while the labile RNA upstream of the mRNA cleavage site (scissors) is indicated by the dashed line. The half arrows downstream of *daaE* represent the stabilizing stem-loop structure. The biogenesis of the fimbriae is depicted above the diagram of the operon. The colors of the proteins correspond to the colors of genes encoding them. See text for the functions of the proteins. OM, outer membrane; IM, inner membrane.

OM

IM

E

C

B

D?

P P

daaF daaA daaB daaC daaD daaP daaE
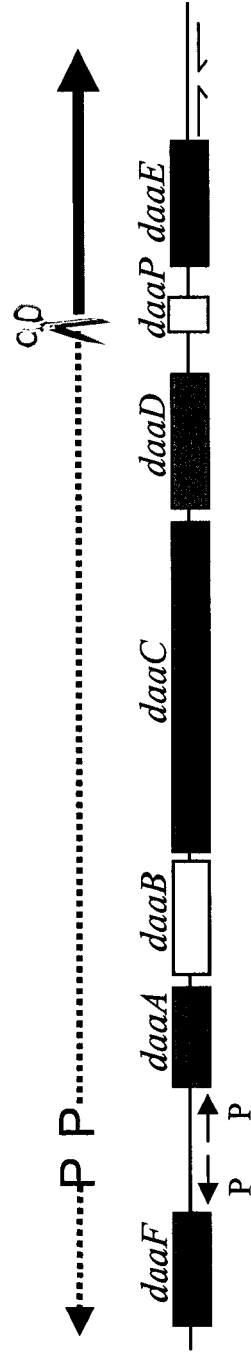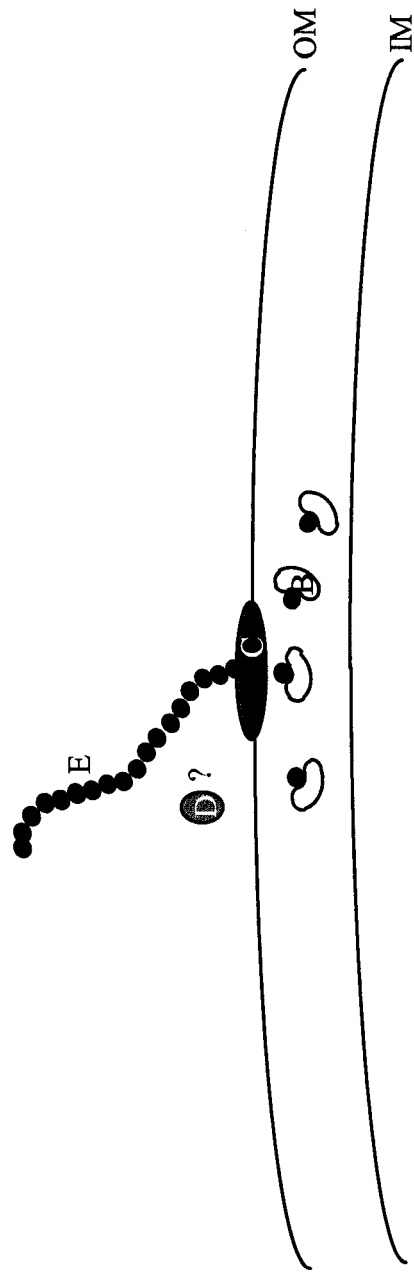
operon also appears to be under a catabolite repression, possibly through the binding of cAMP-CRP to binding sites identified in the promoter (28). The role of the potential IHF-binding site was also determined and it seems that it functions in the expression of the *daa* operon (28).

The products of *daaA* and *daaF* are homologous at the amino acid level to the *papB* and *papI* gene products of the *pap* fimbrial adhesin operon, even though the *daa* and *pap* family are not closely related at the nucleotide level (14, 28). Based on this homology it was proposed that DaaA and DaaF regulate the transcription of the *daa* operon. The *daaB* gene is predicted to encode the periplasmic chaperone protein important for the biogenesis of the fimbrial adhesive structure, while the *daaC* gene product shares homology to the outer memebrane usher proteins, such as FimD and PapC (29). The function of the *daaD* gene product is still unknown, although it is hypothesized that it might mediate invasion of bacteria into the host epithelial tissues (87). The typical organization of fimbrial operons in *E. coli*, including P pili (Pap) and type 1 fimbrial determinants, places the gene encoding the structural subunit near the 5' end of the operon (1, 14). However, in the F1845 fimbrial operon it is the last gene in the operon, *daaE*, which encodes the structural subunit and the adhesin of the fimbriae (29).

Since the structural proteins are required in greater abundance than the accessory proteins during the biogenesis of fimbriae, differential expression of the genes provides a suitable stoichiometry of different fimbrial components. In the *daa* operon this is achieved by an endonucleolytic cleavage of mRNA within the *daaD-E* intercistronic region that creates a stable message encoding only DaaE, while the sequences upstream

of the processing site which encode the accessory proteins are rapidly degraded. Processing of the *daa* transcript was determined to be independent of RNase E, RNase III, and RNase P ((27); see Chapter 3). This suggests that a yet to be identified endonuclease is involved in processing of *daa* mRNA.

Previous work in our laboratory established some of the signals acting *in cis* that are involved in the processing of *daa* mRNA (108, 109). The intercistronic region between *daaD* and *daaE* was found to contain a small open reading frame (ORF) that spans the site of cleavage. This ORF was named *daaP*, for *daa* processing. *daaP* is predicted to encode a peptide of 57 amino acids in length, with a molecular weight of 6.2 kDa and a pI of 10.9 (109). There are no identifiable homologs of *daaP-* encoded protein in the GenBank, EMBL and SWISSPROT databases.

Processing of *daa* mRNA is directly coupled to the translation of *daaP*, since mutations that disrupt the ribosome binding site and result in premature translation termination abolished processing (109). When the reading frame of *daaP* was altered to result in a polypeptide of different amino acid sequence but similar in size to DaaP the *daa* transcript was not processed (109). This suggested that the amino acid sequence of DaaP is also important for processing of *daa* mRNA. Further frameshift analysis of four arbitrary segments of DaaP determined that the amino acids encoded by the final 10 codons downstream of the processing site are crucial for the processing to occur (108). In addition, translation of the region of RNA upstream of the processing site was also determined to be required for processing.

Although these studies have given insight into the sequence elements required for the processing of *daa* transcript to occur, none of the *trans*-acting factors have been identified so far. These findings were consistent with a model of nascent peptide-mediated control of gene expression. We thus hypothesized that ribosomes moving along the 5' portion of *daaP* mRNA could be exposing an important signal in the RNA, and that continued elongation through the final 10 codons would result in an interaction of the nascent peptide with the ribosome (or a ribosome-associated component) to cause cleavage of the mRNA.

The objective of this thesis project was to further characterize the role of the 13 codons of *daaP* in processing and to identify factors involved in the cleavage of *daa* mRNA. By alanine scanning mutagenesis I determined that codons 49, 50 and 51 of *daaP*, encoding a tripeptide Gly-Pro-Pro, are essential for processing of the *daa* transcript. I employed fluorescence activated cell sorting (FACS) and a GFP reporter system as a tool to identify mutants deficient in processing of the *daa* mRNA. Through this screen I found that a putative DEAH-box RNA helicase, HrpA, participates in the endonucleolytic cleavage of *daa* mRNA. Mutational analysis of specific HrpA residues known to play a role in ATP-dependent RNA duplex unwinding in the DEAH-box family of proteins suggests that HrpA may indeed act as an RNA helicase in processing of the *daa* transcript. Additionally, I have implicated ribosome-associated factor SsrA in the processing of *daa* mRNA, supporting the role of the ribosome in the regulation of gene expression in the F1845 fimbrial operon.

CHAPTER 2: MATERIALS AND METHODS

Bacterial strains and media

The *E. coli* strains used in this study are listed in Table 2.1. Bacterial cultures

were grown in Luria Bertani (LB) broth or on Luria agar plates at 37°C (118)

supplemented with the antibiotics ampicillin (100 μg ml^{-1}), kanamycin (25 μg ml^{-1}),

spectinomycin (40 μg ml^{-1}), tetracycline (20 μg ml^{-1}), or chloramphenicol (25 μg ml^{-1}).

DNA manipulation and plasmid construction

Plasmid DNA was isolated by the alkaline lysis method (30), the 'Easy-prep'

method (23), or by using a mini-prep plasmid kit (Qiagen). Restriction endonucleolytic

digestions were performed according to the manufacturer's recommendation (New

England Biolabs). The polymerase chain reaction (PCR) was done using the enzymes

and buffers from Perkin-Elmer and Stratagene. Synthetic oligonucleotide primers were

purchased from Invitrogen and are listed in Table 2.2.

Plasmids used in this study are listed in Table 2.3. Plasmid pVT123, containing a

transcriptional fusion of GFP to *daa* mRNA processing region, was generated as follows.

The *Kpn*I -*Pst*I fragment from pKEN-GFPmut1 (55) was introduced into a low copy

number vector pUFR047 (57) digested with *Kpn*I and *Pst*I, resulting in pUFR047-GFP.

The *daa* mRNA processing region (including *daaP* and a 502 nucleotide deletion of *daaE*

from plasmid pBJC11) followed by a downstream stabilizing stem loop structure was

inserted into pUFR047-GFP as a blunt-*Hind*III fragment. Expression of the

transcriptional fusion is under the control of the *lac* promoter present in the pUFR047. A

control construct was generated in the same manner as pVT123, however it contained a

G49A mutation in DaaP which abolishes processing of *daa* mRNA (108). This plasmid

was designated pVT124. To construct pVT148, *hrpA* was PCR amplified using primers

VTK108 and VTK93 (Table 2.2), digested with *Eco*RI, and ligated into the

chloramphenicol resistance gene of plasmid pACYC184 (45).

Mutagenesis and conjugation

A chemical mutagen 2-aminopurine (2-AP) (Sigma) was used for the mutagenesis

of *E. coli* TA516. A fresh overnight culture of TA516 was diluted into 3 ml of LB

containing 750 μg ml^{-1} 2-AP so that approximately 100 cells were in the inoculum, and

the culture was grown to saturation overnight. This concentration of mutagen increased

the rate of recovery of colonies resistant to a toxic NAD-analog, 6-aminonicotinicacid (6-

ANA), by a factor of approximately 10^2 (83). The mutagenized culture of TA516 strain

(recipient) was then mated on filter discs with a suspension of S17.1 *E. coli* harboring the

GFP-*daa* reporter construct pVT123 (donor) at 37°C for 8 h. The filter discs were

subsequently re-suspended in LB media containing antibiotics to select for

transconjugants. The cultures were grown at 37°C for 12 h to allow sufficient expression

of GFP for fluorescence activated cell sorting.

Fluorescence activated cell sorting (FACS)

Flow cytometry was performed using an Influx Flow Cytometer (Cytopeia, Inc.). A pool of transconjugants in 0.9% NaCl (1:100 dilution of the mating culture) was injected into a 70 μm flow stream comprised of autoclave-sterilized 0.9% NaCl. Excitation was accomplished with a 5W Innova argon laser (Coherent) set to 488 nm emission with ~400 mW power. The flow cytometer was configured to trigger on forward light scatter and to measure the green fluorescence signal passing through a 488 rejection band (RB) and a 520 long pass (LP) filter. Linear amplifiers were used to amplify the output from the photomultipliers.

Control strains with low and high GFP levels were used to calibrate the instrument for sorting. Cells were injected into the stream at a rate of 3×10^4 events sec^{-1}. For the initial round, 10^7 transconjugants were sorted that fell within gates containing the top 2% of cells in terms of GFP fluorescence. The sorted cells were cultured and grown overnight between each round of sorting. In the second round, a total of 1.2×10^6 bacteria were sorted with a sample injection rate of 2×10^4 events sec^{-1}. Again, the top 2% of bacteria in terms of GFP fluorescence were sorted. For the third round of sorting the gates were set to include top 4.5% of green fluorescent bacteria. In this round 10^6 bacteria were sorted with a sample injection rate of 1×10^4 events sec^{-1}. In the fourth and final sort 25% of the most highly GFP fluorescing bacteria were collected. Once again 10^6 bacteria were sorted, but with a sample injection rate of 4×10^3 events sec^{-1}.

RNA isolation and analysis

Total bacterial RNA was isolated from cultures incubated at 37°C overnight (73),

and primer extension analysis was performed according to methods described previously

(27). The oligonucleotides used in the primer extension analysis are listed in Table 2.2.

Mutant isolates from FACS were initially analyzed by semi-quantitative primer

extensions. This analysis was performed using two primers, DA and VTK18, specific for

cleaved product and precursor RNA, respectively. The primer extension results were

quantified using computer-scanned autoradiographs and the ImageQuant software from

Amersham Biosciences. The results were expressed as the ratio of precursor RNA to

cleaved product, with a ratio >1 suggesting a processing defect and a ratio <1

representing no defect.

S1 nuclease protection analysis was performed using the oligonucleotide WPL44

as a probe. WPL44 is complementary to the 46 nt downstream and 21 nt upstream of the

processing site. At the 3' end of the probe, 11 nt of non-complementary sequence were

included to facilitate detection of undigested oligonucleotide. End labeling of the probe,

hybridization and S1 nuclease digestion were performed according to the protocol

described elsewhere (11). The reactions were performed using 10, 50, and 90 units of S1

nuclease (Invitrogen) in parallel, since the precursor and cleavage products have different

sensitivities to S1 nuclease. In some experiments only digestions with 10 units of S1 are

shown. Primer extension and S1 nuclease protection products were resolved on 6%

acrylamide gels in 1X TBE (Tris-Boric acid-EDTA) buffer. S1 nuclease protection

results were quantified using Phosphor Image screens and the ImageQuant software from

Amersham Biosciences. The results were expressed as the percent (%) of total.

Hfr crosses and P1 transduction mapping

The Hfr mapping strains (donor) and strains for P1 transduction mapping are

listed in Table 2.1. In all interrupted mating experiments and P1 transductions the

recipient strain was C65, the mutant deficient in the processing of *daa* mRNA. The

matings were performed according to the protocol of Miller (123). Transconjugants were

selected on LB plates supplemented with tetracycline and ampicillin. P1 bacteriophage

lysate preparation and transductions were carried out essentially as described (124). GFP

levels in the progeny of conjugation and transduction experiments were analyzed in a

Fluoreskan Ascent fluorimeter (Thermo Labsystems) in a 96-well format, with excitation

at 485 nm and emission at 527 nm.

Southern-blot analysis

DNA was isolated from overnight cultures grown at 37°C (175). Genomic DNA

was then digested with *Eco*RI or *Bam*HI, separated on a 1% agarose gel, depurinated,

denatured and neutralized, and then transferred onto a Hybond-XL nylon membrane

(Amersham) according to methods described elsewhere (175). DNA was cross-linked to

the membrane by a UV crosslinker (Ultra-Lum). A DNA probe containing *hrpA* was

PCR-amplified with oligonucleotides VTK92 and VTK93 and labeled with the Random

Labeling kit (Invitrogen). Pre-hybridization buffer was 5 x SSC, 1 x Denhardt solution,

1% SDS and hybridization buffer was 5 x SSC and 1% SDS. The membrane was pre-hybridized for 2 h and hybridized overnight at 65°C. Washes consisted of two 20 min incubations at 65°C in 0.5 x SSC, 0.1% SDS, and one incubation in 0.1 x SSC, 0.1% SDS. The hybridized probe was detected by autoradiography.

Oligonucleotide-directed mutagenesis

Oligonucleotide-directed site-specific mutagenesis was performed using the Quickchange site-directed mutagenesis kit (Stratagene). This approach uses complementary oligonucleotides to introduce desired mutations. The sense strand of oligonucleotides used in the mutagenesis reactions are listed in Table 2.2.

Plasmid pQTN7 (100 ng) was used as a template for alanine scanning mutagenesis of the final ten codons of DaaP. Template was denatured for 30 sec at 95°C. Next, 16 cycles of 95°C for 30 sec, 55°C for 1 min and 68°C for 6 min were carried out in a PTC-100 (MJ Research, Inc.) thermocycler.

Plasmid pVT148 (100 ng) was used as a template for mutagenesis of *hrpA*. The PCR program used for mutagenesis of *hrpA* was similar to the one for mutagenesis of *daaP*, with the exception of an extension step at 68°C for 10 min. The *hrpA* mutagenesis reactions were carried out in a Primus 96 Plus (MWG Biotech) thermocycler. A C-terminal deletion of HrpA was generated by site-directed mutagenesis of pVT148 with the primer VTK119 that is complementary to 27 nucleotides downstream of codon Q463 and 29 nucleotides upstream of codon E1295, resulting in pVT160. For the deletion mutation 18 cycles of the above program were completed. The plasmids carrying *hrpA*

mutations were transformed into competent TOP10 cells after 1h digestion with *Dpn*I. The Big Dye Terminator method and ABI sequencing (PE Applied Biosystems) were used to confirm the presence of desired mutations. The absence of undesired mutations was determined using a mismatch nuclease CELI from celery.

CELI mismatch analysis

Mismatch analysis with CELI nuclease was performed essentially as described (188). Briefly, homoduplex and heteroduplex DNA was obtained by heat-denaturing a sample of either PCR-amplified DNA (using genomic DNA as a template) or linearized plasmid DNA at 95°C for 10 min followed by fast cooling to 85°C at a rate of 2°C/s and then a gradual cooling to 40°C at a rate of 3°C/min in a Primus96 Plus (MWG Biotech) thermocycler to allow random annealing of the denatured DNA strands. PCR fragments of the *rrnC* operon were amplified with primers VTK24+25 (7kb fragment), VTK24+26 (4kb 5' fragment) and VTK25+27 (4kb 3' fragment) from genomic DNA of TA516 strain (wild type) and C65 (mutant). Annealed DNA samples were treated with 1:100 dilution of CELI nuclease (fraction IV, provided by P. Aprikian) in a volume of 20 μl and buffer containing 20 mM HEPES, pH 7.9 and 3 mM $MgCl_2$ for 1 h at 37°C. The reactions were terminated by the addition of TAE loading buffer and electrophoretically separated on a 1.0% agarose gel, followed by staining with GelStar nucleic acid stain (BioWhittaker Molecular Applications).

Recombinational cloning in yeast

For the purpose of generating *rrnC* mutations in isolation and in different combinations on a plasmid, recombinational cloning in *Saccharomyces cervisiae* was employed. This approach relies on the homologous recombination pathway in yeast to construct plasmids using linear DNAs (142, 165). In this cloning strategy, a linearized target plasmid (yeast-*E.coli* shuttle vector) containing a selectable marker is co-transformed with a PCR fragment. The PCR fragment contains the gene of interest and additional 40 bp of homology to the target vector. By homologous recombination a subset of the linear plasmids are recircularized and simultaneously acquire the PCR segment.

Yeast-*E.coli* shuttle vector pRS316 (183) was linearized by digestion with *Sma*I. PCR was used to amplify the region with the desired *rrnC* mutation from the C65 mutant, and the remainder of the *rrnC* operon from the chromosome of wild type strain TA516. Different PCR fragments contained at least 100bp of overlapping sequence. The terminal fragments were generated with primers VTK84 and VTK85 that contain 40nt of homology to pRS316. PCR fragments and the vector were then introduced into yeast strain CRY1-2 (5, 227) by LiAc transformation (76). Yeast colonies with recircularized plasmid that have acquired *rrnC* operon were selected on yeast mimimal media supplemented with ampicillin. DNA was recovered from yeast cells (76) and introduced into electrocompetent *E. coli* DH10B according to the protocol of Sambrook (175). The presence of desired *rrnC* mutant residues in thus generated plasmids pVT140-147 (Table 2.3) were confirmed by ABI automated sequencing.

Ribotyping

To determine the number of rRNA operons in the TA516 strain and in the mutants

isolated by FACS, Southern blot analysis was performed according to the methods of

Asai *et al.* (9). Briefly, chromosomal DNA was extracted, digested with *Bam*HI and *Pst*I

overnight and separated on 0.7% agarose gel. The DNA was transferred onto nylon

membrane, cross-linked, pre-hybridized and hybridized with either Probe I or Probe II

(see below) according to the methods described in the "Southern-blot analysis" section.

Probes I (specific for 16S rRNA) and II (specific for 23S rRNA) were generated as

follows. Probe I: chromosomal DNA of *E. coli* TA516 was used as a template in a PCR

reaction with primers VTK36+31 to generate ~1.2 kb product; this PCR product was

subsequently digested with *Sal*I and *Sma*I resulting in 0.5 kb and 0.56 kb fragments; the

larger 0.56 kb fragment was then gel-purified before being labeled with Random

Labeling Kit as described in the "Southern-blot analysis" section. Probe II:

chromosomal DNA of *E. coli* TA516 was used as a template in a PCR reaction with

primersVTK32+45 to generate ~1.5 kb product; this PCR product was subsequently

digested with *Hpa*I and *Sal*I resulting in ~0.7 kb fragment that was gel purified and used

in hybridization experiments.

In vitro transcription/translation

The *E. coli* coupled transcription/translation system (229) was purchased from

Promega. The reactions contained the following in a total volume of 50 µl: 1 µg

supercolied template DNA (plasmids pWL117R, pWL122R and pWL130R – see Table

2.3), 0.5 mM of each of the 20 amino acids minus methionine, 0.2 μM L-

[^{35}S]methionine (1000 Ci/mmol; NEN), 15 μl T7-*E.coli* S30 extract, 50 ng rifampicin,

and 20 μl S30 premix. Reactions were allowed to proceed at 37°C for 2 hours. For

analysis of the translation products, reactions were precipitated with acetone and

resuspended in gel loading dye (125 mM Tris, pH6.8/ 2% SDS/ 10% glycerol/ 3M urea/

10% β-mercaptoethanol/ 5 μg/ml bromophenol blue), separated by Tricine-SDS-PAGE

(176), and exposed for autoradiography after drying. For analysis of *daa* mRNA

processing the reactions did not contain radioactively labeled methionine, were treated

with RNase free DNase (Promega), phenol/chloroform and chloroform extracted, and

ethanol precipitated before being analyzed by primer extensions with primer DA.

Preparation of *E. coli* S30 extracts

E. coli A19 (see Table 2.1) was grown in LB at 37°C to an optical dentsity (A_{582})

of 0.75. Cell-free extracts (S30 fractions) were prepared according to the method of

Zubay (229). Template mRNA for *in vitro* translation reactions was generated using

MEGA Script In Vitro Transcription kit (Ambion) and linearized plasmids pWL117R,

pWL122R and pWL130R. Translation reaction mixture contained the following in a

total volume of 50 μl: 10 mM MgOAc, 250 mM KOAc, 75 mM NH$_4$OAc, 2.5 μl Premix

I (20x: 3 mg/ml folinic acid, 0.5 M EDTA, 0.5 M DTT, 2% NaN$_3$), 0.48 mg/ml *E. coli*

tRNA (Sigma), 10 mM PEP, 1 ml PEP kinase (2 mg/ml), 2 mM ATP, 0.8 mM GTP, 4%

glycerol, 8 mM HEPES-KOH, 0.16 mM amino acids without methionine, 0.2 μM L-

[^{35}S]methionine (1000 Ci/mmol; NEN), 50ng rifampicin, 0.5μg *in vitro* transcribed RNA

and 10 µl cell-free extract. Reactions were allowed to proceed at 37°C for 2 h. Proteins

were precipitated on ice with trichloroacetic acid (TCA), resuspended in loading buffer,

and heated to 55°C for 10 min before being separated by Tricine-SDS-PAGE. Processing

of *daa* mRNA in S30 extracts was analyzed by primer extensions with primer DA after *in

vitro* translation reactions (with cold methionine) were phenol/chloroform extracted and

ethanol precipitated.

Table 2.1 Bacterial strains used in this study

Strain	**Description**	**Source or reference**
TOP10	F- *mcrA* Δ*(mrr-hsdRMS-mcrBC)* Φ*80lacZ*ΔM15 Δ*lacX74 deoR recA1 endA1 araD139* Δ*(ara-leu)7697 galU galK* λ *rpsL nupG*	Invitrogen
DH5α	F- Φ*80lacZ*ΔM15 Δ*(lacZYA-argF)* U169 *deoR recA1 endA1 hsdR17(r_k-, m_k+) phoA supE44* λ- *thi-1 gyrA96 relA1*	Invitrogen
TA516	Δ6 *rrn* (Δ*EBHG::lacZAD::cat*/pTRNA65)	(9)
S17.1	*E. coli* 294 with integrated plasmid RP4-2 Tc::Mu	(185)
CAG5051	HfrH *nadA57*::Tn*10*	(186)
CAG5052	KL227 *btuB3191*::Tn*10*	(186)
CAG5053	KL208 *zbc-280*::Tn*10*	(186)
CAG5054	KL96 *trpB83*::Tn*10*	(186)
CAG5055	KL16 *zed-3069*::Tn*10*	(186)
CAG8209	KL228 *zgh-3075*::Tn*10*	(186)
CAG8160	KL14 *thi-39*::Tn*10*	(186)
CAG12179	*mgl-500*::Tn*10*	(139)
CAG18640	*zhj-3076*::Tn*10*	(139)
CAG12026	*trg-2*::Tn*10*	(139)
CAG18461	*zdd-235*::Tn*10*	(139)
MC1061	*araD139* Δ*(araA- leu)7697* Δ*(codB-lacI)3galK16 galE15* λ- *e14- mcrA relA rpsL150 spoT1 mcrB9999 hsdR2*	(42)
MC1061ΔhrpA	Δ*hrpA*	(129)
WJW45	W3110 *lacU169*	(33)
WJW45ΔsrmB	Δ*srmB*	(47)
K37	*galK* (wt *ssrA* and *smpB*)	(216)
K8619	*ssrA::cat*	(216)
K8661	K8619 complemented with *ssrA* plasmid pJW28	(216)
MG1693	F- λ- *thy4715 rph-1*	(13)
SK7669	*rne-3071*	(13)
W3110	F- λ- IN*(rrnD-rrnE)1 rph*-1	S. Brown
NC124	W3110 *rnc-105*	D. Court
N2020	*rnpA49*	(4)
TZ136	Δ7 *rrn* strain carrying plasmid pHK-*rrnC-sacB*	C. Squires

Table 2.1 - continued

DH10B	*mrcA Δ(mrr hadRMS mcrBC)*	Invitrogen
CAG18431	*ilv-500*::Tn*10*	(139)
CAG18501	*zie-296*::Tn*10*	(139)
A19	*rna-19 gdhA2 his-95 relA1 spoT1 metB1*	(69)
Q13	A19 *tyrA6 pnp-13*	(168)
CA244	*lacZ trp relA spoT*	(105)
CA244rne	*ams-1*	(105)
CA244cafA	*cafA*	(105)
CA244rne cafA	*ams-1 cafA*	(105)

Table 2.2 – Oligonucleotides used in this study

Oligonucleotides	Sequence[a]
DA	5' GACTGTTCATTGCATATAAGTAAGTTTCTG 3'
VTK18	5' CCAGTGAAAAGTTCTTCTCCTTTACTC 3'
VTK24	5' CGGGTTATCACTTATCAGGTGAGCGTAGC 3'
VTK25	5' CGCCCGTAAGAGGTGGCGCATACCTCACG 3'
VTK26	5' GCCAACATCCTGGCTGTCTGGGCCTTCCC 3'
VTK31	5' CGTGTTGCGAAAATTTGAGAGACTCACG 3'
VTK32	5' CCGGCGAGGGGAGTGAAAAAGAACC 3'
VTK27	5' CGTGAGTCTCTCAAATTTTCGCAACACG 3'
VTK36	5' CCTGGGAACTGCATCTGATACTGGCAAGC 3'
VTK43	5' CGCACCTGAGCGTCAGTCTTCGTCC 3'
VTK44	5' CATCGAGGTGCCAAACACCGCCGTCG 3'
VTK45	5' GGCCATCATTACGCCATTCGTGCAGG 3'
VTK83	5' CGG GTAAGTTCCGACCTGCACGAATGG3'
VTK84	5' <u>CTCCACCGCGGTGGCGGCCGCTCTAGAACTAGTGGATCCCCC</u>CGGGTTATC ACTTATCAGGTG 3'
VTK85	5' <u>CTGGACGGTATCGATAAGCTTGATATCGAATTCCTGCAGCCCC</u>GCCCGTAA GAGGTGGCGCATACC 3'
VTK92	5' GCTGACAGACGAGCACAAAG 3'
VTK93	5' GCTGTAGATAAACATTATTCATC 3'
VTK108	5' <u>CCGGAATTC</u>GCTGACAGACGAGCAC 3'
VTK109[b]	5' GGGGAAACGGGTTCTG<u>C</u>TAAAACGACTCAG 3'
VTK110[b]	5' GGAAACGGGTTCTGGT<u>GC</u>AACGACTCAGTTAC 3'
VTK111[b]	5' GAAACGGGTTCTGGTAAA<u>G</u>CGACTCAGTTACC 3'
VTK112[b]	5' CACTATCATTATTG<u>C</u>CGAAGCGCACGAACG 3'
VTK113[b]	5' CTATCATTATTGACG<u>C</u>AGCGCACGAACGCAG 3'
VTK114[b]	5' CAGGCGTCTGCCAAT<u>GC</u>GCGTAAAGGCCGC 3'
VTK115[b]	5' GCGTCTGCCAATCAG<u>GC</u>TAAAGGCCGCTGTG 3'
VTK116[b]	5' GCCAATCAGCGTAAAG<u>C</u>CCGCTGTGGTCGTG 3'
VTK117[b]	5' CCAATCAGCGTAAAGGC<u>GC</u>CTGTGGTCGTGTG 3'
VTK118[b]	5' GGCCGCTGTGGT<u>GC</u>TGTGTCCGAAGGGATC 3'
VTK119[b]	5' GTCGAAGCACCGGATAAACGCAATATCCAGATTAGCGGTTAACCCTGCTA TTTGCC 3'

Table 2.2 - continued

VTK124[b]	5' GGTGATCGTCGCCG<u>C</u>GGAAACGGGTTCTGG 3'
VTK125[b]	5' CATTATTGACGAAGCG<u>GC</u>CGAACGCAGCCTG 3'
WPL44	5' CGGTGATGCCTTATTCCACGGTCTGCCAGTCCGGTGGCCCCGTGTTCAGCC
	GGTGTTCGCCACCACG<u>TACGCGGACTG</u> 3'
WPL71[b]	5' CCGGCTGAACACGG<u>C</u>GCCACCGGACTGGC 3'
WPL72[b]	5' CGGCTGAACACGGG<u>G</u>CACCGGACTGGCAG 3'
WPL73[b]	5' CTGAACACGGGGCCA<u>G</u>CGGACTGGCAGACC 3'

a. Underlined letters represent non-*daa*, non-*rrnC* or non-*hrpA* sequences, such as restriction endonuclease sites generated to facilitate cloning of PCR products, vector sequences or nucleotides introduced by site-directed mutagenesis.

b. Mutagenesis primers; complimentary oligonucleotides were also used but are not listed.

Table 2.3 - Plasmids used in this study.

Plasmids	**Description**	**Source**
pQTN7	2kb *Sac*I-*Hind*III fragment containing portion of wt *daa* operon cloned into pBluescript-SK+	(109)
pKEN-GFPmut1	Plasmid encoding a FACS-optimized GFP	(55)
pUFR047	Cloning vector; 1-2 copies/cell	(57)
pBJC11	Plasmid containing *daaP∆daaE*+stem loop structure in pBluescript-SK$^+$	B. Cantwell
pACYC184	Low copy number cloning vector	(45)
pVT101	pQTN7 with DaaP G49A mutation; mutagenized with WPL71	(108)
pVT102	pQTN7 with DaaP P50A mutation; mutagenized with WPL72	(108)
pVT103	pQTN7 with DaaP P51A mutation; mutagenized with WPL73	(108)
pVT123	Transcriptional fusion of GFP to wt *daaP* cloned into pURF047	This work
pVT124	Transcriptional fusion of GFP to G49A DaaP cloned into pURF047	This work
pRS316	Yeast-*E. coli* shuttle vector	(183)
pVT140	wt *rrnC* cloned into pRS316 ; *rrnC* amplified from TA516with VTK84 and VTK85 primers	This work
pVT141	C67T, T1865C, G2542A *rrnC* cloned into pRS316; *rrnC* amplified from C65 mutant with VTK84+85	This work
pVT142	C67T *rrnC* cloned into pRS316; VTK84+43 fragment from C65 and VTK36+85 from TA516	This work
pVT143	T1865C *rrnC* cloned into pRS316; VTK84+43 from TA516, VTK36+44 from C65 and VTK83+85 from TA516	This work
pVT144	G2542A *rrnC* cloned into pRS316; VTK84+43 from TA516 and VTK83+85 from C65	This work
pVT145	C67T, T1865C *rrnC* cloned into pRS316; VTK84+44 from C65 and VTK83+85 from TA516	This work

Table 2.3 – continued

pVT146	C67T, G2542A *rrnC* cloned into pRS316; VTK84+43 from C65, VTK36+44 from TA516 and VTK83+85 from C65	This work
pVT147	T1865C, G2542A *rrnC* cloned into pRS316; VTK84+43 from TA516 and VTK36+85 from C65	This work
pVT148	*hrpA* cloned into *Eco*RI site of pACYC184	This work
pVT150	pVT148 with HrpA G105A mutation; mutagenized with VTK109	This work
pVT151	pVT148 with HrpA K106A mutation; mutagenized with VTK110	This work
pVT152	pVT148 with HrpA T107A mutation; mutagenized with VTK111	This work
pVT153	pVT148 with HrpA D197A mutation; mutagenized with VTK112	This work
pVT154	pVT148 with HrpA E198A mutation; mutagenized with VTK113	This work
pVT155	pVT148 with HrpA Q395A mutation; mutagenized with VTK114	This work
pVT156	pVT148 with HrpA R396A mutation; mutagenized with VTK115	This work
pVT157	pVT148 with HrpA G398A mutation; mutagenized with VTK116	This work
pVT158	pVT148 with HrpA R399A mutation; mutagenized with VTK117	This work
pVT159	pVT148 with HrpA R402A mutation; mutagenized with VTK118	This work
pVT160	pVT148 with HrpA deletion (Q463-E1295); mutagenized with VTK119	This work
pVT161	pVT148 with HrpA G100A mutation; mutagenized with VTK124	This work
pVT162	pVT148 with HrpA H200A mutation; mutagenized with VTK125	This work
pWL171	pQTN7 mutagenized to generate destabilized stem loop structure downstream of *daaE*	W. Loomis

Table 2.3 – continued

pWL117R	wt *daaP* under T7 promoter in pBluescript-SK+	W. Loomis
pWL122R	Frameshift mutant of *daaP* under T7 promoter in pBluescript-KS+	W. Loomis
pWL130R	Premature STOP codon mutant of *daaP* under T7 promoter in pBluescript-SK+	W. Loomis

CHAPTER 3: IVOLVEMENT OF *E. coli* ENDORIBONUCLEASES IN PROCESSING OF *daa* mRNA

There is evidence from our laboratory that RNase E and RNase III are not involved in the processing of *daa* mRNA (27). The experiments which determined that the *daa* mRNA processing is not dependent on these endonucleases utilized a construct in which the downstream processed transcript, *daaE*, has a half-life of ~22.5 min. It is possible that in these experiments the role of RNAse E was obscured by processed product that is present long after the shift to the non-permissive temparuture (RNase E mutant is temperature sensitive). The stability of this mRNA is due in part to a stabilizing stem loop structure that forms at the 3' end of the *daaE* transcript (27). Using site-directed mutagenesis, we generated mutations that destabilized the downstream stem loop structure (pWL171). We determined the effect of these mutations on the half-life of *daaE* mRNA by primer extensions. Densitometric analysis of the autoradiograms determined the half-life of the mutant RNA to be ~5min, compared with 15min of the wild type *daaE* mRNA (data not shown).

Results

To investigate the involvement of RNase E, RNase III, and RNase P in the processing of *daa* mRNA, a plasmid containing the destabilized stem loop structure was used in the following backgrounds: conditional RNase E mutant strain SK7669 (*rne-3071*) and its parent strain MG1693, knockout RNase III mutant strain NC124 (*rnc-105*)

and its isogenic parent strain W3110, and the conditional mutant of RNase P strain

N2020 (*rnpA49*) and its isogenic parent strain W3110. All strains were grown to

logarithmic phase at 30°C and then shifted to the non-permissive (for the conditional

mutants) temperature of 44°C for 70min. RNA was then extracted and analyzed by S1

nuclease protection (Figure 3.1). Although the RNA levels differ in the different

backgrounds, no accumulation of precursor transcript was observed in the RNase E, III

and P mutants as compared to the wild type strains. These results confirmed our previous

observation that the RNase E and RNase III are not involved in *daa* mRNA processing,

and provided new data demonstrating that RNase P is not involved in the processing

event.

RNase G is an endonuclease with high homology to N-terminus of RNase E. It

has been reported recently that this enzyme is involved in initiation of decay of specific

transcripts (207). To investigate the role of RNase G in processing of *daa* mRNA we

introduced plasmid pWL171 into an RNase G mutant strain, CAA244cafA and a double

mutant of RNase E and RNase G, CA244cafArne (in addition to wild type parent strain

CA244 and *rne* single mutant in the same background, CA244rne). The cultures were

grown at 30°C to mid logarithmic phase, since the RNase E allele results in a temperature

sensitive phenotype, after which the cultures were incubated at the non-permissive

temperature of 44°C for 10 min. RNA was harvested and processing analyzed by S1

nuclease protection analysis. Although the levels of RNA isolated from the four strains

are different, there is no accumulation of precursor mRNA in any of the mutant strains

Figure 3.1 – RNase E, III and P are not involved in the processing of *daa* mRNA.

Processing of the *daa* mRNA was analyzed by S1 nuclease protection analysis which was performed using oligonucleotide WPL44 (Table 2.2) 5' end-labeled with $\gamma^{32}P$. The probe was hybridized to 10 μg of total RNA isolated from cultures of RNase E temperature sensitive mutant and wild type strains (SK7669 and MG1693, respectively), RNase III mutant and wild type strains (NC124 and W3110, respectively) and RNase P temperature sensitive mutant and wild type strains (N2020 and W3110, respectively) carrying plasmid pWL171 (Table 2.3). All cultures were grown at the permissive temperature (30°C) to mid logarithmic phase after which they were shifted to the non-permissive temperature for the temperature-sensitive mutants (44°C). P, precursor RNA; C, cleaved product.

RNase E   RNase III   RNase P

SK7669   MG1693   NC124   W3110   N2020   W3110

P →

C →
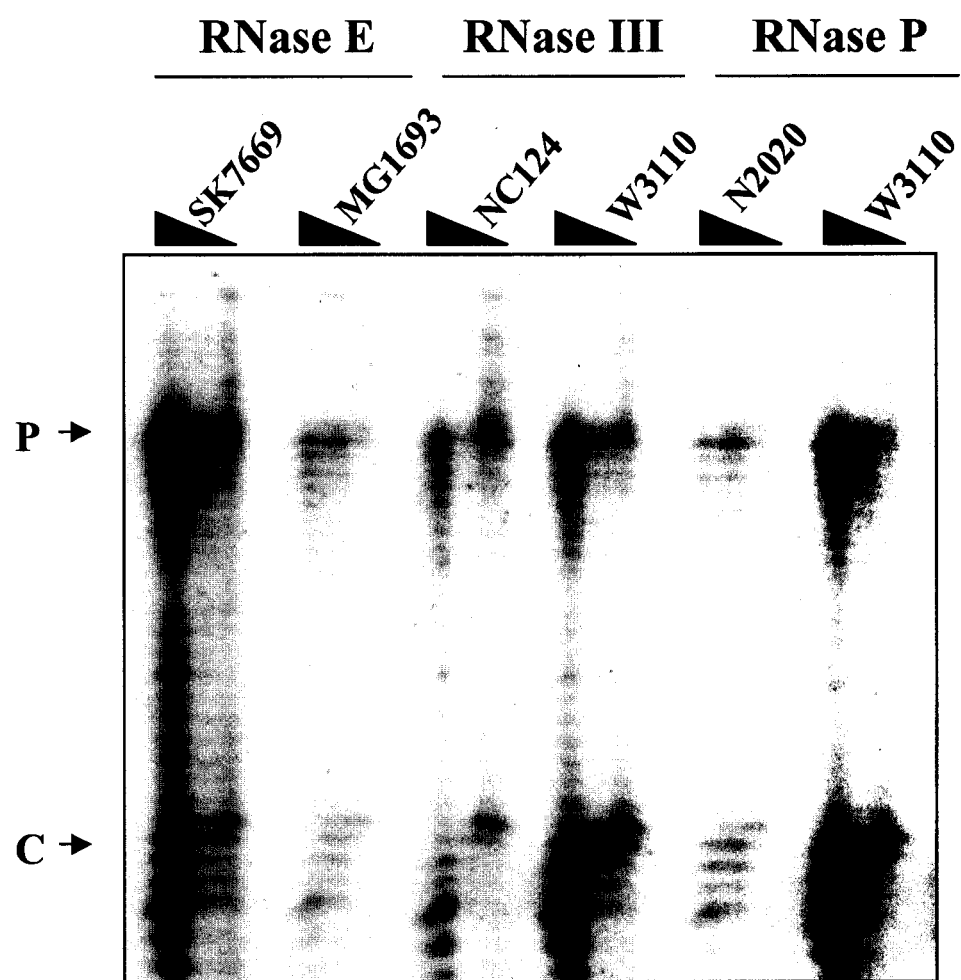
Figure 3.2 – Processing of *daa* mRNA is independent of RNase G.

S1 nuclease protection analysis was performed as described in the legend to Figure 3.1.

RNA was isolated from strain CA244 (wild type) and RNase E (rne), RNase G (cafA)

and RNase G + E (cafA rne) mutant strains generated in the same background and

carrying plasmid pWL171 (Table 2.3). All cultures were grown at the permissive

temperature (30°C) to mid logarithmic phase after which they were shifted to the non-

permissive temperature (44°C) for the temperature-sensitive mutants (rne and cafA rne).

P, precursor RNA; C, cleaved product.
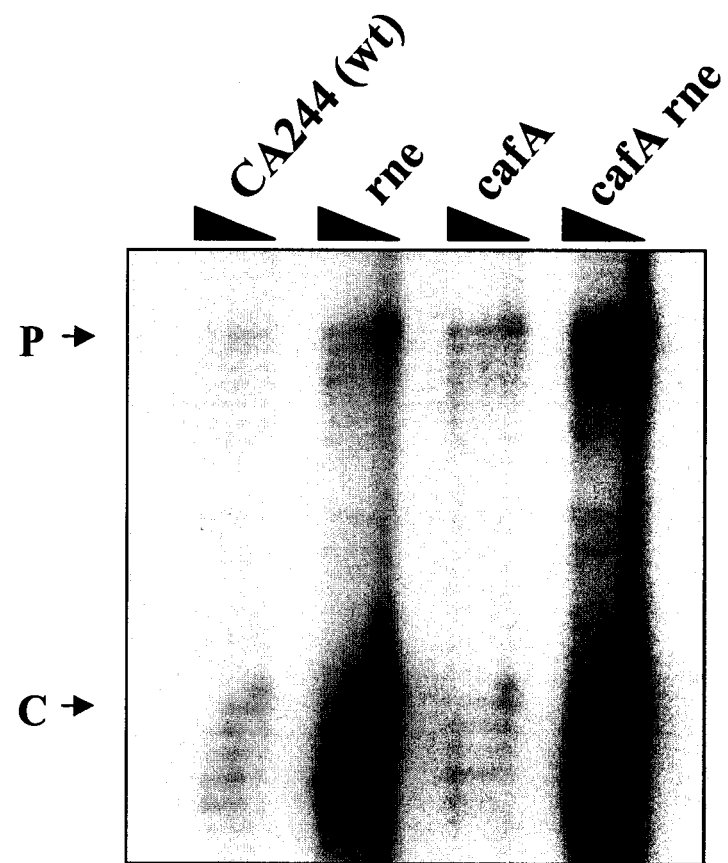
(Figure 3.2). This suggests that RNase G is not responsible for the cleavage of *daa* transcript and confirms that RNase E is not involved.

In addition to RNases E, III, P and G, the four endonucleases known to process mRNA in *E. coli*, RNase I is a major non-specific endonuclease responsible for >99% of the RNase activity in *E. coli* crude extracts (228). RNase I belongs to the T2 superfamily of ribonucleases whose members are present in most organisms, from bacteria to humans. Despite the extensive research on this ribonuclease over many years, the physiological role of RNase I is still unclear. Since mutant strains devoid of RNase I are viable (228) and because there is evidence that this enzyme is often found to associate with 30S ribosomal subunits in extracts (56) we wanted to determine whether RNase I is involved in processing of *daa* mRNA. RNase I mutant strains A19 and Q13 (Table 2.1) were transformed with pWL171 plasmid harboring the destabilized *daa* transcript. Processing of *daa* mRNA in these mutant strains was examined by primer extensions. Figure 3.3 shows that *daa* mRNA is cleaved in A19 and Q13 strains as efficiently as in the wild type strains, suggesting that this general endonuclease is not responsible for the cleavage of the *daa* transcript.

Discussion

The results presented in this chapter confirmed our previous observations and provided additional evidence that the processing of *daa* transcript is independent of major endonucleases known to process mRNA in *E. coli*. Our previous observations regarding the involvement of RNase E and III were based on experiments using a very stable *daa*

Figure 3.3 – RNase I is not involved in the processing of *daa* mRNA.

RNA was isolated from wild type strain DH5α carrying plasmid pQTN7 (with stabilizing

structure downstream of *daaE*) , from the same strain carrying plasmid pWL171 (Table

2.3), and the two RNase I mutant strains A19 and Q13 (also carrying pWL171).

Processing of *daa* mRNA was examined by primer extension analysis using primer DA

(Table 2.2) 5' end-labeled with $\gamma^{32}P$. Reactions were separated on an acrylamide gel next

to a sequencing ladder generated with the same primer (DA).
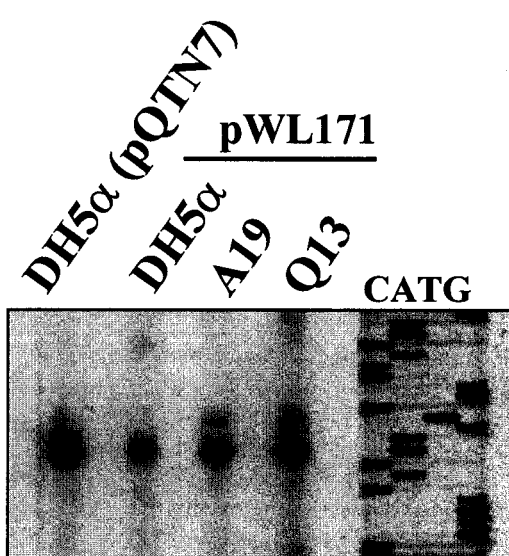
mRNA (calculated half life of ~22.5min) (27). Although RNase E is involved in initiation of decay of very stable transcripts (i.e. *ompA* with half life of 15min, (20)), the role of this enzyme can be masked by long half-lives of messages. Using a destabilized version of the *daa* transcript we were still unable to implicate RNases E, III, P, G and I in the processing of *daa* mRNA.

The current model for the role of RNase E in initiation of mRNA degradation in *E. coli* includes binding of the enzyme to the 5' end of transcripts it affects and preferential endonucleolytic cleavage of single stranded RNA 5' to AU dinucleotides in an AU rich sequences (6). Despite the fact that RNase E is involved in the cleavage of other fimbrial operons (i.e. *papBA* transcript of P-fimbriae (140)) at sequences that show homology to the RNase E preferred sites, the sequence flanking the *daa* mRNA cleavage site (C-U-G - cut - A-A-C) does not resemble the RNase E recognition sequence. Consistent with this observation, the lack of processing defect in the RNase E mutant strain shows that this endonuclease does not play a major role in the processing of *daa* transcript.

In addition to RNase E, RNase III is thought to be another major endonuclease in initiating decay of several mRNAs in *E. coli* (159). It is an enzyme that cleaves double-stranded RNA and the structural motif it recognizes is complex (169). Our preliminary modeling of the *daa* mRNA processing site (W. Loomis, unpublished observation) suggested that it is not in a region of double-stranded RNA. This is consistent with the results presented here (and our previous observation) that an RNase III mutant does not show a defect in the cleavage of *daa* mRNA.

RNase P is an endonuclease that has not been examined previously for its effect on the processing of *daa* mRNA. It is a rybozyme (RNA portion is responsible for catalytic activity) required for 5'-end formation in tRNA, but it can also process specific mRNAs (2, 102). New evidence concerning the effect of the *rnpA-49* mutation on levels of gene expression in *E. coli* suggests that RNase P can regulate gene expression in regions downstream of its cleavage site (102). This enzyme is now thought to be responsible for the some of mRNA decay in a bacterial cell, and the fact that it can initiate degradation of specific mRNAs prompted us to investigate its role in the *daa* mRNA processing. The mutant defective in RNase P function does not result in accumulation of *daa* mRNA precursor (as measured by S1 nuclease protection analysis), suggesting that this endonuclease is also not involved in the degradation of the *daa* transcript.

A homologue of RNase E, RNase G, is involved in processing of *adhE* and *eno* transcripts in *E. coli* (207). Mutations in either RNase E or RNase G in CA244 background had no effect on processing of *daa* mRNA. Additionally, a double mutant CA244cafArne also resulted in wild type processing of *daa* transcript. This suggests that these enzymes do not participate in *daa* mRNA processing and that an unrelated endonuclease is involved.

Finally, we investigated the role of RNase I, a relatively nonspecific endoribonuclease, in the processing of *daa* mRNA. Even though the mutants of RNase I have <1% RNase activity in crude extracts (228), this enzyme is not viewed as a prime candidate for playing a significant role in mRNA decay because of the evidence

suggesting that it is located in the periplasm of the bacterial cell. Our results using

RNase I mutants indicate that this enzyme is not involved in the processing of *daa*

mRNA since they show no processing defect. Therefore, we have excluded a major role

for all of the major endonucleases in *E. coli* in the processing of the *daa* transcript. Our

results are consistent with the possibility that a different, potentially novel, endonuclease

is important in processing of *daa* mRNA and thus in the regulation of gene expression in

E. coli.

CHAPTER 4: CHARACTERIZATION OF A *CIS*-ACTING ELEMENT INVOLVED IN PROCESSING OF *daa* mRNA

Endonucleolytic cleavage of mRNA in the *daa* operon of *E. coli* is responsible for coordinate regulation of genes involved in F1845 fimbrial biogenesis. Translation of a small ORF that spans the site of cleavage, *daaP,* was determined to be required *in cis* for processing of *daa* mRNA to occur. The amino acid sequence of the DaaP polypeptide is also important for processing (109). This suggested a hypothesis that the nascent DaaP peptide interacts with a ribosome or a ribosome-associated component in a manner that facilitates cleavage of the *daa* mRNA in the ribosome. In this chapter I will present experiments that further identified an *in cis* element important for processing of the *daa* transcript.

Results

Previously we have shown that a mutant resulting from a shift in the reading frame of *daaP* and encoding a peptide of similar size but different amino acid sequence failed to mediate processing of the *daa* mRNA. This indicated that the amino acid sequence of DaaP is important for processing (109). To pinpoint the domain of the peptide that is crucial for processing, the sequence of DaaP was divided into four arbitrary segments. Site-directed mutagenesis was utilized to change the reading frame of the four different segments individually. Primer extension and S1 nuclease protection analyses determined that the processing of *daa* mRNA was abolished only when the final

segment, the C-terminal ten amino acids, was frameshifted. This indicated that amino acid sequence of the final ten codons of *daaP* is essential for processing to occur.

To further identify the region of the DaaP peptide important for processing, site-directed mutagenesis was used to individually change each of the final ten codons of DaaP to an alanine. Primer extension analysis showed, that the only codons unable to tolerate mutations were Gly 49, Pro 50 and Pro 51, since when these were changed to an alanine, *daa* message failed to be processed (Figure 4A). S1 nuclease protection analysis of the RNAs encoding the G49A, P50A and P51A mutations, demonstrated that failure to cleave the mutant RNA resulted in an increase in the amount of precursor RNA in the cells (Figure 4B). To eliminate the possibility that the RNA sequence of the GPP tripeptide is important for processing, synonymous mutations of GPP codons were generated in collaboration with Wendy Loomis. Since GGG^{Gly} is a rare codon of glycine, two synonymous changes were introduced into codon 49: GGA^{Gly} which is also a rare codon and GGT^{Gly} which is a commonly used glycine codon (156). Codons 50 and 51 were changed from CCA to CCG and CCG to CCA, respectively, to avoid introducing either of the rare proline codons. Synonymous mutations in these three codons had no effect on processing suggesting that RNA processing is dependent on the tripeptide sequence, GPP (Figure 4C).

Discussion

In this chapter I presented evidence that the processing of *daa* mRNA requires a specific amino acid sequence in the nascent DaaP peptide and that it resembles other

Figure 4 – Alanine scanning mutagenesis of the final 10 codons of *daaP*.

A) Primer extension analysis of *daa* mRNA processing in strains carrying each of the alanine mutations. RNA was isolated and primer extension was performed using primer DA (Table 2.2) 5' end-labeled with γ^{32}P. Reactions were separated on an acrylamide gel next to a sequencing ladder generated with the same primer (DA).

B) S1 nuclease protection analysis was performed using oligonucleotide WPL44 (Table 2.2) 5' end-labeled with γ^{32}P and hybridized to 10 μg of total RNA which was isolated from strains carrying plasmids pQTN7 (wild type), pVT101 (G49A), pVT102 (P50A), and pVT103 (P51A). RNA-probe hybrids were digested with 90, 50 and 10 units of S1 nuclease. Protected products were separated on an acrylamide gel. P, precursor RNA; C, downstream cleaved product.

C) Primer extension analysis of synonymous mutations in codons 49-51. RNA was isolated from strains carrying pQTN7 (wild type GPP) and each of the synonymous mutants and primer extension was performed using primer DA (Table 2.2) 5' end-labeled with γ^{32}P. Reactions were separated on an acrylamide gel next to a sequencing ladder generated with the same primer (DA).

A

CATG N T G P P D W Q T V E CATG

B

CATG WT G49A P50A P51A

← P

← C

C

C A T G WT GPP G49 (ggg to gga) G49 (ggg to ggt) P50 (cca to ccg) P51 (ccg to cca)
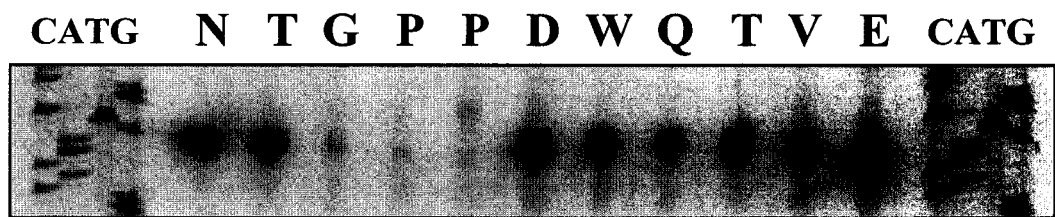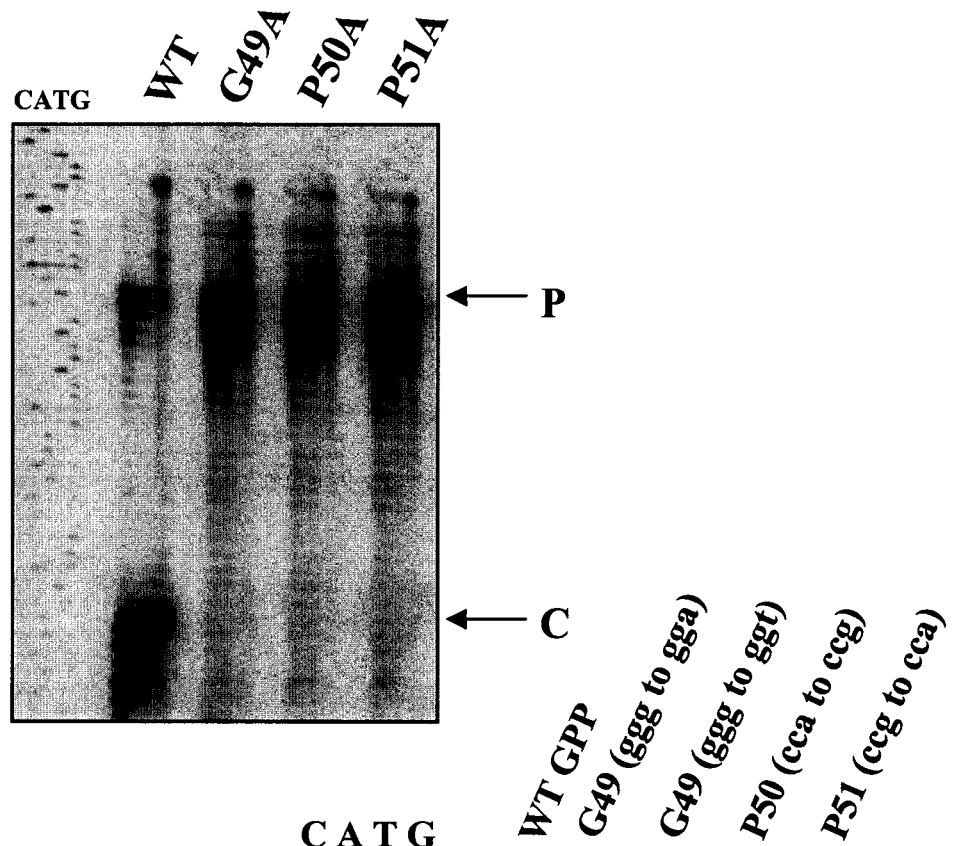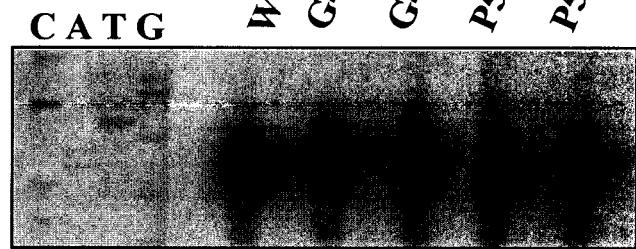
examples of nascent peptide-mediated translational control of gene expression (110, 130, 200). Site-directed mutagenesis of the final ten codons of *daaP* revealed that amino acids 49-51 of DaaP are crucial in promoting cleavage of the *daa* mRNA (Figure 4). The question that remains is: how is the GPP tripeptide involved in processing of *daa* mRNA? Based on the other known systems of translational control it is possible that it interacts with the ribosome (potentially acting close to the peptidyltransferase center) and induces stalling of the ribosome that in turn leads to mRNA cleavage. However, the comparison of the amino acid sequences in effector motifs of nascent peptides does not allow assignment of functional homologies (110), therefore the effect of GPP on the trafficking ribosomes needs to be further examined *in vitro* and *in vivo*.

CHAPTER 5: IDENTIFICATION OF *TRANS*-ACTING FACTORS INVOLVED IN PROCESSING OF *daa* mRNA

Although we knew about the important *in cis* elements needed for processing of the *daa* mRNA, we had no information on the *trans*-acting factors involved. In this chapter I present the data from a genetic screen in which I isolated mutants deficient in processing of *daa* mRNA. Characterization of these mutants aided in identification of novel factors involved in *daa* mRNA cleavage.

Genetic screen for *daa* mRNA processing deficient mutants.

To identify factors involved in the processing of *daa* mRNA, a genetic screen was devised using GFP as a reporter. A gene encoding a FACS-optimized and highly fluorescent GFP was cloned upstream of the *daa* processing region, and the *daaE* mRNA-stabilizing stem-loop structure (27) was placed downstream of the processing site, resulting in plasmid pVT123 (Figure 5.1A). After normal processing, the GFP-*daaP* transcript is quickly degraded because the stabilizing secondary structure is removed, resulting in low GFP levels. A control GFP fusion construct, pVT124, was created with a mutant *daaP* sequence that abolishes processing, i.e. a G49A mutation in DaaP (108). When there is a processing defect, GFP is more highly expressed because the transcript is stabilized by retention of the downstream secondary structure. FACS was used to analyze the levels of GFP in strains harboring the control constructs (Figure 5.1B). Importantly, the strain carrying plasmid pVT123 expresses GFP at a low level, clearly

Figure 5.1 – Genetic screen for *daa* mRNA processing deficient mutants.

A) Plasmid pVT123 was generated as a transcriptional fusion of GFP to the wild type

daa processing region followed by a stabilizing stem loop structure. Control construct

pVT124 is identical to pVT123 except that it contains a G49A mutation in DaaP that

abolishes processing of the *daa* transcript.

B) FACS analysis profiles of control strains. *E. coli* strain TA516 was transformed with

either empty vector pUFR047 (no GFP) or GFP constructs pVT123 and pVT124. GFP

fluorescence levels were measured in 10,000 cells from each of the three populations.

Counts (Y-axis): represents the number of cells; GFP (X-axis): represents GFP

fluorescence levels.
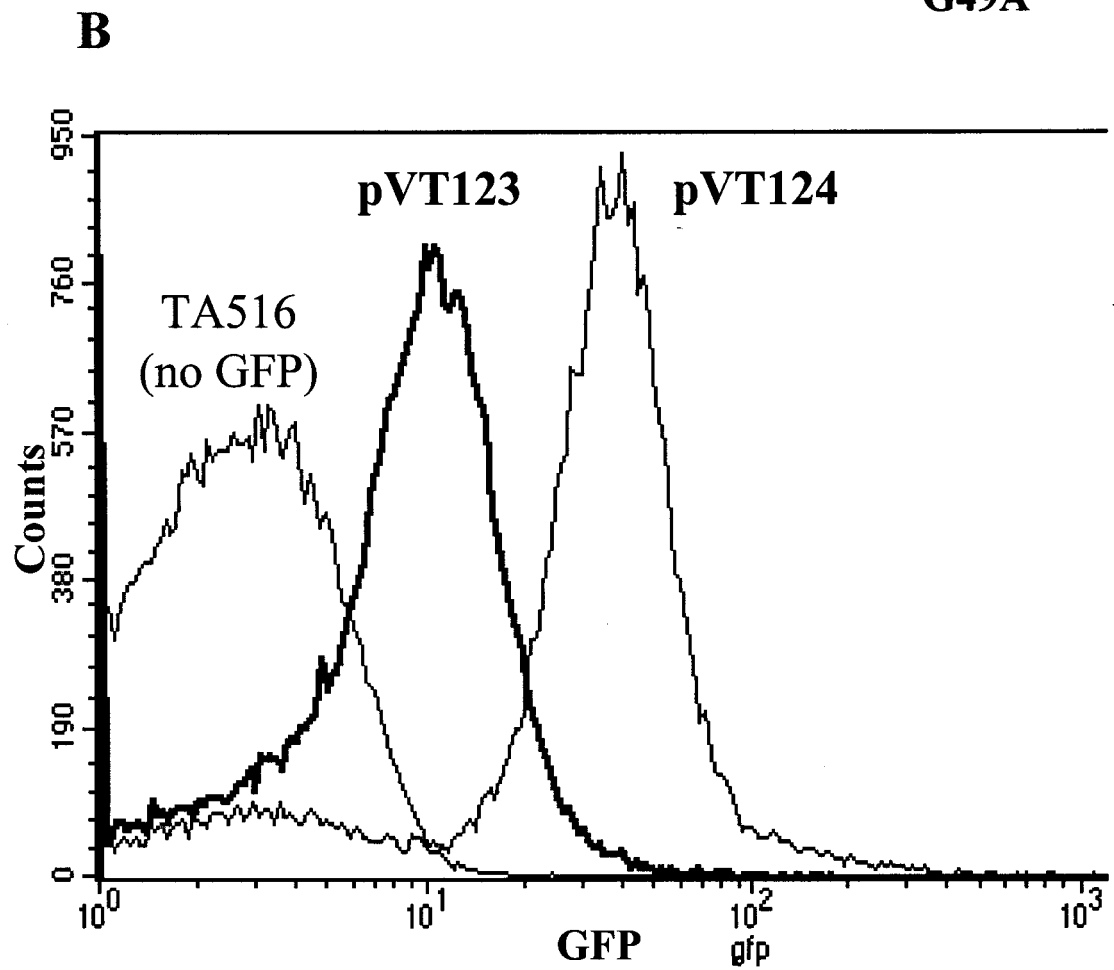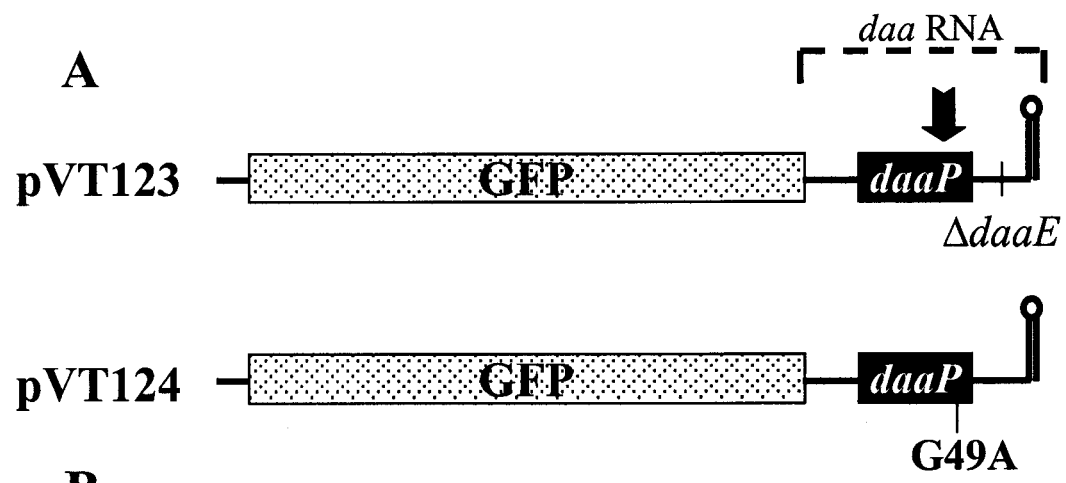
distinct from the high level of GFP expressed by the strain with the non-processing construct pVT124.

Since processing of the *daa* transcript is dependent on translation and there is a possibility of a ribosomal component or a ribosome-associated factor being involved in *daa* mRNA cleavage, *E. coli* strain TA516 (9) with a single copy of an *rrn* operon on the chromosome was chosen for mutagenesis. This strain was mutagenized with the chemical mutagen 2-aminopurine (2-AP) (157). The GFP-containing reporter construct pVT123 was subsequently introduced into the mutagenized TA516 population by conjugation. Approximately 10^7 transconjugants were then subjected to high-speed/high-throughput sorting with the sort window set for the top 2% of high-GFP expressing bacteria. These bacteria were subsequently sorted and grown overnight three more time for a total of four enrichments to achieve a population in which more than 60% of the bacteria were highly fluorescent (Figure 5.2).

Semi-quantitative primer extension analysis was used to determine if there was a *daa* mRNA processing defect in high GFP-expressing mutants isolated by sorting. Two primers, one specific for precursor RNA and one specific for the cleaved product, were simultaneously annealed to the total RNA isolated from five hundred mutant isolates obtained by FACS. Quantitation of the primer extension products revealed that 70% of the mutant isolates had varying degrees of the processing defect (data not shown). A more quantitative analysis of *daa* mRNA processing in representative mutant isolates by S1 nuclease protection showed an increase in the levels of precursor RNA and a reduced amount of cleaved product. My initial analysis of the mutants isolated in the genetic

Figure 5.2 – FACS enrichment for mutants deficient in processing of *daa* mRNA.

The first four panels show representative dot-plots of the mutagenized TA516 population subjected to four connsecutive enrichment sorts. Dashed regions indicate the gated areas from which the bacteria were sorted. The gates in Sorts 1 and 2 were set to include the top 2% of GFP-fluorescing bacteria while the gate in Sort 3 included the top 4.5%. In the final enrichment the top 25% of GFP-fluorescing bacteria were sorted. The final panel is a representative analysis of the mutant population after the four enrichment sorts. GFP, fluorescence level of green fluorescent protein in mutagenized bacteria; FLS, forward light scatter.

Sort 1
2%

Sort 2
2%

Sort 3
4.5%

Sort 4
25%

After sort 4

GFP

FLS
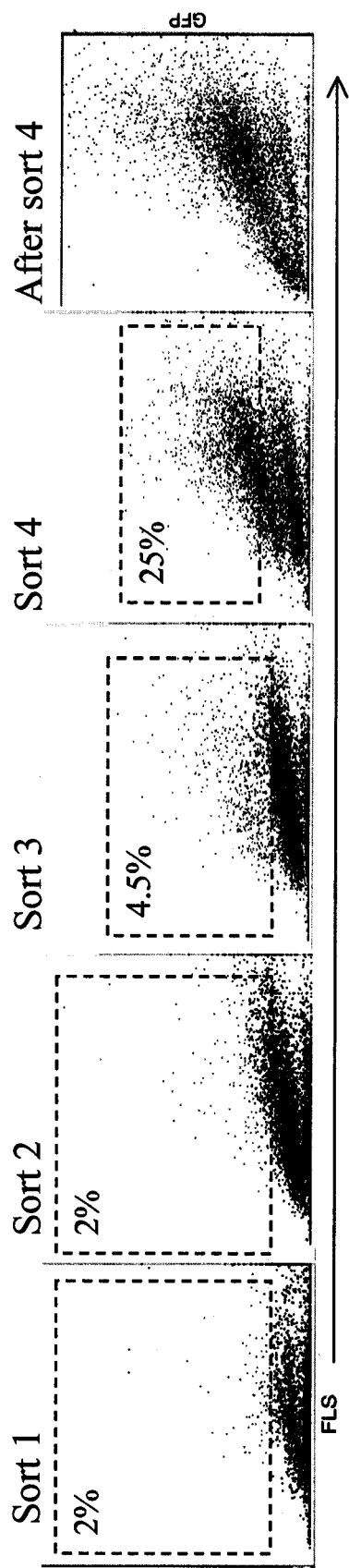
screen revealed that some isolates had a complete lack of processing activity, but on passage regained some activity. No isolate with completely abolished processing of *daa* mRNA has been maintained. One of the high GFP-expressing FACS isolates from the population after the final enrichment, determined to have a *daa* mRNA processing defect by primer extension and S1 nuclease protection, was designated C65 and was used for further analysis. One of the high GFP-expressing FACS isolates from the population after the final enrichment, determined to have a *daa* mRNA processing defect by primer extension and S1 nuclease protection, was designated C65 and was used for further analysis.

Relevance of *rrnC* operon in processing of *daa* mRNA.

The data in our laboratory, prior to the mutagenesis of TA516 strain, suggested a hypothesis that the nascent DaaP peptide controls the processing of the *daa* mRNA by interacting with the ribosome (or a ribosome associated factor) to facilitate cleavage of the transcript in the ribosome. Thus, the initial analysis of FACS isolated mutants focused on the single *rrn* operon in the strain TA516, *rrnC*, as well as the ribosomal proteins. Since the mutagen used, 2-AP, mainly induces point mutations, a mismatch analysis was conducted using CELI nuclease from celery (188).

For the CELI mismatch analysis of *rrnC* operon, 5' 4kb fragment (containing 16S rRNA and a small portion of 23S rRNA), 3' 4kb fragment (containing 23S rRNA) and 7kb fragment (containing the entire operon) were PCR amplified from wild type strain TA516 and processing deficient mutant C65 isolated by FACS (Figure 5.3B).

64

Figure 5.3 – Mismatch analysis of the *rrnC* operon .

A) CEL I nuclease was used for mismatch analysis of the *rrnC* operon. PCR fragments were generated from wild type

(TA516) and C65 mutant and contained the 5' 4kb fragment, the 3' 4kb fragment, or the entire 7kb operon (including the

flanking sequences). In each panel, lanes 1 and 2 correspond to homoduplexes of TA516 and C65 DNA samples,

respectively, while lane 3 corresponds to the heteroduplexes. The arrows indicate the size of the fragments resulting from

the presumed point mutations.

B) Schematic of the *rrnC* operon and the flanking genes. Double-pointed arrows indicated fragments that were predicted

to arise from the mismatch analysis in (A). White stars denote the locations of mutations predicted by the CEL I

analysis and confirmed by automated sequencing.

A

5'*rrnC* 4 kb

1 2 3

2.8 kb
1.2 kb

3'*rrnC* 4 kb

1 2 3

1.8 kb
1.5 kb
0.7 kb

rrnC 7 kb

1 2 3

3.5 kb
1.5 kb
1.2 kb
0.7 kb

B

yieP

1.2 kb

tRNA

16S

3.5 kb

23S

0.7 kb

5S tRNA

yifA

1.5 kb
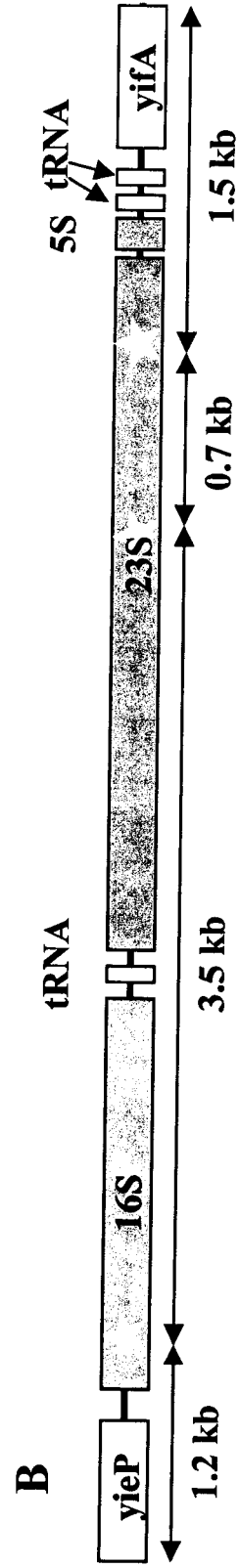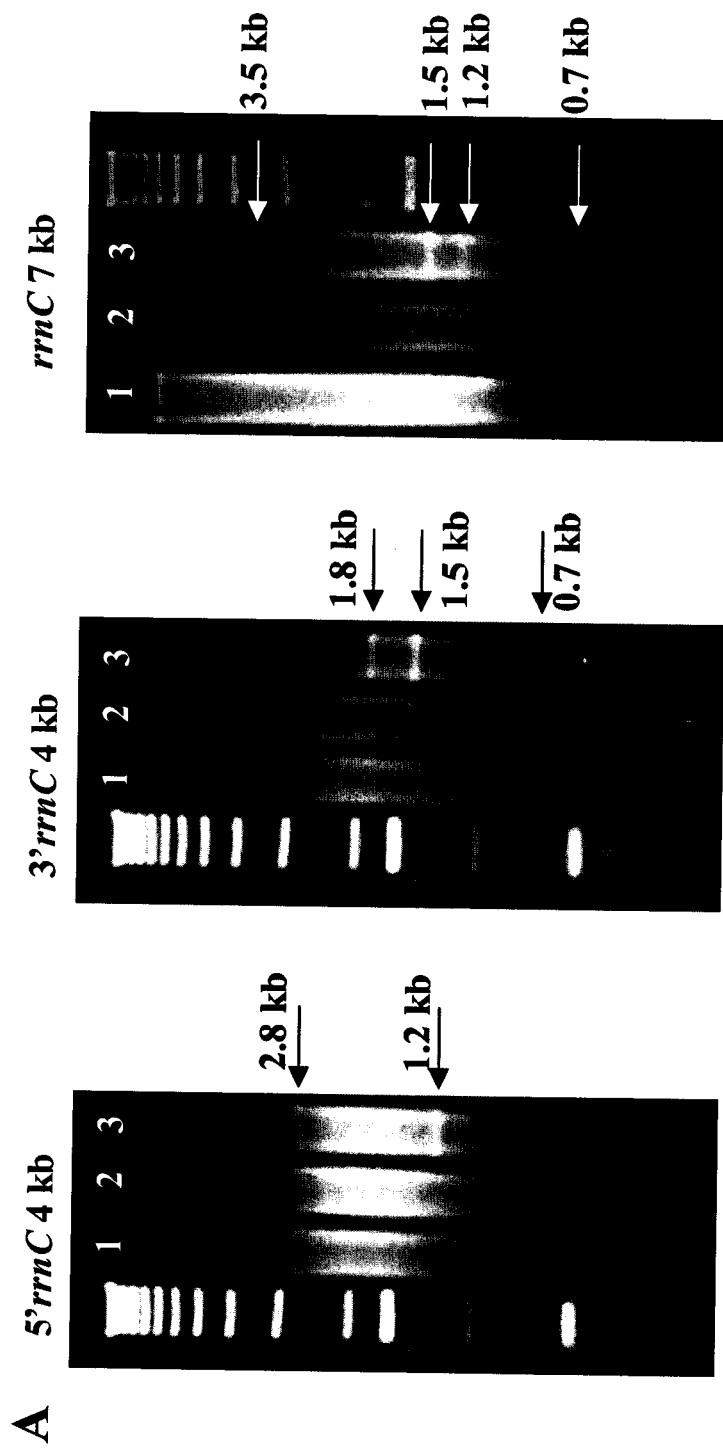
Homoduplex and heteroduplex DNAs were formed and digested with CELI nuclease and products analyzed on agarose gels. Analysis of the 5' fragment resulted in two bands, suggesting the presence of a single mutation in this region (Figure 5.3A). Analysis of the 3' fragment resulted in three bands after CELI digestion, suggesting the presence of two mutations in the 23S rRNA (Figure 5.3A). When the 7kb fragment was used, four bands were observed in the CELI digest of heteroduplexes, further suggesting that C65 mutant contains three mutations in this operon (Figure 5.3A). Automated sequencing of the entire 7kb *rrnC* operon from the C65 mutant revealed the presence of three mutations at the positions predicted by CELI mismatch analysis and at the following residues: C67T (in 16S rRNA), T1865C (in 23S rRNA) and G2542A (in 23S rRNA). All three mutations are transitions, consistent with the type of change caused by 2-AP (157). CELI mismatch analysis of the operons encoding ribosomal proteins and translation factors (~50kb of sequence) revealed no additional mutations (data not shown).

To determine if *rrnC* mutations are important for the processing of the *daa* message, the following approaches were pursued:

Replacement of mutant rrnC *operon with a wild type copy.* A bacteriophage P1 lysate from a strain with a Tn*10* insertion near the *rrnC* operon, CAG18431 (139), was generated. This lysate was then used to transduce the mutant C65, defective in *daa* mRNA processing. Transductants were selected on the basis of antibiotic marker in the transposon. In some transductants the mutant *rrnC* operon was replaced by a wt copy as determined by CELI mismatch analysis and sequencing of the operon (data not shown). To determine the effect of *rrnC* mutation replacement on the processing of the *daa*

mRNA S1 nuclease protection analysis was performed. Figure 5.4 shows that *daa* mRNA processing defect in a strain with wt *rrnC* was not restored, i.e. processing occurred at the level of the original mutant. This suggests two possibilities: first, that the *rrnC* mutations are not relevant for the processing of the *daa* mRNA; and second, that these ribosomal RNA mutations were important initially, but that possible additional mutations accumulated rendering the ribosomal mutations irrelevant.

Site-directed mutagenesis to generate individual rrnC *mutations and mutations in combination.* It is possible that one or more of the *rrnC* mutations identified were important initially and that the other mutations compensated for a possible detrimental effect of these residues on bacterial viability. Thus, recombinational cloning in yeast was used to generate each of the three *rrnC* mutations in isolation and also in combination with others on a plasmid. The plasmids with mutant residues were used to replace the resident pHK-*rrnC-sacB* plasmid from strain TZ136 (by sucrose selection) in which all seven chromosomal ribosomal RNA operons have been inactivated. S1 nuclease protection analysis determined that processing of *daa* mRNA in the strains with plasmids carrying individual and a combination of *rrnC* mutations was not affected, i.e. *daa* message was processed at the wild type level. However, further sequence analysis of mutant plasmids isolated from TZ136 (pVT141-147) strains revealed that all the mutations have been restored to wild type. It is thus possible that in the process of resident-plasmid replacement some plasmid recombination occurred and restored the mutations. This strongly suggested that the *rrnC* mutations had a deleterious effect on the cell.

Figure 5.4 – Restoring *rrnC* operon in C65 mutant does not restore processing of the *daa*

mRNA.

S1 nuclease protection analysis was performed as described in the legend to Figure 3.1.

RNA was isolated from TA516 harboring pVT123 (WT) or pVT124 (G49A), C65 mutant

and C65 in which the *rrnC* operon has been restored to wild type (TA516) sequence by

bacteriophage P1 transduction. RNA-probe hybrids were digested with 90, 50 and 10

units of S1 nuclease and separated on an acrylamide gel. P, precursor RNA; C, cleaved

product.
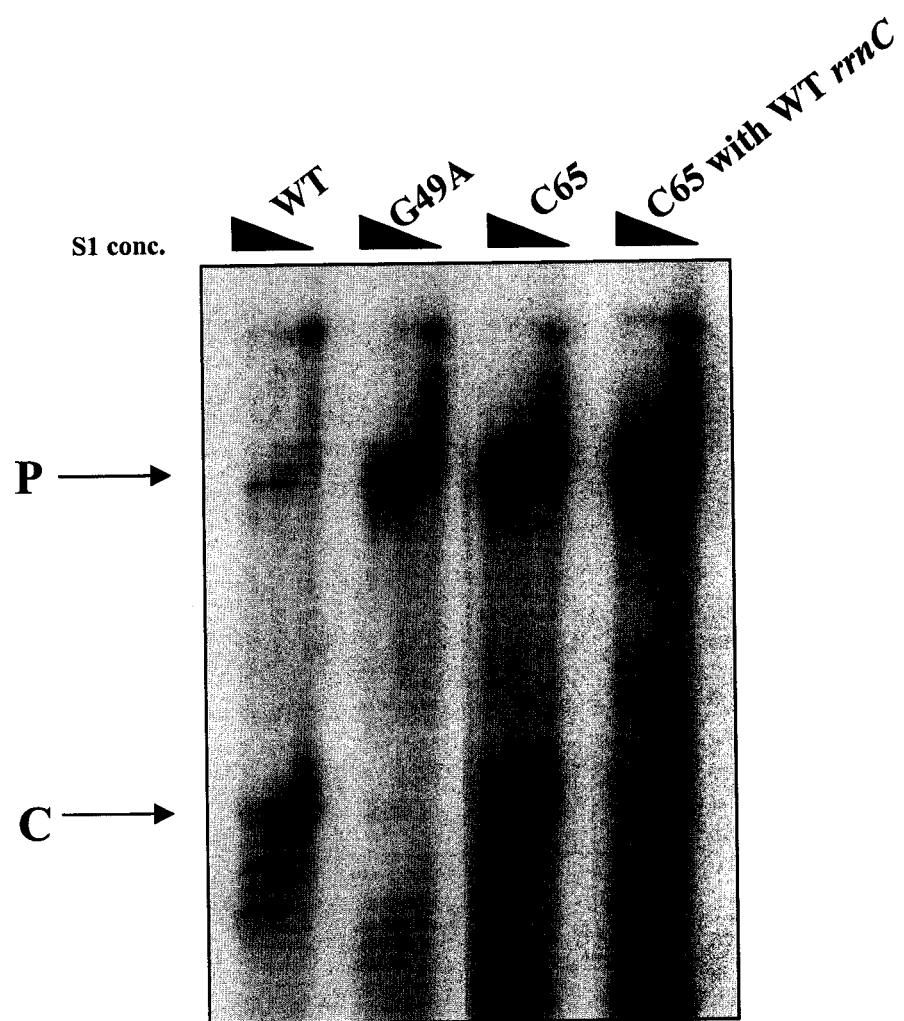
Since the effect of the mutations could not be determined in the absence of wild type *rrn*, a 'diploid'-ribosome experiment was attempted next. For this, the strain with seven ribosomal RNA operons inactivated and one wt operon on a resident plasmid was used. The mutant *rrnC* plasmids were introduced into this strain without replacing the resident plasmid, so that in this strain a wild type and a mutant plasmid encoded ribosomal RNA. The strain with all three *rrnC* mutations on a plasmid had a growth defect, while all the other strains with single and double *rrnC* mutations grew normally (data not shown). Analysis of *daa* mRNA processing in these 'diploid'-ribosome strains revealed a defect in the presence of a construct encoding all three *rrnC* mutations (Figure 5.5). This phenotype, however, was very unstable. Upon passage, in the strain encoding mutant (all three *rrnC* mutations) and wild type ribosomes, processing of *daa* transcript was restored, as was the growth defect. Finally, 'diploid'-ribosome strains were generated by introducing mutant *rrnC* plasmids into the strain with a single wild type copy of rRNA on the chromosome and the other six operons inactivated, TA516. Processing of *daa* mRNA in these 'diploid'-ribosome strains was not affected (Figure 5.6). These data suggest that *rrnC* mutations might affect viability of the bacteria and may not have a direct effect on processing of *daa* mRNA.

The effect of rrnC *mutant residues in isolation on the chromosome.* An alternative way of examining the effect of *rrnC* residues on the processing of *daa* mRNA is to introduce these mutations on the chromosome of TA516. For this purpose, C65 was transduced with a P1 bacteriophage lysate from strain CAG18501 (139) that contains a Tn*10* insertion near *rrnC* (but further away than the Tn*10* insertion in CAG18431). It is

69

Figure 5.5 – Processing of *daa* mRNA in a 'diploid' ribosome experiment in the strain TZ136.

S1 nuclease protection analysis was performed as described in the legend to Figure 3.1. RNA was isolated from the wild type strain TA516 harboring plasmids pVT123 (WT) or pVT124 (G49A), from the mutant C65, and TZ136 harboring plasmids pVT140 (wt *rrnC*), pVT141 (C67T, T1865C, G2542A *rrnC*), pVT142 (C76T *rrnC*), pVT143 (T1865C *rrnC*), pVT144 (G2542A *rrnC*), pVT145 (C67T, T1865C *rrnC*), pVT146 (C67T, G2542A *rrnC*) and pVT147 (T1865C, G2542A *rrnC*). RNA-probe hybrids were digested with 90, 50 and 10 units of S1 nuclease (triangles) and were separated on an acrylamide gel. P, precursor RNA; C, cleaved product.

S1 conc.

WT G49A C65 WT rnc C67T, T186SC, G2542A C67T T186SC G2542A C67T, T186SC C67T, G2542A T186SC, G2542A

P →

C →

Figure 5.6 – Processing of *daa* mRNA in a 'diploid' ribosome experiment in the strain TA516.

S1 nuclease protection analysis was performed as described in the legend to Figure 3.1. RNA was isolated from the wild

type strain TA516 harboring plasmids pVT123 (WT) or pVT124 (G49A), from the mutant C65, and TA516 harboring

plasmids pVT140 (wt *rrnC*), pVT141 (C67T, T1865C, G2542A *rrnC*), pVT142 (C76T *rrnC*), pVT143 (T1865C *rrnC*),

pVT144 (G2542A *rrnC*), pVT145 (C67T, T1865C *rrnC*), pVT146 (C67T, G2542A *rrnC*) and pVT147 (T1865C, G2542A

rrnC). RNA-probe hybrids were digested with 90, 50 and 10 units of S1 nuclease (triangles)and were separated on an

acrylamide gel. P, precursor RNA; C, cleaved product.
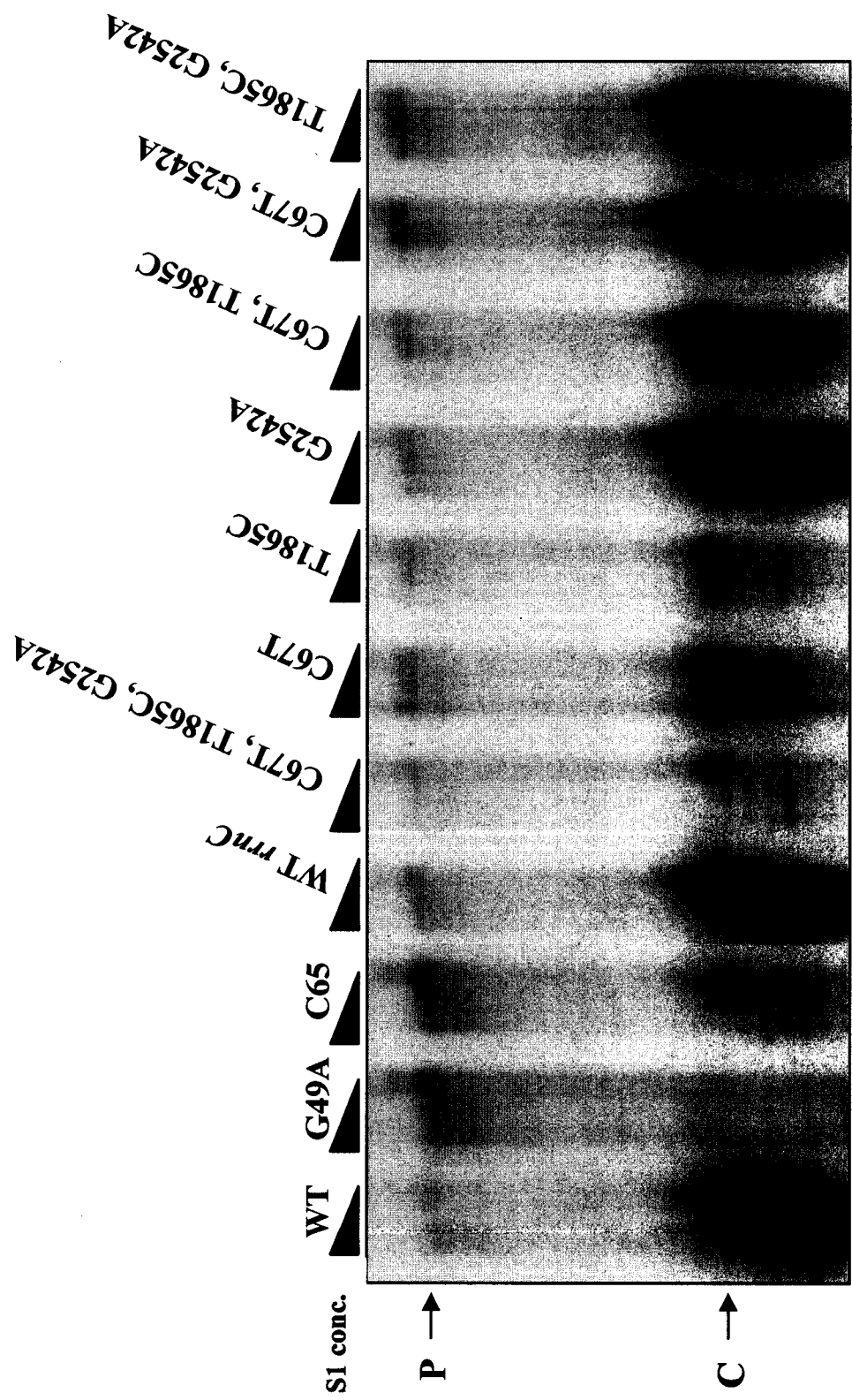
expected that in some of the transductants from this experiment recombination will result in tagging of the mutant *rrnC* operon with Tn*10* without replacing it with the wild type copy. CELI mismatch analysis and sequencing of the *rrnC* region determined that indeed some of the P1(CAG18051) x C65 transductants contained tagged mutant *rrnC* operon (data not shown). Next, a P1 bacteriophage lysate was generated on one of the transductants with a tagged mutant *rrnC* operon and used to transduce wild type strain TA516. Once again, transductants were selected on the basis of the Tn*10* antibiotic marker and analyzed for the presence of *rrnC* mutations by CELI analysis and sequencing (data not shown). In this way *rrnC* mutations from C65 mutant were transferred onto the chromosome of TA516 strain and could be analyzed for their effect on processing of *daa* transcript. S1 nuclease protection analysis revealed that the presence of tagged *rrnC* mutations alone on the chromosome of TA516 had no effect on the processing of *daa* mRNA, since the *daa* transcript was cleaved at wild type levels in this strain (Figure 5.7). These data suggest that all three *rrnC* mutations on the chromosome of TA516 do not cause a defect in the processing of the *daa* mRNA.

Ribotyping analysis of TA516 and FACS-isolated mutants.

One possible explanation for the *rrnC* mutation data is that the mutants isolated by FACS did not arise from TA516 strain, but that during cell sorting contaminants were selected. To test this hypothesis Southern blot analysis of *rrn* operons was performed on TA516 strain used for mutagenesis, mutants isolated by FACS and a donor strain S17.1 from conjugation experiments. This analysis was done according to the methods of Asai

Figure 5.7 – *rrnC* mutations in isolation do not result in a *daa* mRNA processing defect.

S1 nuclease protection analysis was performed as described in the legend to Figure 3.1. RNA was isolated from TA516 harboring pVT123 (WT) or pVT124 (G49A), C65 and four isolates of TA516 into which the *rrnC* mutations were introduced by bacteriophage P1 transduction. RNA-probe hybrids were digested with 90, 50 and 10 units of S1 nuclease and separated on an acrylamide gel. P, precursor RNA; C, cleaved product.
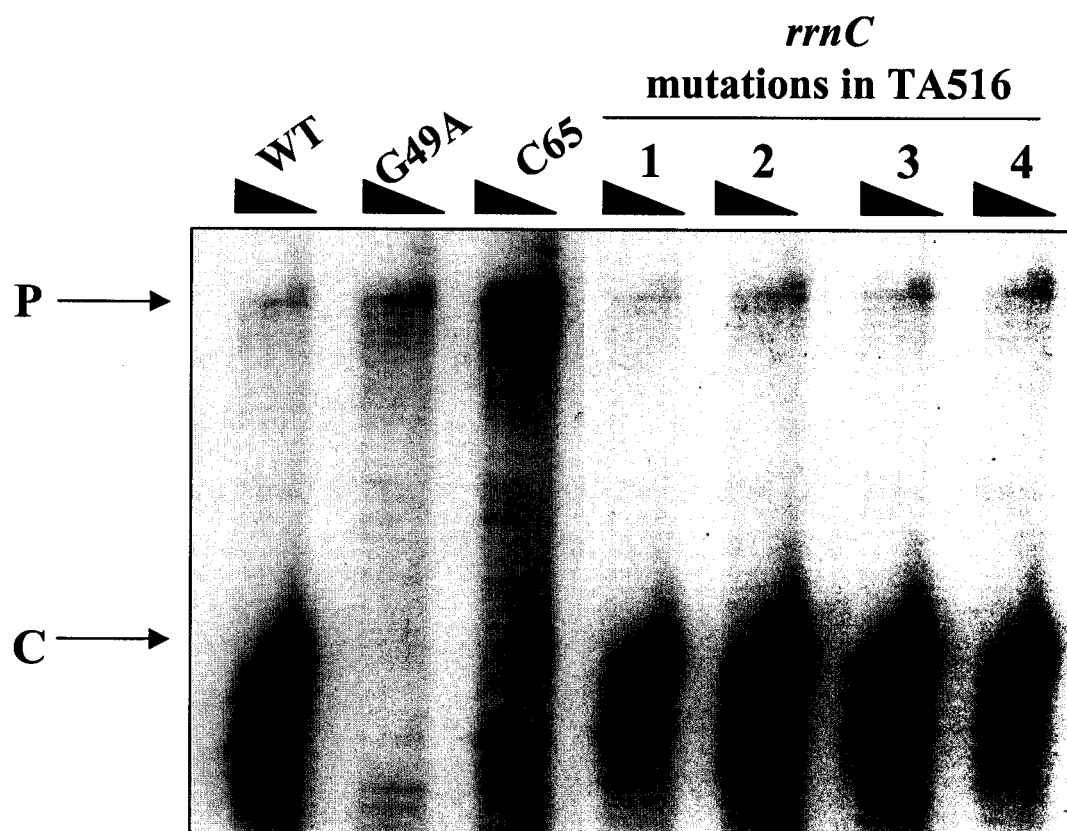
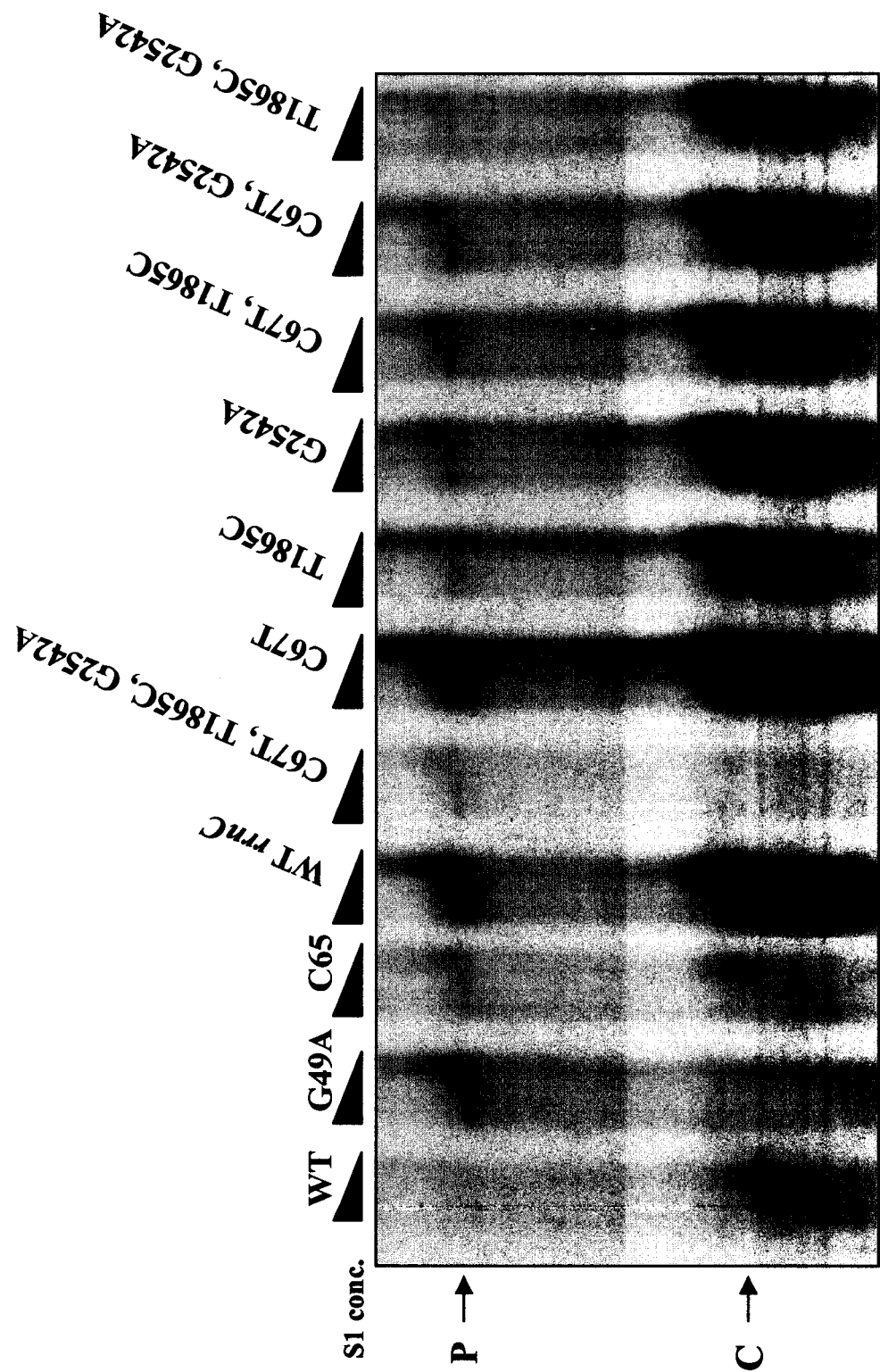*et al.* (9). The schematic diagram of an *rrn* operon is shown in Figure 5.8A and the 16S

and 23S rRNA probes are indicated (Probe I and II, respectively). Control strain in these

experiments was S17.1 and the same strain transformed with pVT123. Analysis of S17.1

with bothe probes shows presence of all seven *rrn* operons and no additional bands

(Figure 5.8B, lanes 6 and 7).

The ribotyping analysis revealed that TA516 band pattern is different than what

was observed by Asai *et al.* (9). There are additional bands present in blots hybridized

with both Probe I and II (Figure 5.8B, lane 1). In the blot with Probe II, in addition to

rrnC and the remnant of *rrnG* bands, a band that runs at the level of *rrnB* operon and a

smaller size fragment (~1 kb) are visible. In the blot with Probe I, TA516 appears to

contain *rrnC* and a doublet that migrates at the level of *rrnB* and *rrnA* in addition to the

small size fragment of ~1 kb.

Analysis of the *rrn* operons present in the FACS-isolated mutants C65, C47, C67

and D19 suggests that they have arisen from TA516, but have restored some of the *rrn*

operons (Figure 5.8B, lanes 2-5). C65 appears to have restored *rrnE* and *rrnD*, while

C47, C67 and D19 isolates appear to have restored *rrnE*. The restoration of *rrnD* operon

by C65 was confirmed by the ability of this isolate to grow on chloramphenicol (*rrnD*

was disrupted by a chloramphenicol resistance gene). Mutant isolates that only restored

rrnE are unable to grow on media containing chloramphenicol. These data indicate that

there was genetic instability of TA516 during or after mutagenesis that resulted in

recombination events and restored some of the *rrn* operons.

Figure 5.8 – Ribotyping analysis of TA516 and mutants isolated by FACS.

A) Schematic diagram of an *rrn* operon with 16S and 23S rRNA porbes indicated as Probe I and Probe II, respectively. This panel of the figure was generated based on a figure from Asai *et al.* (9).

B) Southern blot analysis of *rrn* operons from TA516 and FACS-isolated mutants C65, C47, C67 and D19. Analysis was performed as described in Materials and methods. *rrn* operons are labeled according to Asai *et al.* reference (9). The ~1 kb fragment visible in hybridization of TA516 and mutant strains and not in control *E. coli* K12 was not observed in the Asai *et al.* study (9). Lane 1, TA516; lane 2, C65; lane 3, C47; lane 4, C67; lane 5, D19; lane 6, S17.1 (control strain; used as donor in conjugation experiments); lane 7, S17.1 transformed with pVT123.

A

SacI SmaI SalI SmaI | HpaI EcoRI SalI SacII AluI
16 S | 23S | 5S
Probe I | Probe II

B **Probe I**

1 2 3 4 5 6 7

rrnC
rrnG

rrnE
rrnH

rrnD
rrnB
rrnA

← ~1kb

Probe II

1 2 3 4 5 6 7

rrnC
rrnG

← remnant of rrnG

rrnE
rrnH

rrnD

rrnB
rrnA

← ~1kb
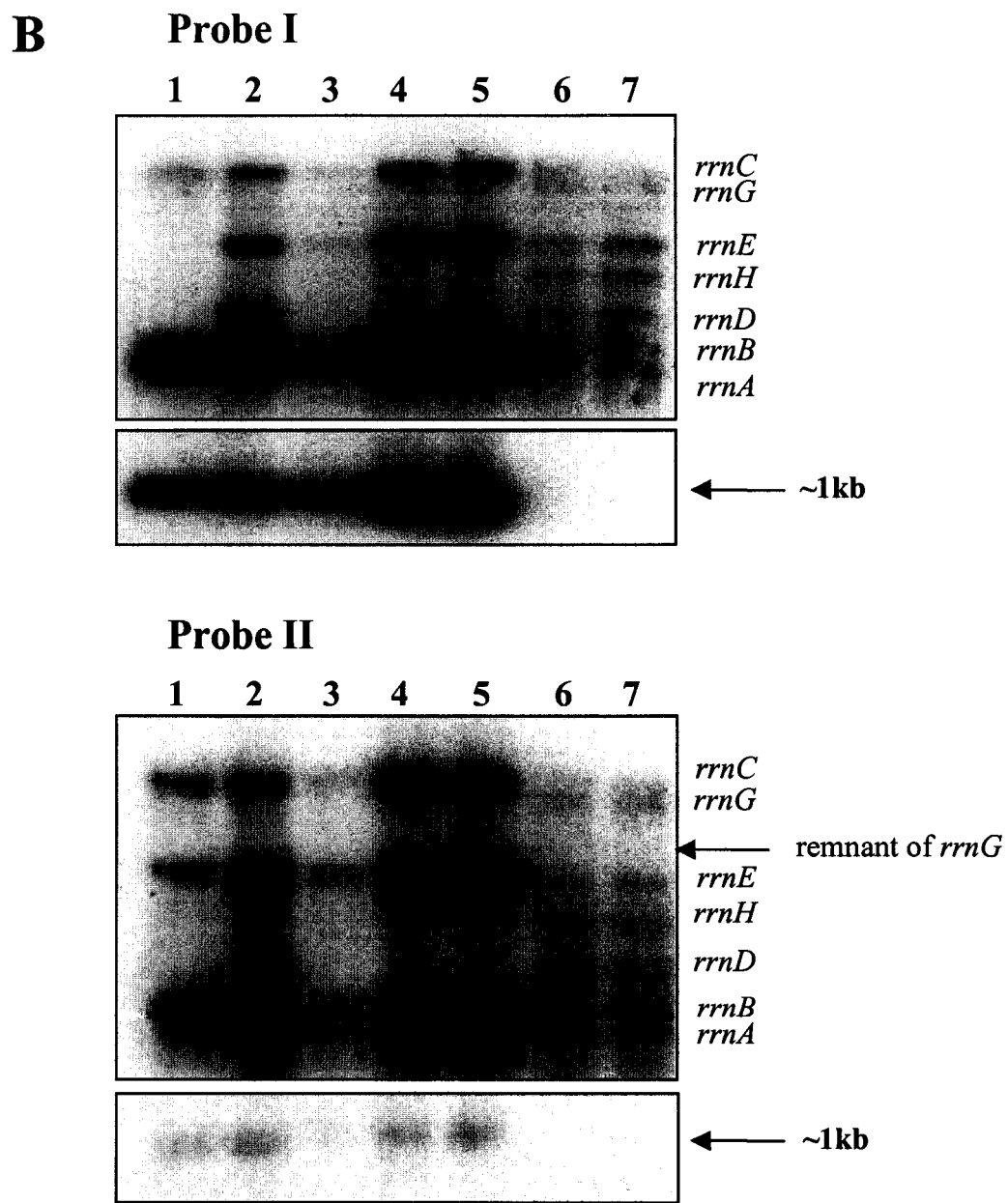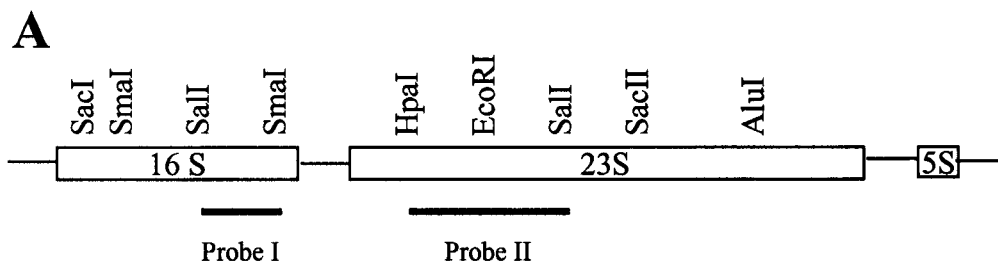
Hfr mapping strategy.

For the initial mapping of mutations, an Hfr mapping set of seven strains (Table 2.1; Figure 5.9A) was employed (186). In these strains, transposon Tn*10* is inserted approximately 20 minutes (min) away from the origin of transfer of each Hfr. These Hfr strains were used as donors and mutant C65 was the recipient in interrupted mating experiments. After selection of transconjugants based on the Tn*10* selectable marker, transconjugants were screened for processing of *daa* mRNA by analyzing GFP levels in a fluorimeter. When a recombination event has occurred resulting in restoration of the processing defect, transconjugants will have low GFP levels. One hundred transconjugants from each of the seven matings were analyzed. We found that 20% of the transconjugants from the mating with CAG5054 Hfr had consistently low levels of GFP. S1 nuclease protection analysis confirmed that in these transconjugants, *daa* mRNA was processed at the level of the wild type (Figure 5.9B, lane 4). Control experiments determined that the transconjugants (CAG5054 x C65) with high GFP levels still had the processing defect as expected (Figure 5.9B, lane 5). In mating C65 with Hfr strains CAG5051 and CAG8160, only 3% and 5% of transconjugants showed low GFP levels respectively, and in only one of the transconjugants from each of those matings was processing restored (data not shown). Because there were so few transconjugants from the matings of C65 with CAG5051 and CAG8160 that had low GFP level correlating with the correct processing phenotype, regions of the chromosome spanned by these two Hfr strains were not analyzed further. CAG5054 Hfr has the origin of transfer at approximately 45 min on the chromosome and the Tn*10* insertion at approximately 25

Figure 5.9 – Hfr mapping of processing deficient mutants.

A) Set of seven Hfr strains used for the initial mapping of mutants isolated in the genetic screen. The approximate origin of transfer for each Hfr is shown with a bar and the arrow indicates the direction of transfer. The bars near the arrow-head indicate the position of Tn*10* transposon insertion. 1, CAG5051; 2, CAG5052; 3, CAG5053; 4, CAG5054; 5, CAG5055; 6, CAG8209; 7, CAG 8160. The figure was reproduced from Singer *et al.* (186).

B) Processing of *daa* mRNA in transconjugants (CAG5054 x C65) with low and high GFP levels. S1 nuclease protection analysis was performed as described in the legend to Figure 3.1. RNA was isolated from wild type strain (TA516 with pVT123, lane 1), G49A control strain (TA516 with pVT124, lane 2), C65 mutant (lane 3), and from transconjugants with low GFP (lane 4) and high GFP (lane 5) as measured by fluorimeter. RNA-probe hybrids were digested with 90, 50 and 10 units of S1 nuclease (triangles) and separated on an acrylamide gel. U, undigested probe; P, precursor RNA; C, cleaved product.

A
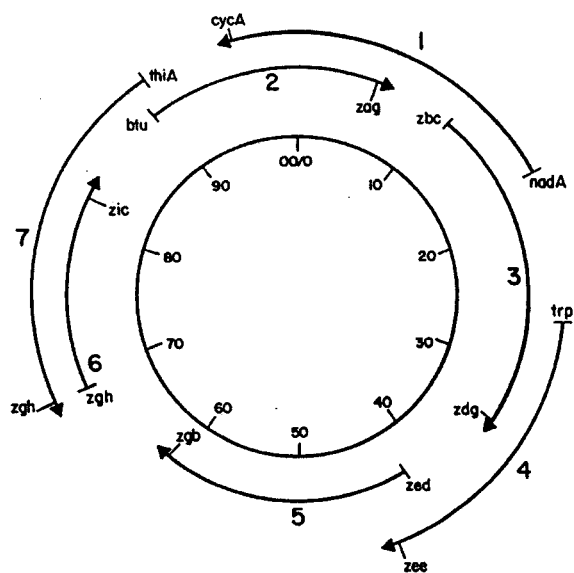
B
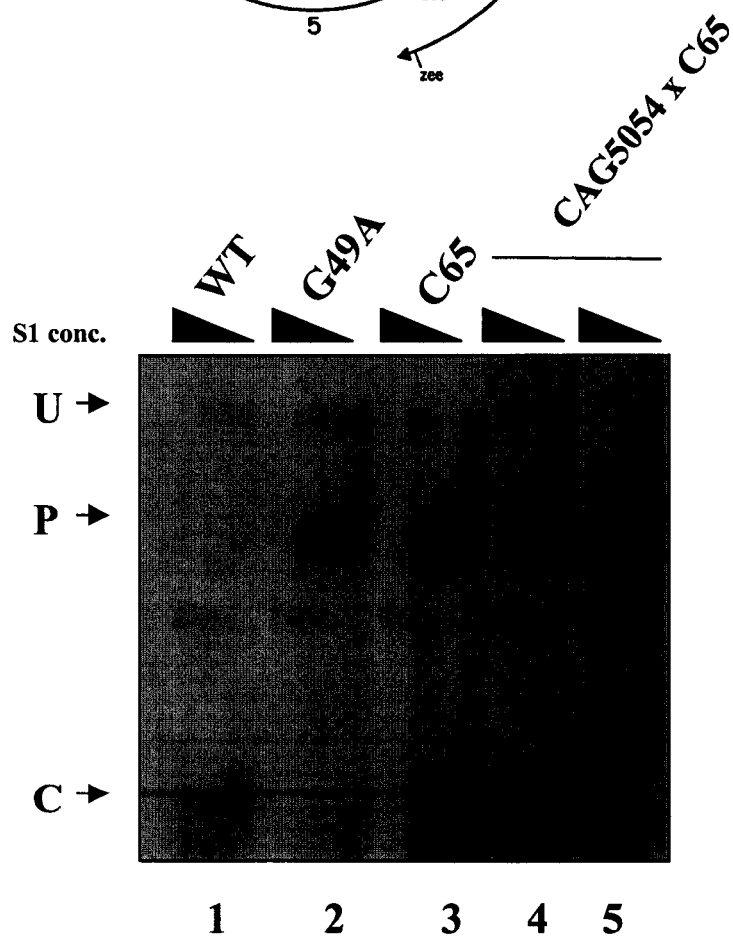
min on the chromosome. Since no transconjugants with low GFP levels were found

using the two Hfr strains that have overlapping regions with CAG5054, i.e. CAG5053

and CAG5055, this suggested that the region of the *E. coli* chromosome in which

recombination results in restoration of the processing defect is between 30 and 40

minutes.

P1 transduction mapping.

To further pinpoint the location of the mutation responsible for the *daa* mRNA

processing defect, a set of P1 mapping strains was utilized (Figure 5.10) (139). These

strains contain Tn*10* insertions at approximately every minute of the *E. coli* chromosome.

Four strains, CAG12179 (map position 30.2 min), CAG18640 (map position 30.9 min),

CAG12026 (map position 32.2 min) and CAG18461 (map position 33.1 min), were used

to generate P1 bacteriophage lysates. P1 transduction was then performed with mutant

C65 as a recipient. The transductants were screened for low GFP levels and restoration

of *daa* mRNA processing. One hundred transductants from each of four experiments

were analyzed. Approximately 30% of transductants generated with the P1 lysate from

CAG12026 and approximately 10% of transductants generated with P1 lysate from

CAG18461 showed low GFP levels. S1 nuclease protection analysis confirmed that

transductants with low GFP level had been restored for *daa* mRNA processing (Figure

5.11, lanes 4 and 6) and that transductants with high GFP levels were still unable to

cleave *daa* mRNA efficiently (Figure 5.11, lanes 5 and 7). None of the transductants

generated with P1 lysates from CAG12179 and CAG18640 strains showed low GFP

Figure 5.10 – A collection of *E. coli* strains with Tn*10* insertions located at approximately

1-min intervals around the chromosome.

Positions of Tn*10* insertions are indicated on the *E. coli* map. Shown for each strain are

its designation, the gene or open reading frame disrupted by the insertion, and the base

pair position. Numbering on the inside of the circle is in minutes. The bracket

corresponds to the region identified in which recombination results in restoration of *daa*

mRNA processing defect (by Hfr mapping). This figure was reproduced from Nichols *et

al.* (139).

E. coli
4,639,221 bp

CAG18442 thrA 425
CAG12093 carB 33,963
CAG12095 leuO 84,350
CAG12025 yadC 150,100
CAG18436 yafC 230,099
CAG18447 proA 261,288
CAG18439 lacI 365,945
CAG12080 b0349 371,180
CAG18091 b0374 393,633
CAG12148 tsx 430,667
CAG12017 b0441 461,486
CAG12154 gsk 500,025
CAG12171 purK 551,279
CAG12149 b0604 637,765
CAG12077 ybeG 655,952
CAG18433 asnB 698,404
CAG12147 nadA 781,532
CAG18493 ig, b0786-b0787 819,871
CAG12034 potf 897,129
CAG18478 ig, ycaD-b0898 946,252
CAG12094 b0940 1,000,952
CAG18486 yccE 1,064,111
CAG12078 yceG 1,154,216
CAG18463 b1160 1,211,084
CAG18497 fadR 1,234,734
CAG12016 ig, kdsA-cha 1,269,233
CAG12169 oppC 1,302,475
CAG18455 trpC 1,317,596
CAG12028 b1309 1,368,905
CAG12179 ydeH 1,399,003
CAG12061 recT 1,412,228
CAG18640 b1377 1,434,058
CAG12026 trg 1,491,930
CAG18461 yddE 1,533,652
CAG12151 ig, b1696-b1696 1,776,386
CAG18464 b1754 1,834,488
CAG18465 b1785 1,869,535
CAG12068 ig, b1820-b1821 1,903,614
CAG18488 eda 1,930,416
CAG12156 uvrC 1,991,244
CAG18451 b1972 2,038,762
CAG12099 ig, yeeF-b2015 2,085,192
CAG12163 galZ 2,173,967
CAG12021 galY 2,175,213
CAG12098 napA 2,299,610
CAG12177 sloS 2,318,294
CAG12178 ylaL 2,341,772
CAG18484 b2274 2,387,022
CAG18467 ig, b2374-b2375 2,491,451
CAG18468 nupC 2,511,317
CAG18470 purC 2,595,619
CAG18481 b2536 2,665,159
CAG18480 nadB 2,708,518
CAG12158 pheA 2,736,076
CAG18642 artD 2,826,375
CAG12173 cysI 2,888,785
CAG12079 fucP 2,932,865
CAG12135 recD 2,948,961
CAG12168 speA 3,082,773
CAG18472 nupG 3,104,395
CAG18475 metC 3,150,485
CAG12184 tolC 3,176,389
CAG12152 alr 3,215,934
CAG12072 nlp 3,332,800
CAG12153 b3219 3,364,914
CAG12075 acrF 3,412,834
CAG12071 smg 3,429,813
CAG18456 yhfT 3,503,687
CAG18638 glgP 3,564,175
CAG18450 ig, ugpB-livF 3,590,125
CAG18492 ig, gltS-yicE 3,826,553
CAG18452 nlpA 3,837,058
CAG18499 ig, ykfW-ykfX 3,873,001
CAG18501 rbsD 3,931,475
CAG18431 ilvD 3,952,161
CAG18491 ig, metR-metE 4,010,549
CAG18496 fadA 4,025,408
CAG18495 b3872 4,063,253
CAG18477 pfID 4,143,393
CAG12165 argE 4,151,734
CAG18500 thiC 4,192,143
CAG12164 melR 4,241,898
CAG18427 yjcS 4,303,986
CAG18488 cadB 4,356,936
CAG12073 cycA 4,427,714
CAG12019 ytfN 4,442,377
CAG18462 chpS 4,446,109
CAG18430 mdoB 4,595,002

Figure 5.11 – Processing of *daa* mRNA in transductants (P1(CAG12026) x C65,

P1(CAG18461) x C65) with low and high GFP levels.

S1 nuclease protection analysis was performed as described in the legend to Figure 3.1.

RNA was isolated from control strains (wild type, lane 1; G49A, lane 2; C65 mutant, lane

3) and transductants with low (lanes 4 and 6) and high (lanes 5 and 7) GFP levels. Probe-

RNA hybrids were digested with 90, 50 and 10 units of S1 nuclease (triangles) and

separated on an acrylamide gel. U, undigested probe; P, precursor RNA; C, cleaved

product.
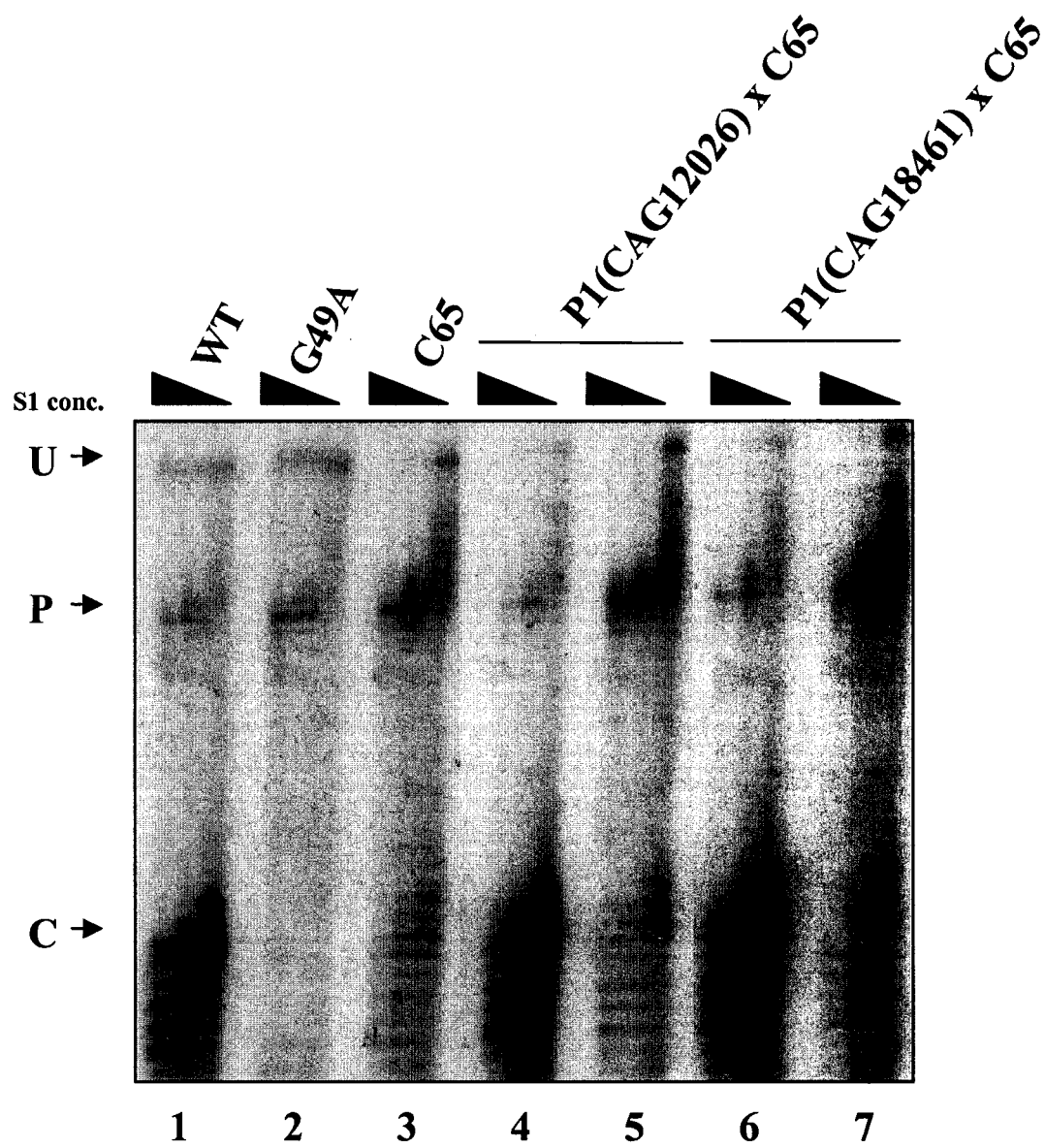
levels. These experiments mapped the mutation responsible for the *daa* processing defect

between 32 and 33 min on the *E. coli* chromosome.

A putative DEAH-box RNA helicase, HrpA, is involved in processing of the *daa* mRNA.

Examination of the sequence for the region of the *E. coli* chromosome around 32

min in GenBank (22) revealed a potentially relevant gene, *hrpA*. Moriya *et al.* identified

this gene during the course of systematic nucleotide sequence analysis of the *terC* region

of the *E. coli* K-12 chromosome (129). The product of *hrpA* was found to have a high

degree of sequence similarity to the products of *PRP2*, *PRP16* and *PRP22* of

Saccharomyces cerevisiae (129). The products of the yeast genes are members of the

DEAH-box RNA helicase family and are involved in RNA splicing (172).

To determine whether *hrpA* is involved in the processing of *daa* transcript we first

attempted to amplify this gene from the chromosomal DNA of the wt strain and from the

genome of the mutant C65. Using *hrpA* specific primers, a ~5kb fragment was amplified

from the wt strain but not from the mutant deficient in processing (Figure 5.12A). PCR

amplification using chromosomal DNA from transductants with restored processing of

daa mRNA (P1(CAG12026) x C65, P1(CAG18461) x C65) also resulted in the correct

size fragment, while no amplicon was present when chromosomal DNA of transductants

deficient in processing was used. The presence of *hrpA* was also examined by Southern

blotting (Figure 5.12B). An *hrpA* specific probe was used to screen a hybridization blot

containing chromosomal DNA from wt, C65 mutant and C65 transductants with wt and

mutant processing. This analysis confirmed that *hrpA* is present in the wt strain and

Figure 5.12 – *hrpA* is deleted from the mutants defective in processing of *daa* mRNA.

A) PCR analysis of *hrpA*. *hrpA* specific primers VTK92 and VTK93 (Table 2.2) were used to amplify ~5kb product from strains with wild type and mutant processing of the *daa* mRNA. Lane 1, TA516 strain; lane 2, C65 mutant; lanes 3 and 4, transductants P1(CAG12026) x C65 (lane 3, transductant with wild type processing; lane 4, transductant with mutant processing); lanes 5 and 6, transductants P1(CAG18461) x C65 (lane 5, transductant with wild type processing; lane 6, transductant with mutant processing).

B) Southern blot analysis of *hrpA* in strains with wild type and mutant processing. Genomic DNA, isolated from same strains as used in A, was digested with restriction endonucleases *Eco*RI (E) and *Bam*HI (B). Blots were hybridized with an *hrpA*-specific probe (VTK92 + 93 PCR fragment amplified from TA516 strain).
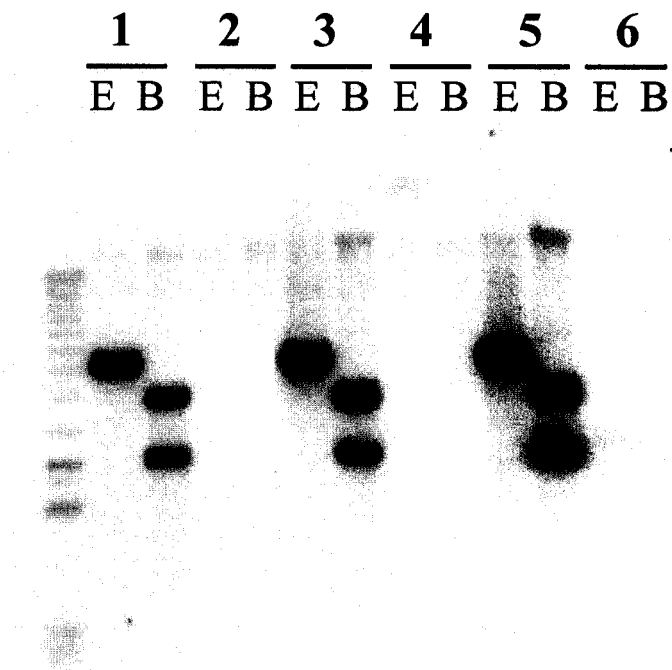
transductants in which processing of *daa* transcript occurs at wt levels, and the gene is absent from the mutant defective in processing as well as from transductants with the processing defect. These results suggest that the product of *hrpA* is involved in *daa* mRNA cleavage. Preliminary PCR analysis has determined that the size of the *hrpA* deletion in the mutant deficient in processing is larger than 16kb (data not shown), but the exact size of the deletion was not determined.

Since the deletion of *hrpA* in the mutant deficient in processing is larger than the size of the gene alone, it is possible that additional gene products present in the deleted region are also involved in processing of *daa* mRNA. To determine if the *hrpA* product would be sufficient to restore processing in the mutant, a ~5kb fragment containing only *hrpA* and its Shine-Dalgarno sequence was inserted into pACYC184, generating plasmid pVT148. This construct was introduced into both the wild type strain and the C65 mutant. S1 nuclease protection analysis of *daa* mRNA transcript cleavage in these strains demonstrated that the presence of *hrpA* alone on a plasmid restored processing in the mutant (Figure 5.13). The presence of pACYC184 alone had no effect on processing (data not shown).

Mutant C65 was selected after chemical mutagenesis and may have acquired additional undefined mutations that could have contributed to the *hrpA*-associated processing defect. We therefore obtained a strain from Dr. K. Isono (129) containing a disrupted allele of *hrpA* and presumably no other mutations on the chromosome. S1 nuclease protection analysis of *daa* mRNA processing in this *hrpA* mutant strain revealed that it has the same processing defect as the mutant isolated by FACS (Figure 5.14).

Figure 5.13 – The DEAH-box RNA helicase HrpA is involved in processing of *daa*

mRNA.

S1 nuclease protection analysis was performed as described in the legend to Figure 3.1.

RNA was isolated form wild type strain carrying plasmids pVT123 (WT) and pVT124

(G49A) and from the mutant C65, as well as from the same strains complemented with a

plasmid encoding *hrpA*, pVT148. RNA probe-hybrids were digested with 90, 50 and 10

units of S1 nuclease (triangles) and resolved on an acrylamide gel. P, precursor RNA; C,

cleaved product.
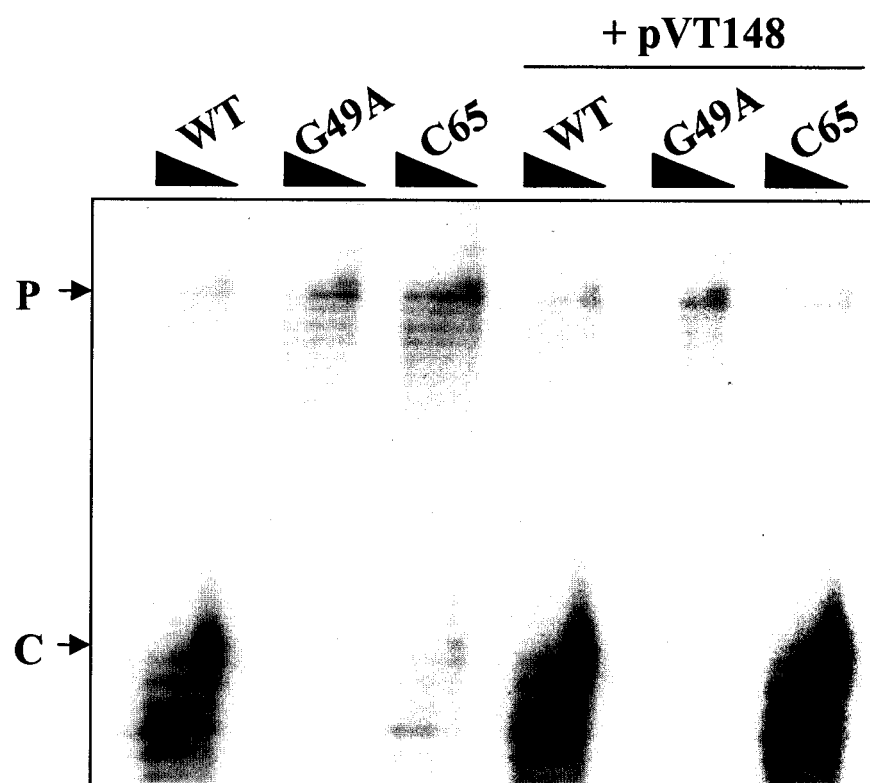
Figure 5.14 – Processing of *daa* mRNA in the *hrpA* deletion strain.

S1 nuclease protection analysis was performed as described in the legend to Figure 3.1.

RNA was isolated from MC1061 strain carrying plasmids pVT123 (WT) and pVT124

(G49A), MC1061ΔhrpA strain carrying plasmid pVT123, and the MC1061ΔhrpA strain

complemented with *hrpA* plasmid pVT148.
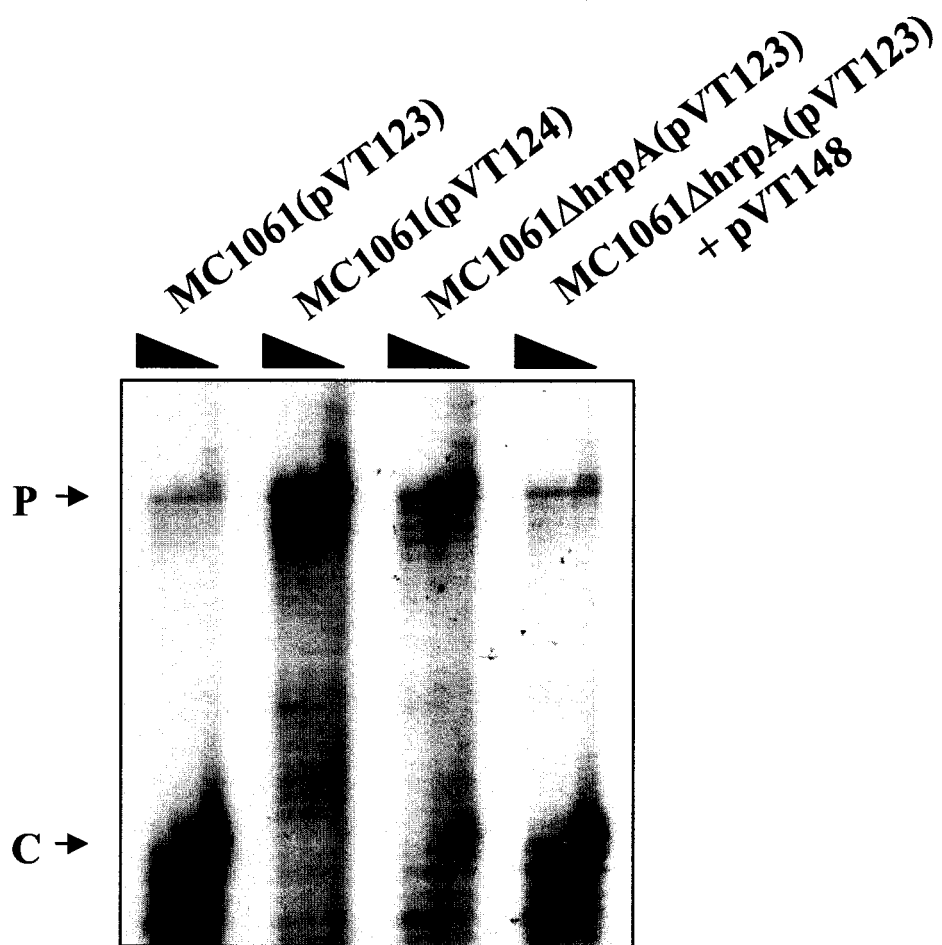
Providing the wild type copy of *hrpA* gene on the pVT148 plasmid complemented the processing defect in the *hrpA* mutant strain to the same extent as in the FACS-isolated mutant. These data suggest that the *hrpA* gene product facilitates cleavage of the *daa* transcript.

A DEAD-box RNA helicase SrmB is not involved in the processing of *daa* mRNA.

In addition to DEAH-box RNA helicases, the related DEAD-box proteins are also members of the large family of putative RNA helicases. The DEAD-box proteins contain the D-E-A-D instead of D-E-A-H motif that gives them their names (106). There are five genes encoding DEAD-box proteins in *E. coli*: *rhlB*, *csdA*, *dbpA*, *rhlE*, and *srmB*. Apart from the *rhlB* gene product that encodes an RNA helicase component of the degradosome (40, 161), the only other gene product from this family with ascribed function is *srmB*. The gene product of *srmB* is a helicase involved in an early step of the assembly of the large ribosomal subunit (47).

To test the hypothesis that any RNA helicase of DEAD/H-box family might be involved in the processing of the *daa* mRNA, we examined the effect of an *srmB* mutation on *daa* mRNA cleavage. An *srmB* deletion mutant and an isogenic wild type strain WJW45 were transformed with plasmids pVT123 and pVT124, and processing of *daa* mRNA in these strains was examined by S1 nuclease protection analysis. Processing was not affected by deletion of the *srmB* gene (Figure 5.15), suggesting that this RNA helicase is not involved in the *daa* transcript cleavage.

Figure 5.15 – The DEAD-box RNA helicase SrmB is not involved in processing of *daa* mRNA.

S1 nuclease protection analysis was performed as described in the legend to Figure 3.1 using RNA isolated from strains WJW45 and WJW45ΔsrmB, carrying pVT123 (WT) or pVT124 (G49A) as indicated. RNA-probe hybrids were digested with 50 and 10 units of S1 nuclease (triangles) and separated on acrylamide gel. The arrows indicated precursor RNA (P) and cleaved product (C).
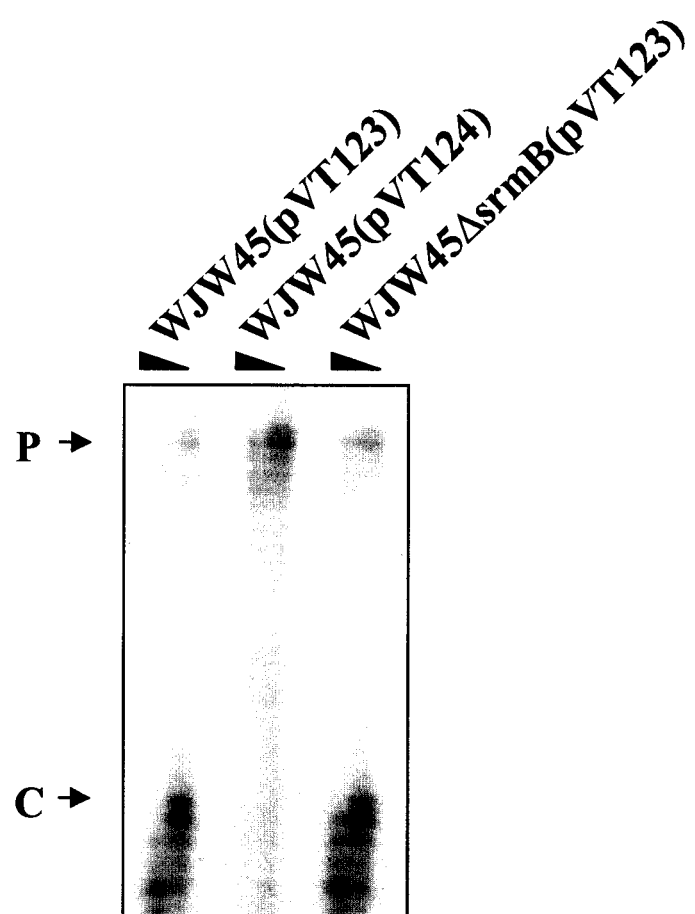
Site-directed mutagenesis of *hrpA*.

The *hrpA* gene product shares sequence similarity with the proteins encoded by the yeast DEAH family genes, *PRP2, PRP16* and *PRP22* (Moriya *et al.*, 1995, Figure 5.16). DEAH family proteins are characterized by the presence of seven to nine conserved sequence motifs (197). These motifs are thought to constitute a component of the active site for nucleic acid-dependent nucleotide triphosphate (NTP) binding and hydrolysis, which is presumably used in the unwinding of dsRNA. All three yeast homologs of HrpA have been shown to possess RNA-dependent ATPase activity (94, 180, 181). Mutational analysis of the yeast proteins Prp16 and Prp22 has revealed that specific residues within conserved motifs I (GETGSGKT), II (DEAH), and VI (QRXGRXGR) are required for their biological activity in pre-mRNA splicing (82, 178). To determine whether the same critical residues within motifs I, II and VI are important for the function of the *hrpA* gene product in the processing of *daa* mRNA, we used site-directed mutagenesis to change these residues to alanine. A plasmid containing wild type *hrpA*, pVT148, was mutagenized and the mutant plasmids were introduced into the mutant deficient in processing of *daa* mRNA (mutant C65). S1 nuclease protection analysis was used to determine whether the mutant *hrpA* plasmids could complement the processing defect.

In motif I, conserved residues G100, G105, K106 and T107 were changed to an alanine. Alanine substitution at the G100 equivalent in Prp16 (G373) had no effect on the function of the yeast protein, while the alanine substitutions at positions equivalent to G105, K106 and T107 (G378, K379 and T380 in Prp16) abolished the function of the

Figure 5.16 – An alignment of HrpA protein sequence with the sequences of yeast splicing factors Prp2, Prp16 and Prp22.

The conserved motifs I, II and VI of DEAH-box RNA helicases are shown in the same order. The alignment was

generated using MACAW alignment utility, version 2.0.5. Filled boxes indicate regions of homology as predicted

by MACAW version 2.0.5. The numbering of the amino acids in HrpA is based on the GenBank entry GI33347548.

asterisk indicates alanine substitutions (see Figure 5.17) in HrpA that could not complement the *daa* mRNA processing

defect of C65 mutant, while the circles indicate alanine substitutions in HrpA that function in the same way as the wild

type HrpA.

HrpA

Prp2

Prp16

Prp22

100 GETGSGKTTQ 110
GETGSGKTTQ
GETGSGKTTQ
GETGSGKTTQ
○ ***
I

197 DEAH 200
DEAH
DEAH
DEAH
** ○
II

395 QRKGRCGRVSEG 406
QRaGRaGRVgpG
QRsGRaGRtapG
QRKGRaGRtgpG
** ** ** *
VI

89
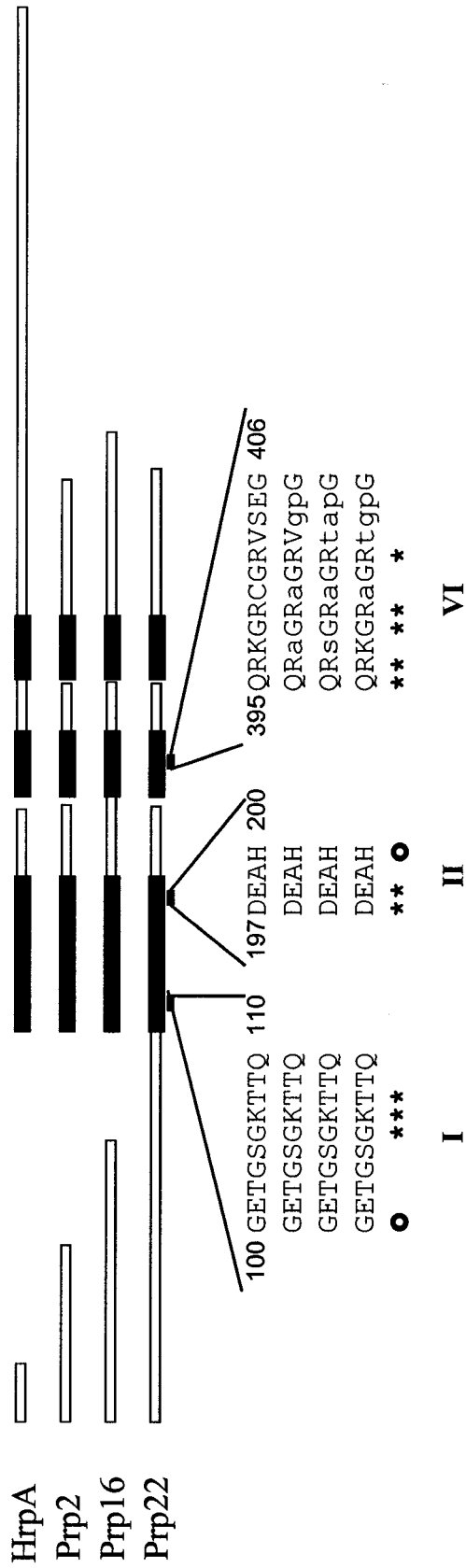
Figure 5.17– Site-directed mutagenesis of HrpA.

S1 nuclease protection analysis was performed as described in the legend to Figure 3.1. RNA was isolated from the wild

type strain harboring plasmids pVT123 (WT) or pVT124 (G49A), from the mutant C65, and mutant C65 transformed

with *hrpA*-encoding plasmids pVT148 (wild type *hrpA*), pVT150-162 (Table 2.3). RNA-probe hybrids were digested

with 10 units of S1 nuclease and were separated on an acrylamide gel. The results of S1 nuclease protection assays were

analyzed using PhosphorImager and ImageQuant software. P, precursor RNA; C, cleaved product.

	WT	G49A	C65	C65 + pVT148	G100A	G105A	K106A	T107A	D197A	E198A	H200A	Q395A	R396A	G398A	R399A	R402A	Δ(Q463-E1295)
P (% total)	4	100	60	10	10	65	53	44	48	56	12	46	37	38	42	51	80
C (% total)	96	0	40	90	90	35	47	56	52	44	88	54	63	62	58	49	20
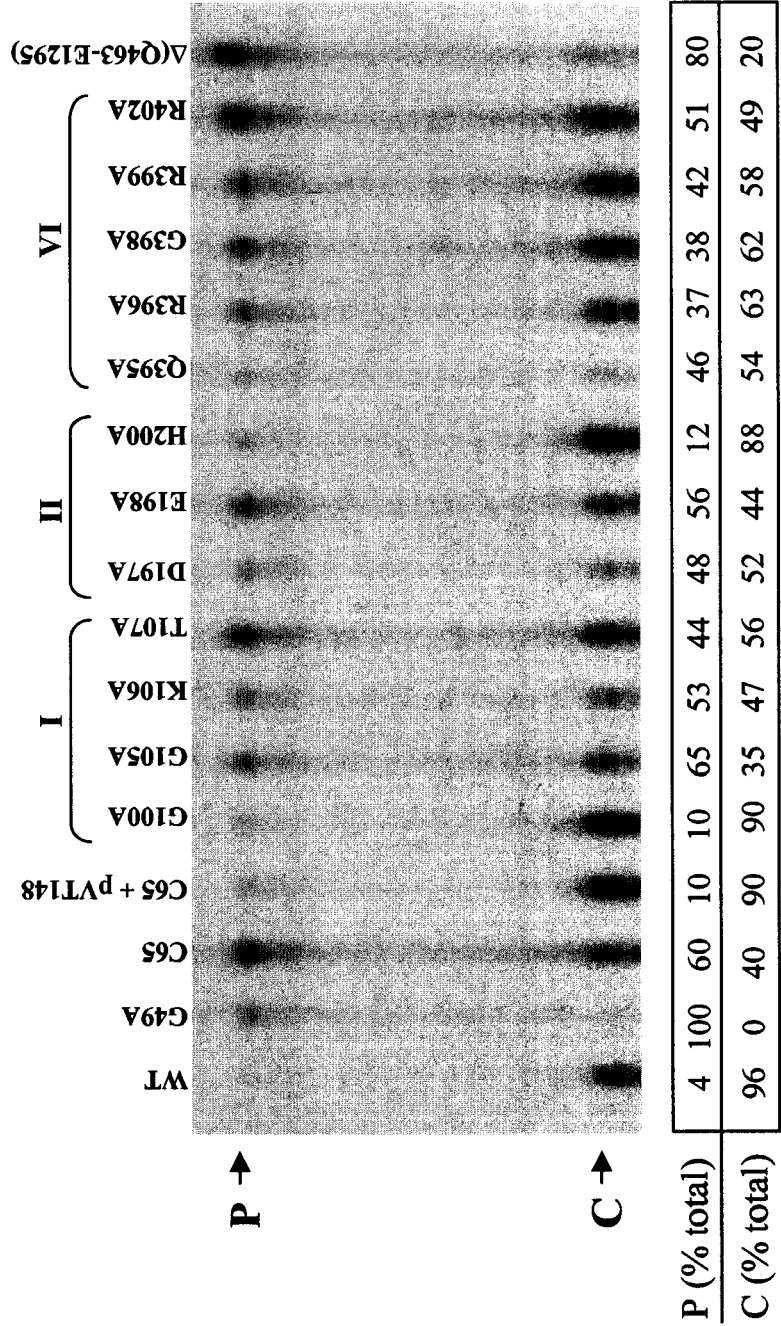
protein. S1 nuclease analysis revealed that pVT161 (with G100A HrpA) could restore

the processing defect of mutant C65, while the presence of pVT150 (G105A HrpA),

pVT151 (K106A HrpA) and pVT152 (T107A HrpA) could not complement the

processing defect (Figure 5.17). In motif II, conserved residues D197, E198 and H200

were mutated to an alanine. The H200 equivalent alanine substitution in Prp16 (H476)

had no effect on the function of the yeast protein in RNA splicing, while the D197 and

E198 equivalents (D473 and E474 in Prp16) abrogated the function of the protein. The

ability of the HrpA mutants in motif II to complement the *daa* mRNA cleavage defect

was similar to that observed with the mutants in motif I. Namely, plasmids encoding

D197A (pVT153) and E198A (pVT154) could not restore processing of the C65 mutant

to wt, while the plasmid encoding H200A (pVT162) could (Figure 5.17), paralleling the

observations with the yeast homolog Prp16. Finally, in motif VI, residues Q395, R396,

G398, R399 and R402 (corresponding to Prp16 residues Q685, R686, G688, R689, and

R692) were changed to an alanine. Plasmids encoding these mutant HrpA residues,

pVT155-159, were unable to complement the defect present in the C65 mutant (Figure

5.17). The corresponding changes in the yeast protein Prp16 abolished its function in

pre-mRNA splicing (82, 178).

The region of the HrpA protein with the highest homology to the conserved

motifs in DEAH-box RNA helicases is located in the N-terminal region of the protein.

The C-terminal portion of HrpA is much longer than its yeast homologs and shows no

significant sequence similarity to other proteins in the database (Figure 5.16). It is

possible that this portion of the HrpA protein, in addition to the conserved motifs, might

also be required for the function of HrpA in the cleavage of *daa* mRNA. To test this hypothesis we generated an in-frame C-terminal deletion of the HrpA protein (ΔQ463-E1295) on a plasmid and used it to complement the C65 mutant. S1 nuclease protection analysis revealed that HrpA encoded on the plasmid pVT160 could not restore the processing defect in the mutant (Figure 5.17). This evidence suggests that despite the presence of intact helicase motifs I-VI, the C-terminal domain of the HrpA protein is essential for its function in the cleavage of the *daa* transcript.

Discussion

Endonucleolytic cleavage of mRNA in the operon encoding F1845 fimbriae is independent of factors known to process mRNA in *E. coli* ((27); also see Chapter 3). In this chapter I presented identification of a putative RNA helicase from the DEAH-box family, HrpA, as an important component of the *daa* mRNA cleavage event. In addition to the mutant selected for in our screening of chemically mutagenized *E. coli* a strain with a defined mutation in *hrpA* alone was unable to efficiently process *daa* mRNA, and both mutants could be complemented with an *hrpA*-encoding plasmid (Figures 5.13 and 5.14). The MC1061 background strain of this *hrpA* mutant is significantly different from the strain TA516 used in our mutagenesis scheme in that it had a full complement of rRNA operons. This strain difference, however, could not account for the processing defect we observed since a sole mutation in *hrpA* was sufficient to cause inefficient cleavage of the *daa* mRNA. These data argue against the involvement of additional undefined mutations in the processing defect in our FACS-selected mutant.

The genetic screen presented here was not exhaustive in that only a single mutant was identified, and additional protein/RNA factors may be required for the processing of the *daa* transcript. In addition, no mutants were found which completely abolished processing. It is possible that a factor essential for viability might also be involved in this process. Based on our previous observations that *daa* mRNA processing depends on translation of DaaP, we hypothesized that a factor essential for processing may be a component of the ribosome (108).

The mutagen we used, 2-AP, is a base analog of adenine that mispairs with cytosine to cause base-pair substitutions of the transition type (157). The fact that we isolated a large deletion that resulted in the processing defect is somewhat surprising and may simply be a serendipitous event. It suggested, however, that there could be additional point mutations on the chromosome of our mutant that are important for the processing defect that may have exerted pressure during the enrichment sorting to allow for the selection of this large deletion. We conducted mismatch analysis on the mutant, focusing on the regions of the chromosome encoding ribosomal factors, and identified point mutations consistent with 2-AP in the single *rrn* operon. However, we have been unable to demonstrate an association of these mutations with the processing defect (see below). Thus, the genetic screen employed here identified only *hrpA* as the important participant in the *daa* mRNA cleavage. It is possible, though, that the *hrpA* mutation, which does not result in a complete lack of processing, may be compensating for additional undefined mutations.

HrpA shares significant homology with the yeast proteins Prp2, Prp16 and Prp22. Based on the presence of seven to nine conserved motifs (depending on the stringency of sequence alignment) these proteins were assigned to the DEAH-box family of RNA helicases. Members of this protein family have been identified in all organisms, ranging from bacteria and viruses to humans, and are involved in major processes of RNA metabolism, including mRNA synthesis, pre-mRNA splicing, ribosome biogenesis, translation and RNA decay (179). Prp2, Prp16 and Prp22 are components of the large ribonucleoprotein assembly, the spliceosome, and participate in the two distinct transesterification reactions that remove introns from eukaryotic transcripts (34, 48, 54). Prp16 and Prp22 have been shown to function as RNA-dependent ATPases that have the ability to unwind RNA duplexes *in vitro* (210, 212). The region of homology of HrpA with the yeast proteins includes conserved Walker motifs A and B (motifs I and II), which are NTP binding motifs found in a wide variety of NTPase enzymes (211). Prp16 mutations can be divided into two classes based on their ability to affect the ATPase function of the protein *in vitro* or the role of Prp16 in pre-mRNA splicing *in vivo* (82, 178). Since ATPase activity for HrpA has not been reported, we used alanine substitutions of the residues in motifs I and II to test the functional conservation between HrpA and the yeast homologs. Only the *hrpA*-encoding plasmids with alanine substitutions at positions equivalent to the residues in Prp16 that had no effect on the function of the yeast protein could restore the ability of the C65 mutant to cleave *daa* mRNA. Alanine substitutions at HrpA residues that in the yeast homolog Prp16 abolished function were unable to complement *daa* mRNA cleavage defect (Figure 5.17).

This suggests that motifs I and II of HrpA may indeed function in NTP binding and hydrolysis, as is known to occur in Prp16, and that this NTPase activity of HrpA is required for its role in *daa* mRNA processing.

Motif VI of DEAH-box RNA helicases has been implicated in NTP binding/hydrolysis and RNA unwinding. The function of Prp16 *in vivo* was abolished when mutants were generated with alanines at HrpA equivalents of amino acids Q395, R396, G398, R399 and R402 in motif VI (82). However, these mutants suffered a more modest defect in ATPase activity *in vitro* than Prp16 mutants in motifs I and II (178). When we introduced alanines at the above-mentioned residues of HrpA motif VI, the plasmids carrying these substitutions could not complement the processing defect of the mutant to the extent that a wild type HrpA-encoding plasmid could. However, the failure of these strains to process *daa* mRNA was not as drastic as in the original mutant or the motif I and II mutants (Figure 5.17). This implies that if motif VI of HrpA acts analogously to the motif VI of Prp16, a threshold NTPase activity might be required for the function of HrpA in processing, as was proposed for the activity of Prp16, and that the role of motif VI may not be limited to NTP hydrolysis. Our alanine mutagenesis data strongly suggests that HrpA shares not only sequence but also functional similarity with the yeast RNA helicase Prp16. Further structure/function and biochemical analyses are needed to verify the homology.

Many DEAH-box proteins contain domains outside of the conserved helicase motifs that have no homologies to other known proteins and are thought to confer specificity. For instance, the N-terminal domain of yeast protein Prp16 is not required for

its function in pre-mRNA splicing but is proposed to be essential for spliceosome binding (82). From the alignment of protein sequences of HrpA and Prp16 we observed that HrpA has a much longer C-terminal tail (Figure 5.16). The amino acid sequence in this C-terminal half of HrpA shows no significant similarity with any protein sequence in the database. A deletion of the residues Q463-E1295 in HrpA could not alleviate the defect in the processing mutant (Figure 5.17), indicating that the truncated HrpA is not functional in processing of *daa* mRNA. The C terminus of HrpA could thus contain a sequence that is required for the appropriate interaction of this putative helicase with its substrate. Additionally, the non-conserved portion of HrpA could be involved in binding of cofactors that might interact with HrpA to promote substrate recognition and facilitate cleavage of the *daa* transcript. A protein cofactor that potentially binds to the HrpA C-terminal half could act to physically modulate HrpA activity through protein-protein interactions or by recruiting a complex of proteins to the HrpA substrate (184). To fully understand the role of HrpA in *daa* mRNA processing, the factors that interact with this putative RNA helicase must be identified and characterized.

This work presents the first implication of a bacterial DEAH-box RNA helicase in processing of mRNA. How might HrpA function in endonucleolytic cleavage of *daa* mRNA? One possibility is that HrpA acts as an RNA helicase in remodeling of RNA. From previous work we know that in addition to a specific amino acid sequence (Gly-Pro-Pro) downstream of the site of cleavage, there is an RNA structural element upstream of the *daa* mRNA processing site that is required for the correct cleavage of the transcript (108). HrpA might be involved in alteration of this RNA structure so that it is in the

correct conformation to allow cleavage of *daa* mRNA. Our previous work has also alluded to the possibility that the RNA cleavage site could be located within the ribosome or at the edge of the ribosome. Thus HrpA might be involved in modifying the structure of ribosomal RNA that is in the vicinity of the processing site which may possess the catalytic activity necessary for *daa* mRNA cleavage. In recent years, the resolution of atomic structures of the ribosome revealed that rRNA participates in the catalysis of peptide bond formation during translation (16, 141). These studies hint that an acid-base catalytic mechanism might be involved in the endonucleolytic cleavage of *daa* mRNA by the rRNA, provided that rRNA is in the appropriate structural conformation. Although RNA unwinding activity *in vitro* has been demonstrated for some putative RNA helicases, the RNA substrates for most of these proteins have not been identified. The *E. coli* protein DbpA, a member of the DEAD-box RNA helicases, is the only example so far for which the ATP-dependent helicase activity has been stimulated by a specific RNA, namely the loop of hairpin 92 of 23S rRNA (61). Therefore, the exact function of HrpA in the processing of *daa* mRNA will be clarified by characterization of its specific RNA substrate.

HrpA could be involved in *daa* mRNA cleavage through modifying protein-RNA interactions. The function of certain DEAH-box family members has been described as processive and directional molecular motors for unwinding regular RNA duplexes (191). However, in the cell, proteins are able to bind RNA, which complicates the ability of RNA helicases to use these RNAs as templates. Thus a hypothesis has been put forth that DEAH-box RNA helicases might have additional functions to disrupt and rearrange

RNA-protein interactions. Such activity of a DEAH-box protein has been demonstrated

for protein NPH-II from vaccinia virus (85). This kinetically well-characterized helicase

is able to displace RNA-binding protein U1A from its template in an ATP-dependent

fashion. NPH-II remains processive during the displacement of U1A, suggesting that it

might be able to switch back and forth between its RNA helicase and protein

displacement roles. HrpA may perhaps be capable of a similar activity in displacing

proteins from its RNA target and by this cause cleavage of the *daa* mRNA.

It is possible that HrpA could contain both helicase and RNase capabilities.

Eukaryotic protein Dicer, a member of the DECH-box family, is involved in processing

long double-stranded RNA precursors into shorter micro RNAs (miRNAs) and small

interfering RNAs (siRNAs), that play a role in a wide variety of cellular processes (80,

226). The N-terminus of Dicer contains a region of helicase homology, while the RNase

activity of the protein is located in the C-terminus (25). Analogously HrpA could have

both the helicase activity suggested by the motifs I, II and VI in its N-terminus, as well as

an RNA cleaving portion residing in the C-terminal tail.

Finally, based on the sequence and functional similarity of HrpA to yeast proteins

Prp2, Prp16 and Prp22, it is interesting to speculate that the eukaryotic spliceosome

might have its origins in bacteria. Since RNA helicases are often found in large

ribonoucleoprotein complexes, it is possible that HrpA is part of such a large complex as

well. We propose that this large complex in the case of HrpA is the ribosome, and that

bacterial ribosome might have retained the functions of both translation and RNA

turnover, which were separated in the eukaryotes.

Using mismatch analysis and CELI nuclease from celery we identified mutant

residues in the *rrnC* operon of mutant C65 deficient in processing and isolated by FACS.

The mutations identified in this region were the only ones found upon examining >50kb

of sequence that included ribosomal RNA and ribosome associated factors and were

consistent with the type of mutations induced by 2-AP.

The mutant residues in *rrnC* of the C65 mutant identified by CELI analysis are in

very interesting regions of the ribosomal structure. The mutation in the 16S rRNA, C67U,

is located in the region of 16S rRNA that forms helix 6 in the secondary and tertiary

structures of the RNA (16, 215). This helix folds into the spur of the small ribosomal

subunit and is distal to the site of mRNA-rRNA interactions. However, the spur helix has

been used to model the P-site tRNA (215). In fact, the spur of one small subunit was

found in the P site of another small subunit in the crystals of 30S subunits (215) and

could potentially interact with the mRNA of an adjacent ribosome. The two mutations

identified in the large subunit, U1865C and G2542A of 23S rRNA, are positioned in

helix 68 of domain IV and helix 91 of domain V, respectively, in the secondary structure

of 23S rRNA. Helix 68 forms bridge 7b between 50S and 30S ribosomal subunits, while

domain V is known to be intimately involved in peptidyl transferase activity of the

ribosome (helix 91 is in the proximity of the nascent peptide exit tunnel) (16). Thus, the

locations of *rrnC* mutations are in line with the hypothesis that an interaction of the

nascent DaaP peptide with the ribosome, perhaps at the entrance to the peptide tunnel,

causes a conformational change in the ribosome that is relayed by the bridging

interactions between the subunits. This finally results in the cleavage of the *daa* mRNA

either by a ribosomal component or an associated factor.

Although the mutant residues we identified in the *rrnC* operon of C65 mutant are consistent with 2-AP and with our hypothesis of how nascent DaaP peptide affects processing of *daa* mRNA by interacting with the ribosome, we were unable to show a direct involvement of *rrnC* residues in the processing of *daa* transcript. First, the replacement of the mutant *rrnC* operon with the wild type copy by P1 transduction could not restore the *daa* mRNA processing defect in the C65 mutant (Figure 5.4). If *rrnC* residues were indeed relevant for processing of *daa* transcript, presence of the wild type copy of the ribosome is expected to alleviate the defect. Second, re-introducing the *rrnC* mutant residues into the TA516 background, also by P1 transduction, did not result in the failure of that mutant strain to cleave *daa* mRNA (Figure 5.7), further supporting the idea that *rrnC* mutations are not relevant for processing of *daa* mRNA.

The replacement experiments, however, did not exclude the possibility that *rrnC* operon was important initially and that accumulation of compensatory mutations (possibly some of the *rrnC* mutations are compensating for the function of others) rendered *rrnC* residues irrelevant. Examination of *rrnC* mutations in isolation and in combination with others (on a plasmid generated by recombinational cloning in yeast) in a genetic background lacking all wild type *rrn* operons suggested that these mutations do not cause a *daa* mRNA processing defect. Possible plasmid recombination in this background, however, resulted in reversion of *rrnC* mutations on the yeast-generated plasmids to wild type residues. It is thus likely that *rrnC* mutations might affect cell viability. rRNA is an essential component of *E. coli* genome, and usually mutations in

rrn operons that affect growth and viability could be compensated for by the presence of additional copies of the operon. In the strains with only a single *rrn* operon on the chromosome or a plasmid, mutations in these genes could cause cell death or growth defect if not recompensed for in some way. To determine whether *rrnC* mutations affected viability vs. *daa* transcript cleavage, we examined *daa* mRNA processing in strains with 'diploid' ribosomes. These experiments also revealed that presence of wild type and mutant ribosomes in a single cell had no effect on the processing of the *daa* mRNA (Figures 5.5 and 5.6).

The fact that wild type *hrpA* on a plasmid can restore processing of *daa* mRNA in the presence of *rrnC* mutations on the chromosome further shows that these residues are probably not responsible for the cleavage of the *daa* transcript. It is still, however, required to separate the effects of *rrnC* mutations on viability and *daa* transcript cleavage. The large deletion present in the C65 mutant could be the compensatory mutation that has arisen because of the pressure exherted by the *rrnC* mutations. The mutants in which *rrnC* mutations were introduced onto the chromosome of TA516 strain by P1 transduction still contain *hrpA* after a single passage (data not shown). This evidence indicates that *rrnC* mutations may not have forced the deletion of *hrpA* (and the processing defect) and that there are potentially additional factors involved.

Ribotyping analysis of TA516 and FACS-isolated mutants suggests that the role of *rrnC* mutations might be more complex. It is very likely that recombination has occured to restore the rRNA operons in TA516 and in the mutant isolates. TA516 appears to be unstable at the level of *rrn* operons because some portions of the operons

were not completely deleted when the strain was generated and this strain is not recombination deficient. Recombination at rRNA operons has been described previously (107), however the mechanism of how it is facilitated is not well understood. Also, at what point the strain TA516 restored some additional rRNA operons is not clear. If it never had a single copy of *rrn*, then the 'diploid' ribosome experiments described above really did not have two operons, but more. The presence of additional wild type copies of *rrn* would obsure any role of *rrnC* mutant residues in processing of *daa* mRNA. Therefore, further analysis is needed to convincingly entangle the role of the mutant *rrnC* residues in processing of *daa* mRNA or on the viability of cells that contain them.

CHAPTER 6: ROLE OF RIBOSOME-ASSOCIATED FACTOR SsrA IN PROCESSING OF *daa* mRNA

The genetic screen used to identify *hrpA* as an important factor in processing of *daa* mRNA was not exhaustive since only a single mutant was identified and the processing in this mutant was not completely abolished. This suggests a possibility that additional protein/RNA components are involved in *daa* mRNA cleavage. I investigated the role of ribosome associated factor SsrA in the processing of *daa* transcript.

Literature overview

Bacterial ribosomes can be stalled at the 3' ends of aberrant transcripts. A system exists to relieve such halted ribosomes and destroy the incomplete peptides synthesized by those ribosomes. It involves a small RNA molecule called tmRNA (encoded by the gene *ssrA*) that contains both tRNA and mRNA activities (92). The process of ribosome rescue and protein tagging by tmRNA has been termed *trans*-translation and seems to be conserved in all eubacteria (97, 214). The initial work on *trans*-translation suggested that the main purpose of tmRNA tagging is to remove incomplete proteins by directed proteolysis so that they might not interfere with the normal growth of the cell. More recently a new model has been proposed for tmRNA tagging in regulation of gene expression. It is now thought that the major biological role of *trans*-translation is in the removal of stalled ribosomes from mRNAs (even intact mRNAs; see below) as means of increasing translation efficiency (218).

The process of *trans*-translation can be broken down into several steps. First, tmRNA is charged with an alanine in its tRNA portion by alanyl-tRNA synthetase (173). Next, alanyl-tmRNA enters the empty A site on the stalled ribosome in the complex with elongation factor Tu and guanosine triphosphate (GTP), in the same manner as tRNA is brought to the ribosome during translation (173). Then, the alanine of tmRNA is transferred to the nascent peptide being synthesized by the stalled ribosome, followed by the translocation of the tmRNA to the P site of the ribosome. At this time the nascent mRNA is released from the ribosome and the mRNA portion of tmRNA becomes the new template for translation. A ten amino acid tag, AANDENYALAA, encoded by the mRNA segment of tmRNA is then translated, followed by the dissociation of the translational ternary complex and release of the tagged peptide (196). The major cytoplasmic protease involved in degradation of tmRNA-tagged peptides is ClpXP that recognizes the C-terminal ALAA sequence of the tag (75, 100). The activity of this protease is enhanced and its binding to the tmRNA-tagged peptide is increased by the ribosome-associated protein, SspB, which specifically binds to the AAND sequence of the tmRNA-tagged peptide (100). Additional proteases were also found to play a role in degrading tmRNA-tagged peptides and they include ClpAP, FtsH, and Tsp (218).

Originally *trans*-translation had been proposed to occur only on the ribosomes stalled at the 3' end of RNAs lacking stop codons, which are thought to be produced by damage, degradation or premature transcription termination (92). Recent investigations have revealed that *trans*-translation can also occur on intact RNAs. Two or more rare arginine codons within intact mRNAs were found to stall ribosomes, and even a single

rare codon could induce *trans*-translation if the congnate tRNA was depleted (81, 171).

Trans-translation can also occur when the ribosomes are stalled on an mRNA because of

inefficient translation termination, as demonstrated with the gene encoding ribokinase,

rbsK (53). In addition, the C-terminal amino acid sequence, including the presence of a

proline residue or an LESG motif, was found to strongly induce *trans*-translation at the

stop codons (194).

Recently tmRNA has been implicated in rescuing ribosomes stalled on damaged

mRNAs generated by toxin-antitoxin system, RelE-RelB (49). RelE of *E. coli* is a global

inhibitor of protein synthesis that is activated by nutritional stres. The activation of this

molecule is dependent on proteolytic degradation of RelE antagonist, RelB. RelE

inihibits translation by cleaving mRNA codons in the ribosomal A site in a sequence

specific way with preference for the stop codon UAG (155). In this system it was found

that tmRNA alleviated RelE toxicity and was required for rapid recovery of translation

(49).

In addition to tmRNA, a small protein SmpB seems to be required for *trans*-

translation to occur. SmpB is needed for the association of tmRNA with ribosomes (91,

219) and for all of tmRNA's functions in *trans*-translation post aminoacylation (182).

Recent crystal structure studies of the tmRNA-SmpB complex suggested a model of its

interaction with the ribosome (77). The tmRNA-SmpB complex fitted into the peptidyl

transferase center of the 50S ribosomal subunit shows that SmpB is oriented towards the

decoding centre of the small ribosomal subunit. The proximity of SmpB to the decoding

center in this model suggests that the C terminus of SmpB acts as an anticodon stem

mimic, while the tmRNA could loop outside the ribosome near the elongation factor binding site and deliver its mRNA component into the active site of the small ribosomal subunit.

Results

One effect of *trans*-translation in rescuing stalled ribosomes may be endonucleolytic cleavage of the nascent mRNA. To determine whether tmRNA participates in processing of *daa* mRNA we introduced plasmid pQTN7 (109), which encodes the *daa* processing region into *E. coli* K37 and into the isogenic construct K8619 harboring an *ssrA* mutation (217). Processing was examined by primer extension analysis. Total bacterial RNA was isolated from strains DH5α (pQTN7), K37 (pQTN7) and K8619 (pQTN7) (73) and annealed to DA primer 5' end-labeled with γ-^{32}P (28). Reverse transcription was performed with MMLV-RT at 37°C for 1h, after which the reactions were run on a 6% acrylamide gel next to a sequencing ladder generated with the same primer (DA). Figure 6.1 shows that *daa* mRNA is inefficiently processed in the *ssrA*-deficient strain, as indicated by accumulation of extension products extending beyond the *daa* cleavage site (lane 3). This implicates the involvement of tmRNA in *daa* transcript cleavage.

Primer extension analysis, however, does not allow us to asses the level of precursor RNA since this RNA is too large to enter the gel. For this purpose processing of *daa* mRNA in the *ssrA*-deficient strain was examined by S1 nuclease protections. RNA was isolated from strains DH5α, K37, and K8619 transformed with plasmid

Figure 6.1 – *daa* mRNA processing in *ssrA* deficient strain.

Primer extension analysis was performed using RNA isolated from strains DH5α, K37

and K8619 (all harboring plasmid pQTN7) with primer DA (Table 2.2) 5' end-labeled

with $\gamma^{32}P$. Reactions were separated on an acrylamide gel next to a sequencing ladder

generated with the same primer (DA). The arrow indicates the sequence at which *daa*

mRNA is cleaved.
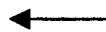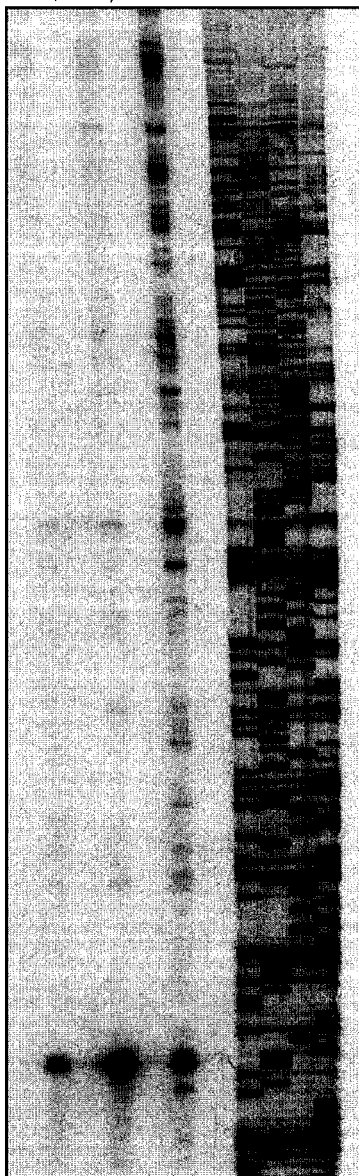
pVT123 and hybridized to a 5' end-labeled oligonucleotide WPL44. The S1 nuclease

protection analysis indicates that there is an accumulation of precursor *daa* mRNA in the

ssrA-deficient strain as compared to the wild type strain (Figure 6.2), suggesting that

tmRNA is indeed necessary for efficient cleavage of the *daa* transcript. Processing of

daa mRNA in the *ssrA*-deficient strain was restored to wild type levels by providing a

wild type copy of *ssrA* on a plasmid (pJW28) (216), further supporting the role of *ssrA* in

processing of the *daa* transcript.

In a genetic screen utilizing green fluorescent protein (GFP) and fluorescence

activated cell sorting (FACS), we have also identified a putative DEAH-box RNA

helicase, HrpA, as an important participant in the processing of *daa* mRNA (Chapter 5).

Deletion of *hrpA* results in cells with defective mRNA processing. Since mutation of

ssrA results in a processing defect without fully eliminating all cleavage of the *daa*

mRNA, we investigated the effect of a double *ssrA hrpA* mutation. We introduced an

hrpA mutation onto the chromosome of K8619 by P1 transduction, using a P1

bacteriophage lysate generated on *E. coli* strain MC1061Δ*hrpA* (129). Deletion of *hrpA*

in the double mutant strain was confirmed by *hrpA*-specific PCR (data not shown).

Processing of *daa* mRNA in the *ssrA hrpA* mutant was examined by S1 nuclease

protection analysis as described above, except that only 10 units of S1 nuclease was used

in digestion reactions. RNA was isolated from single and double mutant strains, as well

as from the wild type strain transformed with either plasmid pVT123 which encodes wild

type *daa* mRNA, or a control plasmid pVT124 that encodes mutant *daa* mRNA with a

G49A mutation in DaaP that abolishes processing (108). The S1 nuclease reactions were

Figure 6.2 – SsrA is are required for efficient processing of *daa* mRNA.

S1 nuclease protection analysis of *daa* mRNA processing was performed as described in

the legend to Figure 3.1. RNA was isolated from strain K37 (wild type) harboring

plasmids pVT123 or pVT124, from K8619 (*ssrA* deficient) and K8661 (*ssrA*

complemented) both carrying pVT123. RNA-probe hybrids were digested with 90, 50

and 10 units of S1 nuclease (triangles) and separated on an acrylamide gel. P, precursor

RNA; C, cleaved product.
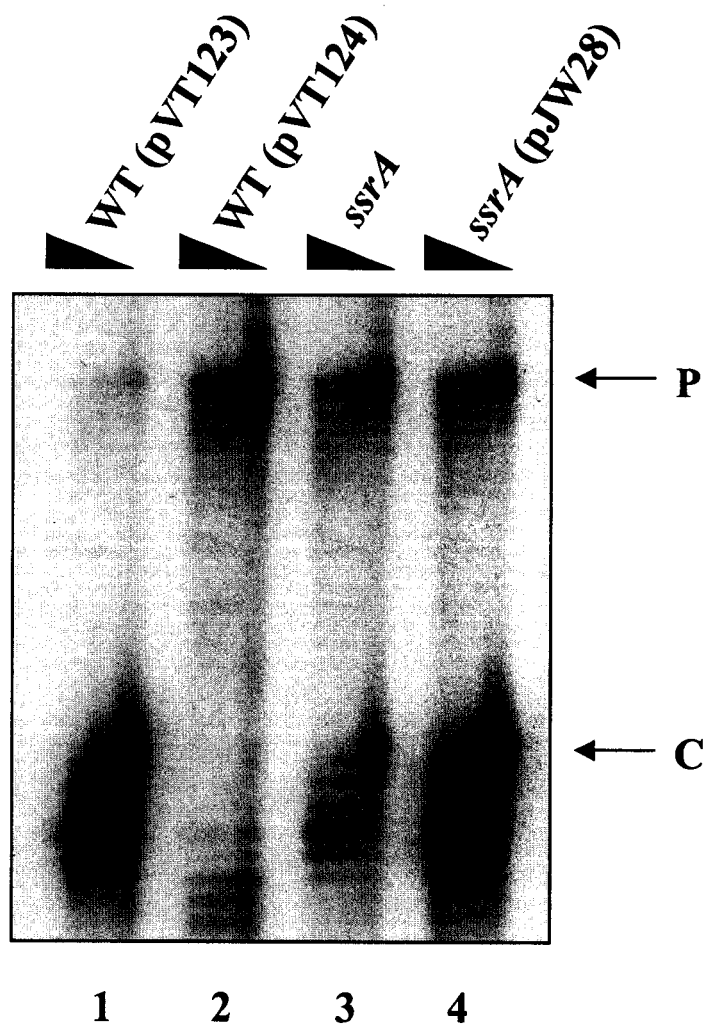
resolved on an acrylamide gel. Figure 6.3 shows that the double mutant *ssrA hrpA* (lane 5) has a *daa* mRNA processing defect greater than that of single *ssrA* or *hrpA* mutants (lanes 3 and 4, respectively). Addition of and *hrpA*-encoding plasmid, pVT148, to the *ssrA hrpA* double mutant ameliorated the defect in *daa* mRNA processing to the level of processing observed in the single *ssrA* mutant strain (Fig. 6.3, lane 6).

Discussion

The data presented in this chapter indicate that tmRNA is involved in the endonucleolytic cleavage of *daa* mRNA. The demonstration of a ribosome-associated factor affecting the processing of this transcript supports our hypothesis that the ribosome plays an important role in the cleavage of *daa* mRNA. While the role of the tmRNA in the rescue of stalled ribosomes and *trans*-translation has been clearly established, it still remains to be determined whether the ribosome is stalled on *daa* mRNA and whether the DaaP peptide is tagged for degradation by tmRNA. Previous work from our laboratory indicates that translation of the entire *daaP* gene is not required for processing to occur (108). It is possible then that if DaaP were indeed tagged by tmRNA, it would not be at the stop codon, but perhaps at an internal site in the coding region ; this could even be the site of *daa* mRNA cleavage. Therefore, the involvement of tmRNA in processing of *daa* transcript would support the proposal by Roche and Sauer (171) that tagging intact mRNAs requires ribosome-associated cleavage of mRNA generating the 3'-end needed for *trans*-translation. Regardless of whether the DaaP peptide is tagged or not, the

Figure 6.3 – *hrpA* deletion amplifies the effect of *ssrA* mutation on *daa* mRNA

processing.

S1 nuclease protection analysis was performed as described in the legend to Figure 3.1.

RNA was isolated from wild type strain K37 carrying plasmids pVT123 or pVT124 ,

from *ssrA* and *hrpA* single mutant strains (K8619 and MC1061ΔhrpA, respectively) and

from the double mutant strain *ssrA hrpA* (K8619ΔhrpA). All single and double mutant

strains are harboring plasmid pVT123. RNA-probe hybrids were digested with 10 units

of S1 nuclease and ran on an acrylamide gel. The % of precursor RNA (P) and cleaved

product (C) was determined after the analysis of S1 nuclease protection results with the

ImageQuant software.

	WT (pVT123)	WT (pVT124)	ssrA	hrpA	ssrA hrpA	ssrA hrpA (pVT148)
	1	2	3	4	5	6
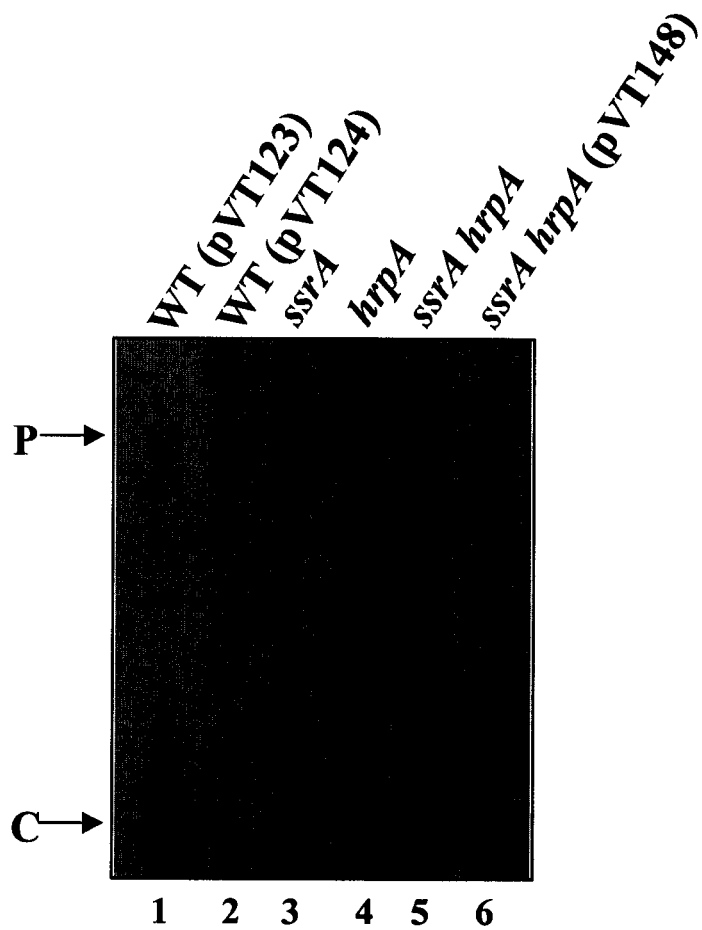
P (% total)	6	100	53	61	76	39
C (% total)	94	0	47	39	24	61

involvement of tmRNA in the processing of *daa* mRNA implicates this factor in a form of gene regulation in *E. coli* that has not been described previously.

The *daa* mRNA processing defect in the *ssrA* mutant is amplified and processing is almost completely abolished in the presence of the *hrpA* mutation. We recently identified HrpA as a component of *daa* mRNA processing (Chapter 5); however, those studies did not exclude the possible involvement of additional factors. The enhanced effect of the double *ssrA hrpA* mutation on *daa* mRNA processing suggests that these gene products may interact to allow more efficient cleavage of the *daa* transcript. This interaction is further supported by the ability of an *hrpA*-encoding plasmid, pVT148, to complement the processing defect in the *ssrA hrpA* double mutant to the level of processing in the single *ssrA* mutant. Yeast homologs of HrpA are part of the large ribonucleoprotein complex, the spliceosome, and we hypothesize that HrpA might be in a similar complex in bacteria. Karzai and Sauer (90) identified a complex of protein factors that interact with tmRNA. It is not known if HrpA is a part of the tmRNA complex. Our results suggest that this possibility should be investigated.

In conclusion, data presented here implicate ribosome-associated factor tmRNA in the endonucleolytic cleavage of mRNA in the *daa* fimbrial operon of *E. coli*. A putative RNA helicase, HrpA, is also involved in this process, and it appears that both of these factors are required for the efficient processing of *daa* mRNA.

CHAPTER 7: *IN VITRO* SYSTEM FOR ANALYSIS OF *daa* mRNA PROCESSING

In addition to the genetic analysis of *daa* mRNA processing, we were also

interested in dissecting the processing event by a biochemical approach. Availability of

an *in vitro* processing system is likely to be crucial for identifying additional factors

involved in processing of *daa* mRNA. An *in vitro* system is also needed to further our

understanding of the factors we have identified through genetic approaches as being

involved in the *daa* transcript cleavage: HrpA, SsrA and SmpB, and the ribosome. In

this chapter we present an attempt at utilization of commercially available *E. coli* S30

extracts for *in vitro* analysis of *daa* mRNA processing reactions, as well as optimization

of conditions for the processing reaction in this cell free system.

Analysis of translation and processing of *daa* mRNA in commercially available S30 extracts.

To start development of an *in vitro* system for analysis of processing of the *daa*

transcript, commercially available *E. coli* S30 extract (Promega) was utilized. Unlike

eukaryotic systems where transcription and translation occur sequentially, in *E. coli*

transcription and translation occur simultaneously within the cell. *In vitro E. coli*

translation systems are thus usually designed to perform the same way and are termed

"coupled" since both transcription and translation take place in the same tube under the

same reaction conditions. During transcription, the 5' end of the RNA becomes available

for ribosomal binding and undergoes translation while its 3' end is still being

transcribed. This early binding of ribosomes to the RNA maintains transcript stability and promotes efficient translation.

Similar to the systems for *in vivo* high-level protein expression, the coupled transcription/translation systems rely on the use of bacteriophage T7 polymerase and T7 promoters. The Promega S30 System facilitates the transcription/translation of DNA sequences cloned in plasmid or lambda vectors containing a T7 promoter by providing an extract that contains T7 RNA polymerase for transcription and all necessary components for translation. Promega's T7 S30 extract is prepared by modifications of the method described by Zubay (229) from an *E. coli* strain B deficient in OmpT endoproteinase and *lon* protease, which results in greater stability of expressed proteins that would otherwise be degraded by these proteases. The T7 S30 system contains an S30 Premix without amino acids that is optimized for each lot of S30 extract and contains all other required components, including rNTPs, tRNAs, an ATP-regenerating system and appropriate salts. Amino acid mixtures lacking cysteine, methionine or leucine are provided to facilitate radiolabeling of translation products.

For the analysis of processing of *daa* mRNA in the Promega S30 extracts, wild type and non-processing mutants (premature STOP codon and frameshift mutants of *daaP* (109)) *daa* processing regions were inserted under the control of bacteriophage T7 promoter to generate constructs pWL117R, pWL130R and pWL122R, respectively (Table 2.3). Reactions were performed according to the manufacturer's instructions and were analyzed for the presence of the DaaP peptide by Tricine-SDS-PAGE and processing of *daa* mRNA by primer extensions.

Tricine-SDS-PAGE results revealed that DaaP is translated in the commercially available S30 extracts (Figure 7.1A). A protein of expected size (~6.2 kDa) is produced from wild type *daaP* template, pWL117R. No translation product is visible when the premature STOP codon mutant, pWL130R, is used as a template in the *in vitro* reactions (lane 3). This result is expected because a peptide of only two amino acids in length is synthesized in this case and is too small to be visualized on the gel. The frameshift mutant, pWL122R, template also results in an *in vitro* translated product (lane 4). The peptide generated from the frameshifted *daaP* is of slightly smaller size relative to the peptide encoded by the wild type *daaP* sequence. The additional protein bands (MW ~7.6 kDa) visible in lanes containing all of the *daaP* constructs are probably due to translation of endogenous mRNAs present in the extract (possibly a result of incomplete degradation of RNA during extract preparation). These same bands are present in lane 1 containing the vector control provided in the Promega kit. The translation of DaaP in the *in vitro* extract used here appears to be efficient since the peptides with three methionines (in the case of wild type DaaP) and a single methionine (in the case of frameshifted peptide) can be detected in samples after a 2h reaction time.

Coupled transcription/translation reactions using the same templates as above were also analyzed for the processing of *daa* mRNA by primer extensions and S1 nuclease protection assays. Figure 7.1B,C shows that wild type *daa* mRNA was processed correctly in the *in vitro* reactions, while the mutants known not to be processed

Figure 7.1 – *In vitro* analysis of *daa* mRNA processing utilizing commercially available *E. coli* S30 extracts.

A) Translation of DaaP in Promega S30 extracts. Products of the coupled transcription/translation reactions with control DNA template (PinPoint), pWL117R (wild type *daaP*), pWL130R (premature STOP codon mutant of *daaP*) and pWL122R (frameshift mutant of *daaP*) were precipitated with acetone and examined by Tricine-SDS-PAGE analysis. The sizes of the molecular weight standards are shown on the left. The arrow indicates the apparent position of the DaaP peptide synthesized in the S30 extracts.

B) Analysis of *daa* mRNA processing in the S30 extracts. RNA was isolated from the coupled transcription/translation reactions programmed with pWL117R, pWL122R and pWL130 R and used in primer extension reactions with primer DA (Table 2.2) 5' end-labeled with γ^{32}P. The reactions in the left-side panel were performed with 90 µg of RNA, while the reactions in the right set of lanes contained 30 µg of RNA. Control processing reactions (*in vivo*) were performed with RNA isolated from DH5α harboring pQTN7.

C) S1 nuclease protection analysis of *daa* mRNA processing in the S30 extracts. RNA was isolated as in (B) and subjected to S1 nuclease protection as described in the legend to Figure 3.1. P, precursor RNA; C, cleaved product.

A

kDa

PinPoint pLWL117R pWL130R pWL122R

203
116
83
48.7
33.4
28.2
20.7
7.6

← DaaP

B

CAT G   pQTN7 pWL117R pWL122R pWL130R   pQTN7 pWL117R pWL122R pWL130R

C

CATG   pQTN7 pWL117R pWL122R pWL130R

← P

← C
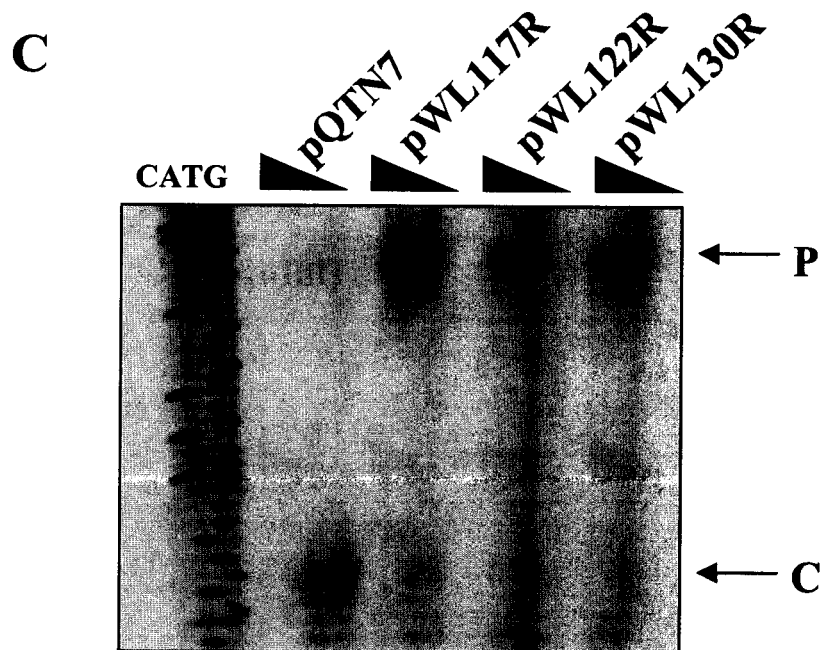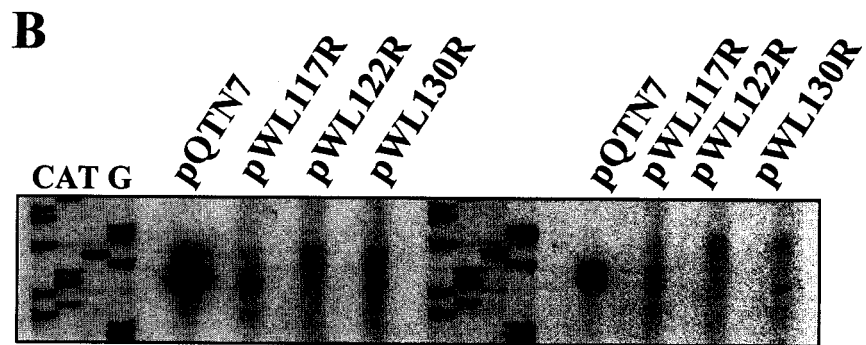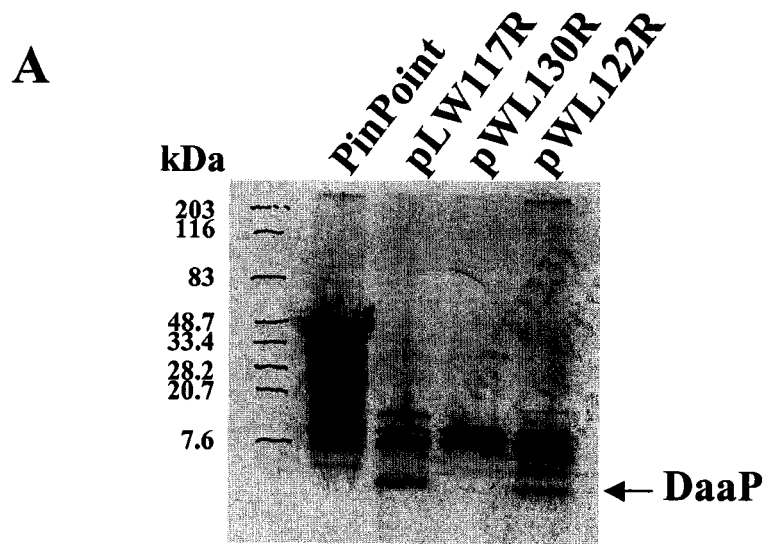
in vivo also failed to be processed in the S30 extracts. Although the *in vitro* processing in this system is much less efficient relative to *in vivo* processing, it is encouraging that a specific processing product was seen in reactions with wild type *daaP* template. These data demonstrate the potential utility of a cell-free translation system for investigation of *daa* mRNA processing.

Optimization of the *in vitro* system for *daa* mRNA processing.

The preliminary work described above shows cleavage of the *daa* mRNA in the commercially available S30 extracts, however the processing was not very efficient. Since the commercially available extracts are optimized for *in vitro* translation of the control mRNA, we attempted to optimize the cell-free system for processing of *daa* mRNA by preparing the extracts in our laboratory. We wanted to experiment with the parameters that can be varied and which are critical for performance of the cell-free transcription/translation system (99), including divalent cations, tRNA and amino acid concentrations.

The S30 extracts were prepared by the method of Zubay (229) from an RNase I⁻ *E. coli* strain, A19, to prevent degradation of the RNA in the extracts. Unlike with the commercially available extracts where all of the components necessary for the *in vitro* transcription and translation are provided in the kit, the extracts we prepared required the addition of all the individual components. These included the divalent cations, nucleotide triphosphates, amino acids, tRNA, source of energy, T7 RNA polymerase and the prepared S30 extracts. The competency of these extracts for translation of DaaP was first

attempted in a coupled transcription/translation system using pWL117R DNA as a template. The initial experiments, however, resulted in no detectable peptide (data not shown). Next, *in vitro* translation was tested in 'uncoupled' reactions. The *daa* mRNA was generated using an *in vitro* transcription kit (from a linearized DNA template) and was subsequently incubated with the S30 extracts (in the presence of 10 mM $Mg(OAc)_2$ and 250 mM KOAc). The incorporation of ^{35}S-methionine into DaaP was analyzed by Tricine-SDS-PAGE. Figure 7.2A shows that *in vitro* translation in our S30 extracts resulted in visible protein bands when wild type and frameshifted *daaP* mRNA were used as templates (lanes 1 and 2), but no product is seen with the mRNA transcribed from the premature STOP codon mutant (lane 3). The mutant DaaP resulting from the frameshift mutation is of slightly smaller molecular weight than the wild type DaaP, as was observed with the commercially available extracts. The difference between the translation products from our extracts and those generated in the Promega extracts is their molecular weight. In Figure 7.2A, wild type and mutant DaaP appear at the level of the 7.6 kDa protein standard band, and are larger in size than the peptides observed with Promega extracts (Figure 7.1A). This is possibly due to a difference in protein precipitation procedures (acetone was used to precipitate proteins from the Promega extracts, while TCA was used with our extracts). Irrespective of the disparity in the size of proteins seen between the two different extracts, these data indicate that the S30 extracts generated in our laboratory are translation competent in the 'uncoupled' reactions.

Figure 7.2 – *In vitro* analysis of *daa* mRNA processing: 'uncoupled'

transcription/translation reactions in S30 extracts.

A) Translation of DaaP in 'uncoupled' transcription/translation reactions. RNA was

generated from templates pWL117R, pWL122R and pWL130R by using *in vitro*

transcription reactions and then added to the S30 extracts (generated in our laboratory)

for protein synthesis. Products of the *in vitro* translation reactions were precipitated with

TCA and analyzed by Tricine-SDS-PAGE. The sizes of the molecular weight standards

are shown on the left. The arrow indicates that the DaaP product was generated in these

in vitro reactions.

B) Primer extension analysis of *daa* mRNA processing in 'uncoupled'

transcription/translation reactions. RNA was isolated from the same reactions as in (A)

and annealed to primer DA (Table 2.2) 5' end-labeled with γ^{32}P. Reactions were

separated on an acrylamide gel next to a sequencing ladder generated with the same

primer (DA). Control processing reaction (*in vivo*) was performed with RNA isolated

from DH5α strain harboring pQTN7.

C) Analysis of RNA integrity. RNA generated by *in vitro* transcription reactions was

analyzed on an acrylamide gel. Molecular weight standards are denoted on the right.

A

kDa

203
116
83
48.7
33.4
28.2
20.7
7.6

pWL117R
pWL122R
pWL130R

DaaP

1   2   3

B

C ATG

pQTN7 (*in vivo*)
pWL117R
pWL122R
pWL130R

C

pWL117R
pWL122R
pWL130R

bp

2000
1200
800
400

200

100
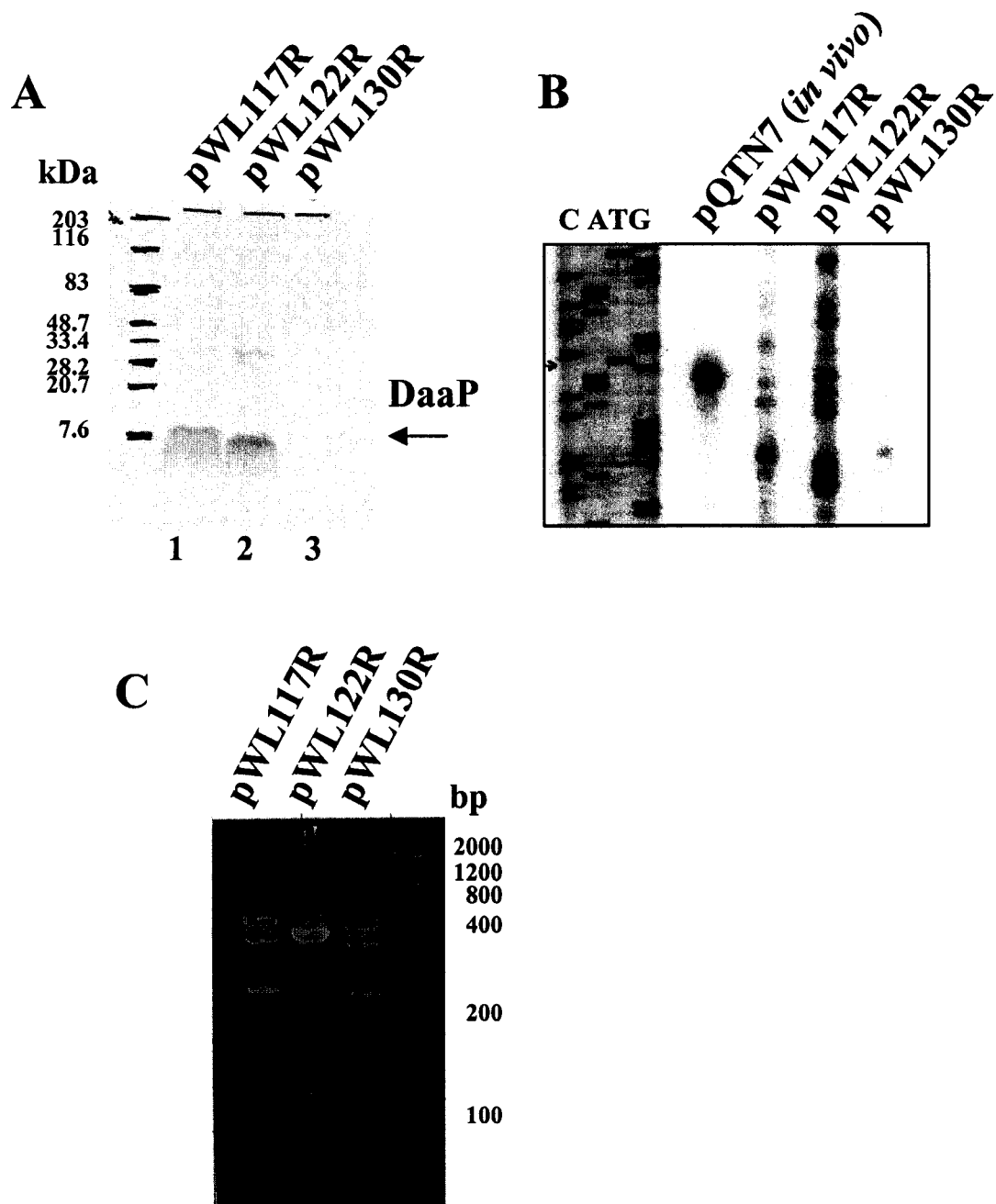
Since translation is required for the processing of *daa* mRNA and we observed

translation in the 'uncoupled' reaction, we examined *daa* mRNA processing in our S30

extracts under the same conditions. Similar to the analysis of DaaP peptide, *daa* mRNA

(from wild type and non-processing mutant templates) was generated by *in vitro*

transcription and used to program the S30 extracts for translation. After 2 h incubation

with the extracts under the same conditions as for protein analysis, RNA was precipitated

and analyzed for processing of *daa* mRNA by primer extensions. A number of different

attempts at processing analysis resulted in undetectable processing of *daa* transcript with

the wild type *daa* mRNA as a template (Figure 7.2B). A possible explanation for this

result is that the *daa* mRNA generated *in vitro* is degraded and is not suitable for

detection of the processing event in the cell-free system. Electrophoretic analysis of the

in vitro transcribed *daa* mRNA shows that indeed some of the RNA is degraded (Figure

7.2C).

Since in a coupled transcription/ translation system RNA is continuously made by

the RNA polymerase and is protected from degradation by the translation machinery, the

above observation suggested that the coupled transcription/translation system should be

revisited. Initially, no translation of DaaP could be observed with the coupled system

using our S30 extracts. In those experiments a very low concentration of T7 RNA

polymerase was used (0.003 units/µl) and it is possible that there was an insufficient

amount of transcript made to result in efficient translation. We repeated the coupled

experiments with 1000 fold more T7 RNA polymerase and looked for translation of DaaP

by incorporation of ^{35}S-methionine on Tricine-SDS-PAGE. Figure 7.3A shows that

Figure 7.3 - *In vitro* analysis of *daa* mRNA processing: 'coupled'

transcription/translation reactions in S30 extracts.

A) Translation of DaaP in 'coupled' transcription/translation reactions. pWL117R,

pWL122R and pWL130R were used to program 'coupled' transcription/translation

reactions in the S30 extracts (generated in our laboratory). Protein products of these

reactions were precipitated with TCA and analyzed by Tricine-SDS-PAGE. The sizes of

the molecular weight standards are shown on the left. The arrow indicates the

approximate size of DaaP product.

B) Primer extension analysis of *daa* mRNA processing in 'coupled'

transcription/translation reactions. RNA was isolated from the same reactions as in (A)

and annealed to primer DA (Table 2.2) 5' end-labeled with $\gamma^{32}P$. Reactions were

separated on an acrylamide gel next to a sequencing ladder generated with the same

primer (DA). Control processing reaction (*in vivo*) was performed with RNA isolated

from DH5α strain harboring pQTN7. In addition, a control reaction with RNA from the

S30 extracts (no DNA template added) was also included.

C) Analysis of RNA integrity. RNA generated by the 'coupled' reactions was analyzed

on an acrylamide gel. Molecular weight standards are denoted on the right.
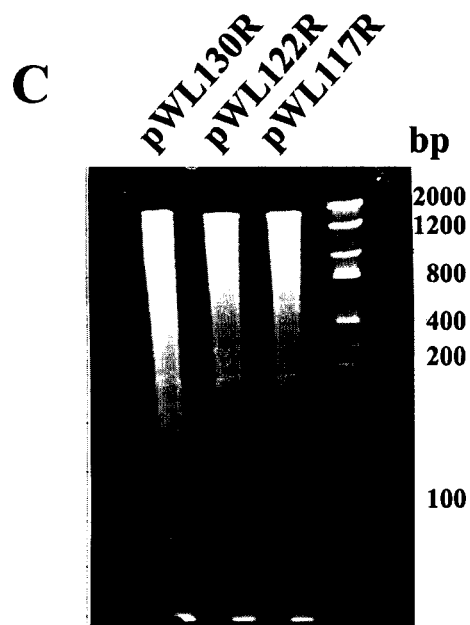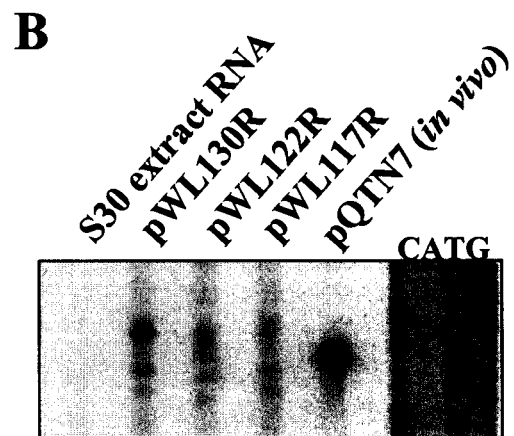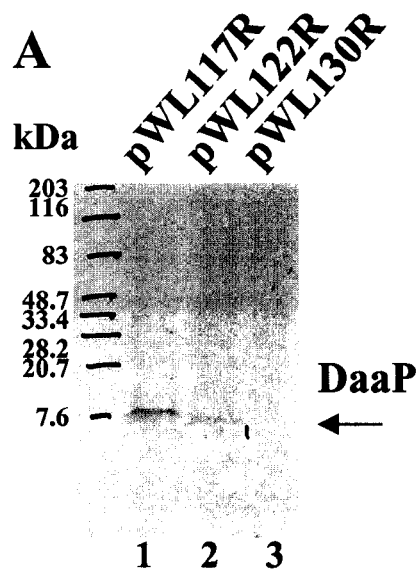
when the amount of RNA polymerase is increased DaaP peptide can be detected when wild type and frameshifted *daa* templates are used (lanes 1 and 2) and no peptide is seen with the premature STOP codon mutant (lane 3). The sizes of the observed peptides are identical to those seen in the 'uncoupled' reactions. This suggests that the S30 extracts we prepared can be used for the analysis of translation. The processing of *daa* mRNA in the coupled system was analyzed next. The reactions were performed as for the protein analysis (except that the 'cold' methionine was used). After 2 h incubation with the S30 extracts RNA was precipitated and analyzed by primer extensions. Once again, no predicted *daa* mRNA processing product could be seen with the wild type template (Figure 7.3B) and the RNA generated in the coupled reactions also appeared to be degraded (Figure 7.3C). These data suggests that although our S30 extracts are adequate for DaaP translation, the conditions required for *daa* mRNA processing to occur and be detected in this cell-free system are complex and require more rigorous experimentation.

Discussion

Our understanding of numerous mechanisms of gene regulation in bacteria, including the *parD* stability system of plasmid R1 (60) and tryptophanase (*tna*) operon of *E. coli* (74) among others, has greatly benefited from biochemical studies in cell-free conditions. Genetic analysis of *daa* mRNA processing described in the previous chapters can be greatly complemented by a biochemical approach. However, no *in vitro* system for the examination of *daa* mRNA processing has been available. We, therefore, sought to develop a cell-free *daa* mRNA processing reaction.

To instigate development of an *in vitro* system for *daa* mRNA processing, commercially available S30 extracts were utilized. The most common application of S30 extracts is the synthesis of small amounts of radiolabeled protein; consequently the extracts are usually optimized for protein yield. Proteins expressed in the S30 extract also may be used for a variety of functional transcription and translation studies. We performed coupled transcription/translation reaction experiments in the Promega S30 extracts and detected both translation and processing of *daa* mRNA (Figure 7.1). This suggests that *daa* transcript processing can occur in a cell-free system. DaaP translation was quite efficient in these extracts (which is important since processing is translation dependent), as would be expected for extracts that are optimized for protein synthesis. The processing of *daa* mRNA, however, although detectable occurred with greatly reduced efficiency relative to the processing *in vivo*. A system that more accurately resembles the *in vivo* processing is desirable for biochemical analysis. Since the composition of the commercially available extracts, premixes and other solutions provided in the kit is unavailable, it is difficult to experiment with the reaction conditions to improve the competency of the extracts for processing of *daa* mRNA. We, thus, resorted to generating the S30 extracts in our laboratory.

The S30 extracts we made were tested for their capacity to translate DaaP and also for processing of *daa* mRNA. In both coupled transcription/translation reactions and in 'uncoupled' reactions, translation of DaaP from a wild type and frameshifted template was observed (Figures 7.2 and 7.3), suggesting that both transcription and translation components of the extract are functional. However, no *daa* transcript cleavage could be

detected in the extracts under the conditions in which translation occurs. Examination of the mRNA integrity after both 'uncoupled' reactions and coupled transcription/translation indicate that the RNA was degraded. This suggests that the conditions in the cell-free system we generated, although adequate for translation, are not adequate for processing of the *daa* mRNA.

It is interesting, in light of the fact that processing is translation dependent, that DaaP seems to be quite unstable *in vivo*, since the peptide can only be detected in immunoblot assays if it contains a C-terminal HSV (define) fusion tag (Wendy Loomis, unpublished observation). When this C-terminal tag stabilizes the peptide, however, the efficiency of *daa* mRNA processing is greatly reduced ((109) and unpublished observation). This is further evidence that optimum translation and stabilized DaaP are not necessary prerequisites for optimum processing of the *daa* transcript.

It is apparent from the experiments with the S30 extracts we generated that RNA degradation prevents detection of *daa* mRNA processing. Our extracts were made from an *E. coli* strain deficient in RNase I to prevent RNA degradation. In addition, RNase inhibitors were added to the reaction mixes during both coupled transcription/translation and 'uncoupled' experiments. However, this was not sufficient to eliminate RNA decay prior to examination of *daa* transcript processing. Possible solutions to this problem may include preparation of S30 extracts from *E. coli* Q13 that in addition to RNase I mutation is deficient in PNPase, one of the major exonucleases in *E. coli*. The use of specific exonuclease inhibitors (which should soon be available from Roche) may also prevent some of the RNA decay.

Another reason for our inability to detect *daa* mRNA cleavage in the S30 extracts may be in the currently available constructs of *daa* processing region under the T7 promoter. The constructs we have been employing do not contain the 3' stabilizing stem loop structure that is present when processing is examined *in vivo*. Therefore, addition of the sequence encoding this secondary structure may be required to alleviate degradation of transcript in the extracts and result in conditions for detection of *daa* mRNA processing. Also, since we do not fully understand all the sequence requirements for *daa* mRNA processing (for example the instability element in the 5' UTR, (108)), constructs with variable lengths of the *daa* processing region should be assembled to determine which one is best suited for the *in vitro* analysis. Finally, different vectors for *in vitro* transcription/translation are now available from Invitrogen and Roche and should be explored for possible improvement of detection of *daa* mRNA processing.

After the problem of RNA degradation is eliminated and processing of *daa* mRNA can be visualized in the S30 extracts, additional parameters may be optimized. These include concentrations of DNA template, critical cations (Mg^{2+}, K^+, $NH4^+$), amino acids and tRNA, as well as reaction times and temperatures. As mentioned previously, the commercially available systems for *in vitro* translation include premixes with all the components optimized for protein synthesis. In addition, published uses of non-commercial S30 extracts only contain information about the conditions for most efficient protein synthesis. Thus, the greatest challenge in developing a useful cell-free system for processing of *daa* transcript will be to identify parameters that will allow for sufficient translation activity without compromising the *daa* mRNA processing event.

CHAPTER 8: CONCLUSIONS AND FUTURE DIRECTIONS

The goal of this thesis project was to identify factors involved in processing of *daa* mRNA. I tested the hypothesis that the nascent DaaP regulates processing of the *daa* transcript by interacting with the ribosome or a ribosome associated factor resulting in the cleavage of the mRNA within the ribosome. Although I could not implicate the ribosome directly in the cleavage of *daa* mRNA, I have discovered an essential *in cis* element and also previously unknown *trans* acting factors that are important for the efficient processing of the *daa* transcript.

I confirmed our previous observations and provided new evidence that major endonucleases known to be involved in the processing of mRNA in *E. coli* are not responsible for the cleavage of the *daa* transcript. Mutant alleles of RNase E, III, P, G and I did not result in a *daa* mRNA processing defect. This suggests that a novel endonucleolytic activity is crucial for the processing of the mRNA in this fimbrial operon.

In an attempt to understand the role of the nascent DaaP in the processing of the *daa* mRNA, translation of which was known to be important (108, 109), I determined that a tripeptide sequence in the C-terminus of DaaP is essential for processing to occur. Codons 49-51 of DaaP, encoding Gly-Pro-Pro, could not be changed to an alanine suggesting that this amino acid sequence is required for RNA processing. The requirement of DaaP translation and the GPP tripeptide for *daa* mRNA processing are consistent with the models of nascent peptide regulation of gene expression through an

interaction with the ribosome (110, 130, 200). Although the mechanism by which the GPP tripeptide induces processing of the *daa* transcript is not known, it is likely that it interacts with the ribosome in some way. It possibly causes a conformational change in the ribosome to result in the cleavage of the RNA by the ribosome or an associated factor. To better understand how GPP affects processing and mRNA-ribosome interactions further experimentation will be required.

While we had data to suggest a model of nascent peptide mediated gene expression in the *daa* operon, we had no information on *trans*-acting factors involved in this process. Through a chemical mutagenesis and a genetic screen that utilized a GFP reporter construct and FACS, I isolated mutants that were deficient in *daa* mRNA processing activity. I pinpointed the location of the mutation in the processing-deficient strains by Hfr and P1 transduction mapping. These experiments led to identification of a novel factor in mRNA processing in *E. coli*, a putative DEAH-box RNA helicase HrpA. The biological role of this gene product was not known previously, however it's putative function as an RNA helicase had been proposed base on the high sequence similarity it shares with yeast proteins of DEAH-box RNA helicase family, Prp2, Prp16 and Prp22. The yeast homologs of HrpA are part of the ribonucleoprotein complex, the spliceosome, and are involved in pre-mRNA splicing (172). Site-directed mutagenesis experiments based on the sequence homology of HrpA with the yeast DEAH family of RNA helicases indicate a functional resemblance: mutations in *hrpA* corresponding to mutations in yeast proteins that abolished function in pre-mRNA splicing rendered *hrpA* incapable of complementing the *daa* mRNA processing defect, while mutations in *hrpA* corresponding

to mutations with no effect on the yeast proteins similarly had no effect on the ability of the bacterial gene to complement the mRNA processing defect in the mutant strain. This is the first demonstration that a DEAH-box RNA helicase is involved in the processing of mRNA in *E. coli*.

What is the possible mechanism of HrpA action in *daa* mRNA processing? The potential roles of HrpA include RNA remodeling, modification of RNA-protein interactions as well as endonucleolytic activity, and these roles cannot be distinguished based on sequence similarities. The mutagenesis data suggest that HrpA may be a true NTPase, like the yeast homologs, and use the NTP binding/hydrolysis for its function in mRNA processing. The NTPase function of HrpA, however, needs to be confirmed by biochemical analysis.

Although HrpA seems to be crucial for efficient processing of the *daa* mRNA, the mutants lacking *hrpA* are not completely defective in *daa* transcript cleavage. In these strains a low level of processing is detectable. In addition, the mutant I isolated had suffered a deletion of *hrpA*, and this was unlikely to have occurred through the action of the mutagen I used, 2-aminopurine. This suggests that additional factors participate in the mRNA processing events. Based on our hypothesis and the role of nascent DaaP ribosomal components, either rRNA or ribosomal proteins, were not ruled out as possible effectors of *daa* mRNA processing. Mismatch analysis of the single rRNA operon present on the chromosome of the strain I used for mutagenesis and the operons encoding ribosomal proteins and translation factors tested this hypothesis. By this approach I identified three point mutations in the rRNA operon, one in 16S and two in 23S rRNA,

and no other mutations. The mutant residues I identified were changed in accordance to the chemical mutagen 2-AP, and were in locations of the secondary/tertiary structure of rRNA that based on our hypothesis of nascent peptide regulation could be responsible for *daa* mRNA cleavage. While the rRNA mutations are very exciting, I have been unable to establish their role in the defective processing phenotype. Replacing the rRNA mutations in the mutant strain C65 with the wild type copy by P1 transduction did not restore the processing of the mutant. Moreover, re-introducing the rRNA mutations into the wild type background did not result in a processing defect. The main reason why I am unable to detect a processing defect with all three mutations present and in all the different experiments is that ribotyping analysis revealed presence of additional *rrn* operons in TA516 and FACS-isolated mutants. This is consistent with the possible selection of a spontaneous compensatory mutation, either the *hrpA* mutation or other unknown mutations, which now renders the rRNA mutations irrelevant to the processing phenotype.

Although I was unable to dissect the role of the rRNA mutations in the processing of *daa* mRNA, I did identify ribosome-associated factor SsrA as an important element of the processing event. This gene product is involved in *trans*-translation, a system known to release stalled ribosomes from truncated messages and to target the incomplete peptides for degradation (218). Once the *daa* mRNA is cleaved it generates an aberrant transcript on which the ribosome is likely stalled, and this mRNA is a probable substrate for SsrA tagging. Unfortunately we have been unsuccessful in detecting SsrA-tagged DaaP. However, mutant in *ssrA* causes inefficient processing of the *daa* mRNA, which

suggests that SsrA is involved in the efficient cleavage of *daa* transcript prior to its tagging. Interestingly, *ssrA hrpA* double mutant exhibit an additive effect on processing of *daa* transcript, indicating that an interaction between SsrA and HrpA is involved in *daa* mRNA processing. If indeed HrpA interacts with the ribosome-associated factor SsrA, it might likely be part of the ribosome itself. This would support the intriguing possibility that processing of certain mRNAs in bacteria is analogous to the pre-mRNA splicing in eukaryotes. Thus a bacterial RNA helicase might be a component of the large ribonucleoprotein complex, i.e. the ribosome, which gave rise to the eukaryotic complex of RNA helicases, the spliceosome. This hypothesis, however, needs to be tested experimentally.

Future directions

Although the work presented here demonstrates new insights into the endonucleolytic cleavage of *daa* mRNA, there are many remaining issues that need to be addressed. The first is the role of HrpA in the processing of *daa* mRNA. The NTPase activity of HrpA and its potential RNA unwinding activity need to be examined to further support the functional homology of HrpA with the yeast homologs found in the spliceosome. It would be of interest to perform further structure/function analysis of HrpA, possibly based on the predicted structure of the protein (which could be modeled on the crystal structures of DEAD-box RNA helicases, such as eIF4e (41). Comparative structures studies have been used to deduce function in other helicases (63).

Whether HrpA interacts with the ribosome also needs to be investigated, and this will require an *in vitro* system of *daa* mRNA processing that is still not available. Once and efficient cell-free system is developed, it would be of interest to generate S30 extracts from the *hrpA* mutant strain and try to supply the purified HrpA protein to such extracts to asses processing of the mRNA. Based on the *in vivo* evidence that the *hrpA* mutation alone does not result in complete lack of *daa* mRNA processing, the *in vitro* system could be used to identify the additional components required for processing. Moreover, the biological substrate specificity for HrpA needs to be determined. Does this helicase act on the *daa* transcript, on ribosomal RNA or on a complex of RNA and proteins? Additionally, it is imperative to determine the role of HrpA in degradation of other bacterial mRNAs. This could be examined by determining whether the decay of specific transcripts is affected in the *hrpA* mutant strain, possibly in an expression microarray analysis.

It will also be important to establish the function of HrpA in F1845 fimbrial biogenesis and the ability of bacteria that express these fimbriae to cause disease. Unpublished electron microscopy studies from our laboratory indicate that mutations which abolish processing of *daa* mRNA result in undetectable fimbriae on the surface of bacterial cells (Wendy Loomis, unpublished observation). Additional preliminary evidence suggests that failure to process Dr-family fimbrial operons leads to decreased colonization of the mouse kidney. Thus, it would be interesting to determine whether an RNA helicase could be a virulence determinant. Mutants deficient in *hrpA* can be generated in the clinical strain that expresses F1845 fimbriae on the chromosome and the

effect of this mutation on processing of *daa* mRNA, fimbrial biogenesis, receptor binding and mouse kidney colonization can be examined.

The second remaining issue that needs further consideration is the role of ribosomal RNA in processing of *daa* mRNA. The *rrnC* residues I identified by mismatch analysis could still be contributing to the processing of *daa* mRNA, but in the mutant C65 their effect might be obscured by the presence of wild type *rrn* operons that were restored by recombination. One possible way of defining the role of *rrnC* residues in processing of *daa* transcript is in a modified 'hybrid' ribosome experiments with *rrnC* operon under tight regulation. Individual *rrnC* mutant residues, as well as combinations of different mutations, can be engineered into a low copy number vector and under tightly regulated promoter. These constructs can then be introduced into the strain that carries only a singe copy of wild type rRNA operon on the chromosome, the expression of mutant ribosomes induced, and the effect of the mutations on processing of mRNA examined upon induction. A more stable strain with single *rrn* operon is diserable for these analyses and could potentially be used in 'diploid' ribosome experiments that I have attempted. Alternatively, the role of the *rrnC* residues can be assessed in an *in vitro* system. When the *in vitro* processing system is optimized, mutant ribosomes with different mutant rRNA residues can be assembled (202) and the processing of *daa* mRNA can be examined in the presence of such mutant ribosomes.

Finally, the issue of whether ribosomes are stalled on *daa* mRNA also needs to be resolved. As mentioned previously, it is likely that the ribosomes are stalled on the *daa* mRNA once the RNA is endonucleolytically cleaved and becomes substrate for SsrA

tagging. However, it is not clear whether the ribosome stalls prior to or during the processing of the mRNA. The reason for exploring this question is to determine whether DaaP acts similarly to other nascent peptides that are known to stall ribosomes (200) or whether it presents a novel system of gene regulation. This issue could be examined in a cell-free system, further supporting the crucial need for an efficient *in vitro* processing reaction. Therefore, it appears that while genetic approaches were useful in identifying the factors involved in processing of *daa* mRNA, biochemical analyses will be essential in dissecting the mechanism by which these factors execute the RNA cleavage reaction.

REFERENCES

1. **Abraham, J. M., C. S. Freitag, J. R. Clements, and B. I. Eisenstein.** 1985. An invertible element of DNA controls phase variation of type 1 fimbriae of Escherichia coli. Proc Natl Acad Sci U S A **82**:5724-7.

2. **Alifano, P., C. Piscitelli, V. Blasi, F. Rivellini, A. G. Nappo, C. B. Bruni, and M. S. Carlomagno.** 1992. Processing of a polycistronic mRNA requires a 5' cis element and active translation. Mol Microbiol **6**:787-98.

3. **Apirion, D.** 1973. Degradation of RNA in Escherichia coli. A hypothesis. Mol Gen Genet **122**:313-22.

4. **Apirion, D.** 1980. Genetic mapping and some characterization of the rnpA49 mutation of Escherichia coli that affects the RNA-processing enzyme ribonuclease P. Genetics **94**:291-9.

5. **Aprikian, P., B. Moorefield, and R. H. Reeder.** 2001. New model for the yeast RNA polymerase I transcription cycle. Mol Cell Biol **21**:4847-55.

6. **Arraiano, C. M., and L. E. Maquat.** 2003. Post-transcriptional control of gene expression: effectors of mRNA decay. Mol Microbiol **49**:267-76.

7. **Arraiano, C. M., S. D. Yancey, and S. R. Kushner.** 1988. Stabilization of discrete mRNA breakdown products in ams pnp rnb multiple mutants of Escherichia coli K-12. J Bacteriol **170**:4625-33.

8. **Arthur, M., C. E. Johnson, R. H. Rubin, R. D. Arbeit, C. Campanelli, C. Kim, S. Steinbach, M. Agarwal, R. Wilkinson, and R. Goldstein.** 1989. Molecular epidemiology of adhesin and hemolysin virulence factors among uropathogenic Escherichia coli. Infect Immun **57**:303-13.

9. **Asai, T., D. Zaporojets, C. Squires, and C. L. Squires.** 1999. An Escherichia coli strain with all chromosomal rRNA operons inactivated: complete exchange of rRNA genes between bacteria. Proc Natl Acad Sci U S A **96**:1971-6.

10.   **August, J. T., P. J. Ortiz, and J. Hurwitz.** 1962. Ribonucleic acid-dependent ribonucleotide incorporation. I. Purification and properties of the enzyme. J Biol Chem **237:**3786-93.

11.   **Ausubel, F. M., R. Brent, R. E. Kingston, D. D. Moore, J. G. Seidman, J. A. Smith, and K. Struhl.** 1994. Current Protocols in Molecular Biology. John Wiley & Sons, New York.

12.   **Babitzke, P., L. Granger, J. Olszewski, and S. R. Kushner.** 1993. Analysis of mRNA decay and rRNA processing in Escherichia coli multiple mutants carrying a deletion in RNase III. J Bacteriol **175:**229-39.

13.   **Babitzke, P., and S. R. Kushner.** 1991. The Ams (altered mRNA stability) protein and ribonuclease E are encoded by the same structural gene of Escherichia coli. Proc Natl Acad Sci U S A **88:**1-5.

14.   **Baga, M., M. Goransson, S. Normark, and B. E. Uhlin.** 1985. Transcriptional activation of a pap pilus virulence operon from uropathogenic Escherichia coli. Embo J **4:**3887-93.

15.   **Baga, M., M. Norgren, and S. Normark.** 1987. Biogenesis of E. coli Pap pili: papH, a minor pilin subunit involved in cell anchoring and length modulation. Cell **49:**241-51.

16.   **Ban, N., P. Nissen, J. Hansen, P. B. Moore, and T. A. Steitz.** 2000. The complete atomic structure of the large ribosomal subunit at 2.4 A resolution. Science **289:**905-20.

17.   **Bardwell, J. C., P. Regnier, S. M. Chen, Y. Nakamura, M. Grunberg-Manago, and D. L. Court.** 1989. Autoregulation of RNase III operon by mRNA processing. Embo J **8:**3401-7.

18.   **Barry, G., C. Squires, and C. L. Squires.** 1980. Attenuation and processing of RNA from the rplJL--rpoBC transcription unit of Escherichia coli. Proc Natl Acad Sci U S A **77:**3331-5.

19.   **Barry, G., C. L. Squires, and C. Squires.** 1979. Control features within the rplJL-rpoBC transcription unit of Escherichia coli. Proc Natl Acad Sci U S A **76:**4922-6.

20.   **Belasco, J., and G. Brawerman.** 1993. Control of messenger RNA stability. Academic Press, San Diego.

21.   **Belasco, J. G., G. Nilsson, A. von Gabain, and S. N. Cohen.** 1986. The stability of E. coli gene transcripts is dependent on determinants localized to specific mRNA segments. Cell **46:**245-51.

22.   **Benson, D. A., I. Karsch-Mizrachi, D. J. Lipman, J. Ostell, and D. L. Wheeler.** 2003. GenBank. Nucleic Acids Res **31:**23-7.

23.   **Berghammer, H., and B. Auer.** 1993. "Easypreps": fast and easy plasmid minipreparation for analysis of recombinant clones in E. coli. Biotechniques **14:**524, 528.

24.   **Berisio, R., F. Schluenzen, J. Harms, A. Bashan, T. Auerbach, D. Baram, and A. Yonath.** 2003. Structural insight into the role of the ribosomal tunnel in cellular regulation. Nat Struct Biol **10:**366-70.

25.   **Bernstein, E., A. A. Caudy, S. M. Hammond, and G. J. Hannon.** 2001. Role for a bidentate ribonuclease in the initiation step of RNA interference. Nature **409:**363-6.

26.   **Bernstein, J. A., A. B. Khodursky, P. H. Lin, S. Lin-Chao, and S. N. Cohen.** 2002. Global analysis of mRNA decay and abundance in Escherichia coli at single-gene resolution using two-color fluorescent DNA microarrays. Proc Natl Acad Sci U S A **99:**9697-702.

27.   **Bilge, S. S., J. M. Apostol, Jr., M. A. Aldape, and S. L. Moseley.** 1993. mRNA processing independent of RNase III and RNase E in the expression of the F1845 fimbrial adhesin of Escherichia coli. Proc Natl Acad Sci U S A **90:**1455-9.

28.   Bilge, S. S., J. M. Apostol, Jr., K. J. Fullner, and S. L. Moseley. 1993. Transcriptional organization of the F1845 fimbrial adhesin determinant of Escherichia coli. Mol Microbiol **7**:993-1006.

29.   Bilge, S. S., C. R. Clausen, W. Lau, and S. L. Moseley. 1989. Molecular characterization of a fimbrial adhesin, F1845, mediating diffuse adherence of diarrhea-associated Escherichia coli to HEp-2 cells. J Bacteriol **171**:4281-9.

30.   Birnboim, H. C., and J. Doly. 1979. A rapid alkaline extraction procedure for screening recombinant plasmid DNA. Nucleic Acids Res **7**:1513-23.

31.   Blum, E., A. J. Carpousis, and C. F. Higgins. 1999. Polyadenylation promotes degradation of 3'-structured RNA by the Escherichia coli mRNA degradosome in vitro. J Biol Chem **274**:4009-16.

32.   Bouvet, P., and J. G. Belasco. 1992. Control of RNase E-mediated RNA degradation by 5'-terminal base pairing in E. coli. Nature **360**:488-91.

33.   Britton, R. A., B. S. Powell, S. Dasgupta, Q. Sun, W. Margolin, J. R. Lupski, and D. L. Court. 1998. Cell cycle arrest in Era GTPase mutants: a potential growth rate-regulated checkpoint in Escherichia coli. Mol Microbiol **27**:739-50.

34.   Burgess, S., J. R. Couto, and C. Guthrie. 1990. A putative ATP binding protein influences the fidelity of branchpoint recognition in yeast splicing. Cell **60**:705-17.

35.   Cao, G. J., and N. Sarkar. 1992. Identification of the gene for an Escherichia coli poly(A) polymerase. Proc Natl Acad Sci U S A **89**:10380-4.

36.   Cao, J., and A. P. Geballe. 1996. Coding sequence-dependent ribosomal arrest at termination of translation. Mol Cell Biol **16**:603-8.

37.   Cao, J., and A. P. Geballe. 1996. Inhibition of nascent-peptide release at translation termination. Mol Cell Biol **16**:7109-14.

38. **Cao, J., and A. P. Geballe.** 1998. Ribosomal release without peptidyl tRNA hydrolysis at translation termination in a eukaryotic system. Rna **4:**181-8.

39. **Cao, J., and A. P. Geballe.** 1995. Translational inhibition by a human cytomegalovirus upstream open reading frame despite inefficient utilization of its AUG codon. J Virol **69:**1030-6.

40. **Carpousis, A. J.** 2002. The Escherichia coli RNA degradosome: structure, function and relationship in other ribonucleolytic multienzyme complexes. Biochem Soc Trans **30:**150-5.

41. **Caruthers, J. M., E. R. Johnson, and D. B. McKay.** 2000. Crystal structure of yeast initiation factor 4A, a DEAD-box RNA helicase. Proc Natl Acad Sci U S A **97:**13080-5.

42. **Casadaban, M. J., and S. N. Cohen.** 1980. Analysis of gene control signals by DNA fusion and cloning in Escherichia coli. J Mol Biol **138:**179-207.

43. **Casaregola, S., A. Jacq, D. Laoudj, G. McGurk, S. Margarson, M. Tempete, V. Norris, and I. B. Holland.** 1992. Cloning and analysis of the entire Escherichia coli ams gene. ams is identical to hmp1 and encodes a 114 kDa protein that migrates as a 180 kDa protein. J Mol Biol **228:**30-40.

44. **Case, C. C., E. L. Simons, and R. W. Simons.** 1990. The IS10 transposase mRNA is destabilized during antisense RNA control. Embo J **9:**1259-66.

45. **Chang, A. C., and S. N. Cohen.** 1978. Construction and characterization of amplifiable multicopy DNA cloning vehicles derived from the P15A cryptic miniplasmid. J Bacteriol **134:**1141-56.

46. **Chang, C. P., D. H. Vesole, J. Nelson, M. B. Oldstone, and M. F. Stinski.** 1989. Identification and expression of a human cytomegalovirus early glycoprotein. J Virol **63:**3330-7.

47. **Charollais, J., D. Pflieger, J. Vinh, M. Dreyfus, and I. Iost.** 2003. The DEAD-box RNA helicase SrmB is involved in the assembly of 50S ribosomal subunits in Escherichia coli. Mol Microbiol **48:**1253-65.

48. **Chen, J. H., and R. J. Lin.** 1990. The yeast PRP2 protein, a putative RNA-dependent ATPase, shares extensive sequence homology with two other pre-mRNA splicing factors. Nucleic Acids Res **18**:6447.

49. **Christensen, S. K., and K. Gerdes.** 2003. RelE toxins from bacteria and Archaea cleave mRNAs on translating ribosomes, which are rescued by tmRNA. Mol Microbiol **48**:1389-400.

50. **Coburn, G. A., and G. A. Mackie.** 1999. Degradation of mRNA in Escherichia coli: an old problem with some new twists. Prog Nucleic Acid Res Mol Biol **62**:55-108.

51. **Coburn, G. A., and G. A. Mackie.** 1996. Differential sensitivities of portions of the mRNA for ribosomal protein S20 to 3'-exonucleases dependent on oligoadenylation and RNA secondary structure. J Biol Chem **271**:15776-81.

52. **Coburn, G. A., and G. A. Mackie.** 1998. Reconstitution of the degradation of the mRNA for ribosomal protein S20 with purified enzymes. J Mol Biol **279**:1061-74.

53. **Collier, J., E. Binet, and P. Bouloc.** 2002. Competition between SsrA tagging and translational termination at weak stop codons in Escherichia coli. Mol Microbiol **45**:745-54.

54. **Company, M., J. Arenas, and J. Abelson.** 1991. Requirement of the RNA helicase-like protein PRP22 for release of messenger RNA from spliceosomes. Nature **349**:487-93.

55. **Cormack, B. P., R. H. Valdivia, and S. Falkow.** 1996. FACS-optimized mutants of the green fluorescent protein (GFP). Gene **173**:33-8.

56. **Datta, A. K., and D. P. Burma.** 1972. Association of ribonuclease I with ribosomes and their subunits. J Biol Chem **247**:6795-801.

57. **De Feyter, R., Y. Yang, and D. W. Gabriel.** 1993. Gene-for-genes interactions between cotton R genes and Xanthomonas campestris pv. malvacearum avr genes. Mol Plant Microbe Interact **6**:225-37.

58. **Degnin, C. R., M. R. Schleiss, J. Cao, and A. P. Geballe.** 1993. Translational inhibition mediated by a short upstream open reading frame in the human cytomegalovirus gpUL4 (gp48) transcript. J Virol **67:**5514-21.

59. **Deutscher, M. P., and N. B. Reuven.** 1991. Enzymatic basis for hydrolytic versus phosphorolytic mRNA degradation in Escherichia coli and Bacillus subtilis. Proc Natl Acad Sci U S A **88:**3277-80.

60. **Diaz, R., K. Nordstrom, and W. L. Staudenbauer.** 1981. Plasmid R1 DNA replication dependent on protein synthesis in cell-free extracts of E. coli. Nature **289:**326-8.

61. **Diges, C. M., and O. C. Uhlenbeck.** 2001. Escherichia coli DbpA is an RNA helicase that requires hairpin 92 of 23S rRNA. Embo J **20:**5503-12.

62. **Donovan, W. P., and S. R. Kushner.** 1986. Polynucleotide phosphorylase and ribonuclease II are required for cell viability and mRNA turnover in Escherichia coli K-12. Proc Natl Acad Sci U S A **83:**120-4.

63. **Du, M. X., R. B. Johnson, X. L. Sun, K. A. Staschke, J. Colacino, and Q. M. Wang.** 2002. Comparative characterization of two DEAD-box RNA helicases in superfamily II: human translation-initiation factor 4A and hepatitis C virus non-structural protein 3 (NS3) helicase. Biochem J **363:**147-55.

64. **Dunn, J. J., and F. W. Studier.** 1973. T7 early RNAs and Escherichia coli ribosomal RNAs are cut from large precursor RNAs in vivo by ribonuclease 3. Proc Natl Acad Sci U S A **70:**3296-3300.

65. **Frank, J., J. Zhu, P. Penczek, Y. Li, S. Srivastava, A. Verschoor, M. Radermacher, R. Grassucci, R. K. Lata, and R. K. Agrawal.** 1995. A model of protein synthesis based on cryo-electron microscopy of the E. coli ribosome. Nature **376:**441-4.

66. **Gabashvili, I. S., S. T. Gregory, M. Valle, R. Grassucci, M. Worbs, M. C. Wahl, A. E. Dahlberg, and J. Frank.** 2001. The polypeptide tunnel system in the ribosome and its gating in erythromycin resistance mutants of L4 and L22. Mol Cell **8:**181-8.

67.   **Gay, D. A., S. S. Sisodia, and D. W. Cleveland.** 1989. Autoregulatory control of beta-tubulin mRNA stability is linked to translation elongation. Proc Natl Acad Sci U S A **86:**5763-7.

68.   **Gay, D. A., T. J. Yen, J. T. Lau, and D. W. Cleveland.** 1987. Sequences that confer beta-tubulin autoregulation through modulated mRNA stability reside within exon 1 of a beta-tubulin mRNA. Cell **50:**671-9.

69.   **Gesteland, R. F.** 1966. Isolation and characterization of ribonuclease I mutants of Escherichia coli. J Mol Biol **16:**67-84.

70.   **Ghosh, S., and M. P. Deutscher.** 1999. Oligoribonuclease is an essential component of the mRNA decay pathway. Proc Natl Acad Sci U S A **96:**4372-7.

71.   **Giron, J. A., T. Jones, F. Millan-Velasco, E. Castro-Munoz, L. Zarate, J. Fry, G. Frankel, S. L. Moseley, B. Baudry, J. B. Kaper, and et al.** 1991. Diffuse-adhering Escherichia coli (DAEC) as a putative cause of diarrhea in Mayan children in Mexico. J Infect Dis **163:**507-13.

72.   **Godefroy-Colburn, T., and M. Grunberg-Manago.** 1972. Polynucleotide phosphorylase. Enzymes **7:**533-574.

73.   **Goluszko, P., S. L. Moseley, L. D. Truong, A. Kaul, J. R. Williford, R. Selvarangan, S. Nowicki, and B. Nowicki.** 1997. Development of experimental model of chronic pyelonephritis with Escherichia coli O75:K5:H-bearing Dr fimbriae: mutation in the dra region prevented tubulointerstitial nephritis. J Clin Invest **99:**1662-72.

74.   **Gong, F., and C. Yanofsky.** 2001. Reproducing tna operon regulation in vitro in an S-30 system. Tryptophan induction inhibits cleavage of TnaC peptidyl-tRNA. J Biol Chem **276:**1974-83.

75.   **Gottesman, S., E. Roche, Y. Zhou, and R. T. Sauer.** 1998. The ClpXP and ClpAP proteases degrade proteins with carboxy-terminal peptide tails added by the SsrA-tagging system. Genes Dev **12:**1338-47.

76.   **Guthrie, C., and G. R. Fink.** 1991. Guide to yeast genetics and molecular biology. Academic Press, San Diego.

77.   **Gutmann, S., P. W. Haebel, L. Metzinger, M. Sutter, B. Felden, and N. Ban.** 2003. Crystal structure of the transfer-RNA domain of transfer-messenger RNA in complex with SmpB. Nature **424:**699-703.

78.   **Hajnsdorf, E., F. Braun, J. Haugel-Nielsen, J. Le Derout, and P. Regnier.** 1996. Multiple degradation pathways of the rpsO mRNA of Escherichia coli. RNase E interacts with the 5' and 3' extremities of the primary transcript. Biochimie **78:**416-24.

79.   **Hajnsdorf, E., F. Braun, J. Haugel-Nielsen, and P. Regnier.** 1995. Polyadenylylation destabilizes the rpsO mRNA of Escherichia coli. Proc Natl Acad Sci U S A **92:**3973-7.

80.   **Hannon, G. J.** 2002. RNA interference. Nature **418:**244-51.

81.   **Hayes, C. S., B. Bose, and R. T. Sauer.** 2002. Stop codons preceded by rare arginine codons are efficient determinants of SsrA tagging in Escherichia coli. Proc Natl Acad Sci U S A **99:**3440-5.

82.   **Hotz, H. R., and B. Schwer.** 1998. Mutational analysis of the yeast DEAH-box splicing factor Prp16. Genetics **149:**807-15.

83.   **Hughes, K. T., B. T. Cookson, D. Ladika, B. M. Olivera, and J. R. Roth.** 1983. 6-Aminonicotinamide-resistant mutants of Salmonella typhimurium. J Bacteriol **154:**1126-36.

84.   **Jallat, C., V. Livrelli, A. Darfeuille-Michaud, C. Rich, and B. Joly.** 1993. Escherichia coli strains involved in diarrhea in France: high prevalence and heterogeneity of diffusely adhering strains. J Clin Microbiol **31:**2031-7.

85.   **Jankowsky, E., C. H. Gross, S. Shuman, and A. M. Pyle.** 2001. Active disruption of an RNA-protein interaction by a DExH/D RNA helicase. Science **291:**121-5.

86. **Jordi, B. J., I. E. op den Camp, L. A. de Haan, B. A. van der Zeijst, and W. Gaastra.** 1993. Differential decay of RNA of the CFA/I fimbrial operon and control of relative gene expression. Journal of Bacteriology **175**:7976-81.

87. **Jouve, M., M. I. Garcia, P. Courcoux, A. Labigne, P. Gounon, and C. Le Bouguenec.** 1997. Adhesion to and invasion of HeLa cells by pathogenic Escherichia coli carrying the afa-3 gene cluster are mediated by the AfaE and AfaD proteins, respectively. Infect Immun **65**:4082-9.

88. **Kaberdin, V. R., A. Miczak, J. S. Jakobsen, S. Lin-Chao, K. J. McDowall, and A. von Gabain.** 1998. The endoribonucleolytic N-terminal half of Escherichia coli RNase E is evolutionarily conserved in Synechocystis sp. and other bacteria but not the C-terminal half, which is sufficient for degradosome assembly. Proc Natl Acad Sci U S A **95**:11637-42.

89. **Kaga, N., G. Umitsuki, K. Nagai, and M. Wachi.** 2002. RNase G-dependent degradation of the eno mRNA encoding a glycolysis enzyme enolase in Escherichia coli. Biosci Biotechnol Biochem **66**:2216-20.

90. **Karzai, A. W., and R. T. Sauer.** 2001. Protein factors associated with the SsrA.SmpB tagging and ribosome rescue complex. Proc Natl Acad Sci U S A **98**:3040-4.

91. **Karzai, A. W., M. M. Susskind, and R. T. Sauer.** 1999. SmpB, a unique RNA-binding protein essential for the peptide-tagging activity of SsrA (tmRNA). Embo J **18**:3793-9.

92. **Keiler, K. C., P. R. Waller, and R. T. Sauer.** 1996. Role of a peptide tagging system in degradation of proteins synthesized from damaged messenger RNA. Science **271**:990-3.

93. **Kennell, D., and H. Riezman.** 1977. Transcription and translation initiation frequencies of the Escherichia coli lac operon. J Mol Biol **114**:1-21.

94. **Kim, S. H., J. Smith, A. Claude, and R. J. Lin.** 1992. The purified yeast pre-mRNA splicing factor PRP2 is an RNA-dependent NTPase. Embo J **11**:2319-26.

95.   **Kisselev, L. L., and R. H. Buckingham.** 2000. Translational termination comes of age. Trends Biochem Sci **25:**561-6.

96.   **Klug, G., C. W. Adams, J. Belasco, B. Doerge, and S. N. Cohen.** 1987. Biological consequences of segmental alterations in mRNA stability: effects of deletion of the intercistronic hairpin loop region of the Rhodobacter capsulatus puf operon. Embo J **6:**3515-20.

97.   **Knudsen, B., J. Wower, C. Zwieb, and J. Gorodkin.** 2001. tmRDB (tmRNA database). Nucleic Acids Res **29:**171-2.

98.   **Kushner, S. R.** 2002. mRNA decay in Escherichia coli comes of age. J Bacteriol **184:**4658-65; discussion 4657.

99.   **Lesley, S. A.** 1995. Preparation and use of E. coli S-30 extracts. Methods Mol Biol **37:**265-78.

100. **Levchenko, I., M. Seidel, R. T. Sauer, and T. A. Baker.** 2000. A specificity-enhancing factor for the ClpXP degradation machine. Science **289:**2354-6.

101. **Levine, M. M., C. Ferreccio, V. Prado, M. Cayazzo, P. Abrego, J. Martinez, L. Maggi, M. M. Baldini, W. Martin, D. Maneval, and et al.** 1993. Epidemiologic studies of Escherichia coli diarrheal infections in a low socioeconomic level peri-urban community in Santiago, Chile. Am J Epidemiol **138:**849-69.

102. **Li, Y., and S. Altman.** 2003. A specific endoribonuclease, RNase P, affects gene expression of polycistronic operon mRNAs. Proc Natl Acad Sci U S A **100:**13213-8.

103. **Li, Y., K. Cole, and S. Altman.** 2003. The effect of a single, temperature-sensitive mutation on global gene expression in Escherichia coli. Rna **9:**518-32.

104. **Li, Z., and M. P. Deutscher.** 2002. RNase E plays an essential role in the maturation of Escherichia coli tRNA precursors. Rna **8:**97-109.

105. **Li, Z., S. Pandit, and M. P. Deutscher.** 1999. RNase G (CafA protein) and RNase E are both required for the 5' maturation of 16S ribosomal RNA. Embo J **18:**2878-85.

106. **Linder, P., P. F. Lasko, M. Ashburner, P. Leroy, P. J. Nielsen, K. Nishi, J. Schnier, and P. P. Slonimski.** 1989. Birth of the D-E-A-D box. Nature **337:**121-2.

107. **Liu, S. L., and K. E. Sanderson.** 1998. Homologous recombination between rrn operons rearranges the chromosome in host-specialized species of Salmonella. FEMS Microbiol Lett **164:**275-81.

108. **Loomis, W. P., J. T. Koo, T. P. Cheung, and S. L. Moseley.** 2001. A tripeptide sequence within the nascent DaaP protein is required for mRNA processing of a fimbrial operon in Escherichia coli. Mol Microbiol **39:**693-707.

109. **Loomis, W. P., and S. L. Moseley.** 1998. Translational control of mRNA processing in the F1845 fimbrial operon of Escherichia coli. Mol Microbiol **30:**843-53.

110. **Lovett, P. S., and E. J. Rogers.** 1996. Ribosome regulation by the nascent peptide. Microbiol Rev **60:**366-85.

111. **Lublin, D. M., and J. P. Atkinson.** 1989. Decay-accelerating factor: biochemistry, molecular biology, and function. Annu Rev Immunol **7:**35-58.

112. **Lundberg, U., and S. Altman.** 1995. Processing of the precursor to the catalytic RNA subunit of RNase P from Escherichia coli. Rna **1:**327-34.

113. **Lupski, J. R., and G. N. Godson.** 1984. The rpsU-dnaG-rpoD macromolecular synthesis operon of E. coli. Cell **39:**251-2.

114. **Mackie, G. A.** 1998. Ribonuclease E is a 5'-end-dependent endonuclease. Nature **395:**720-3.

115. **Mackie, G. A.** 1991. Specific endonucleolytic cleavage of the mRNA for ribosomal protein S20 of Escherichia coli requires the product of the ams gene in vivo and in vitro. J Bacteriol **173**:2488-97.

116. **Mackie, G. A., and J. L. Genereaux.** 1993. The role of RNA structure in determining RNase E-dependent cleavage sites in the mRNA for ribosomal protein S20 in vitro. J Mol Biol **234**:998-1012.

117. **Mackie, G. A., J. L. Genereaux, and S. K. Masterman.** 1997. Modulation of the activity of RNase E in vitro by RNA sequences and secondary structures 5' to cleavage sites. J Biol Chem **272**:609-16.

118. **Maniatis, T., E. F. Fritsch, and J. Sambrook.** 1982. Molecular cloning. A Laboratory Manual. Cold Spring Harbor Laboratory Press, Cold Spring Harbor, NY.

119. **Marujo, P. E., F. Braun, J. Haugel-Nielsen, J. Le Derout, C. M. Arraiano, and P. Regnier.** 2003. Inactivation of the decay pathway initiated at an internal site by RNase E promotes poly(A)-dependent degradation of the rpsO mRNA in Escherichia coli. Mol Microbiol **50**:1283-94.

120. **McDowall, K. J., and S. N. Cohen.** 1996. The N-terminal domain of the rne gene product has RNase E activity and is non-overlapping with the arginine-rich RNA-binding site. J Mol Biol **255**:349-55.

121. **McDowall, K. J., R. G. Hernandez, S. Lin-Chao, and S. N. Cohen.** 1993. The ams-1 and rne-3071 temperature-sensitive mutations in the ams gene are in close proximity to each other and cause substitutions within a domain that resembles a product of the Escherichia coli mre locus. J Bacteriol **175**:4245-9.

122. **McNicholas, P., R. Salavati, and D. Oliver.** 1997. Dual regulation of Escherichia coli secA translation by distinct upstream elements. J Mol Biol **265**:128-41.

123. **Miller, J. H.** 1972. Experiments in molecular genetics. Cold Spring Harbor Laboratory, [Cold Spring Harbor, N.Y.].

124. **Miller, J. H.** 1992. A short course in bacterial genetics : a laboratory manual and handbook for Escherichia coli and related bacteria. Cold Spring Harbor Laboratory Press, Plainview, N.Y.

125. **Milligan, R. A., and P. N. Unwin.** 1986. Location of exit channel for nascent protein in 80S ribosome. Nature **319:**693-5.

126. **Misra, T. K., and D. Apirion.** 1979. RNase E, an RNA processing enzyme from Escherichia coli. J Biol Chem **254:**11154-9.

127. **Mohanty, B. K., and S. R. Kushner.** 2002. Polyadenylation of Escherichia coli transcripts plays an integral role in regulating intracellular levels of polynucleotide phosphorylase and RNase E. Mol Microbiol **45:**1315-24.

128. **Mohanty, B. K., and S. R. Kushner.** 2000. Polynucleotide phosphorylase, RNase II and RNase E play different roles in the in vivo modulation of polyadenylation in Escherichia coli. Mol Microbiol **36:**982-94.

129. **Moriya, H., H. Kasai, and K. Isono.** 1995. Cloning and characterization of the hrpA gene in the terC region of Escherichia coli that is highly similar to the DEAH family RNA helicase genes of Saccharomyces cerevisiae. Nucleic Acids Res **23:**595-8.

130. **Morris, D. R., and A. P. Geballe.** 2000. Upstream open reading frames as regulators of mRNA translation. Mol Cell Biol **20:**8635-42.

131. **Morschhauser, J., B. E. Uhlin, and J. Hacker.** 1993. Transcriptional analysis and regulation of the sfa determinant coding for S fimbriae of pathogenic Escherichia coli strains. Molecular & General Genetics **238:**97-105.

132. **Mudd, E. A., A. J. Carpousis, and H. M. Krisch.** 1990. Escherichia coli RNase E has a role in the decay of bacteriophage T4 mRNA [published erratum appears in Genes Dev 1990 Jun;4(6):1078]. Genes Dev **4:**873-81.

133. **Mudd, E. A., P. Prentki, D. Belin, and H. M. Krisch.** 1988. Processing of unstable bacteriophage T4 gene 32 mRNAs into a stable species requires Escherichia coli ribonuclease E. Embo J **7:**3601-7.

134. **Nakamura, Y., and K. Ito.** 2002. A tripeptide discriminator for stop codon recognition. FEBS Lett **514**:30-3.

135. **Nakatogawa, H., and K. Ito.** 2002. The ribosomal exit tunnel functions as a discriminating gate. Cell **108**:629-36.

136. **Nakatogawa, H., and K. Ito.** 2001. Secretion monitor, SecM, undergoes self-translation arrest in the cytosol. Mol Cell **7**:185-92.

137. **Newbury, S. F., N. H. Smith, and C. F. Higgins.** 1987. Differential mRNA stability controls relative gene expression within a polycistronic operon. Cell **51**:1131-43.

138. **Newbury, S. F., N. H. Smith, E. C. Robinson, I. D. Hiles, and C. F. Higgins.** 1987. Stabilization of translationally active mRNA by prokaryotic REP sequences. Cell **48**:297-310.

139. **Nichols, B. P., O. Shafiq, and V. Meiners.** 1998. Sequence analysis of Tn10 insertion sites in a collection of Escherichia coli strains used for genetic mapping and strain construction. J Bacteriol **180**:6408-11.

140. **Nilsson, P., and B. E. Uhlin.** 1991. Differential decay of a polycistronic Escherichia coli transcript is initiated by RNaseE-dependent endonucleolytic processing. Mol Microbiol **5**:1791-9.

141. **Nissen, P., J. Hansen, N. Ban, P. B. Moore, and T. A. Steitz.** 2000. The structural basis of ribosome activity in peptide bond synthesis. Science **289**:920-30.

142. **Noskov, V. N., N. Kouprina, S. H. Leem, I. Ouspenski, J. C. Barrett, and V. Larionov.** 2003. A general cloning system to selectively isolate any eukaryotic or prokaryotic genomic region in yeast. BMC Genomics **4**:16.

143. **Nowicki, B., A. Labigne, S. Moseley, R. Hull, S. Hull, and J. Moulds.** 1990. The Dr hemagglutinin, afimbrial adhesins AFA-I and AFA-III, and F1845 fimbriae of uropathogenic and diarrhea-associated Escherichia coli belong to a family of hemagglutinins with Dr receptor recognition. Infect Immun **58**:279-81.

144. **Nowicki, B., M. Martens, A. Hart, and S. Nowicki.** 1994. Gestational age-dependent distribution of Escherichia coli fimbriae in pregnant patients with pyelonephritis. Ann N Y Acad Sci **730:**290-1.

145. **Nowicki, B., L. Truong, J. Moulds, and R. Hull.** 1988. Presence of the Dr receptor in normal human tissues and its possible role in the pathogenesis of ascending urinary tract infection. Am J Pathol **133:**1-4.

146. **Ogle, J. M., D. E. Brodersen, W. M. Clemons, Jr., M. J. Tarry, A. P. Carter, and V. Ramakrishnan.** 2001. Recognition of cognate transfer RNA by the 30S ribosomal subunit. Science **292:**897-902.

147. **Okada, Y., M. Wachi, A. Hirata, K. Suzuki, K. Nagai, and M. Matsuhashi.** 1994. Cytoplasmic axial filaments in Escherichia coli cells: possible function in the mechanism of chromosome segregation and cell division. J Bacteriol **176:**917-22.

148. **Oliver, D., J. Norman, and S. Sarker.** 1998. Regulation of Escherichia coli secA by cellular protein secretion proficiency requires an intact gene X signal sequence and an active translocon. J Bacteriol **180:**5240-2.

149. **Ono, M., and M. Kuwano.** 1979. A conditional lethal mutation in an Escherichia coli strain with a longer chemical lifetime of messenger RNA. J Mol Biol **129:**343-57.

150. **Ow, M. C., and S. R. Kushner.** 2002. Initiation of tRNA maturation by RNase E is essential for cell viability in E. coli. Genes Dev **16:**1102-15.

151. **Ow, M. C., Q. Liu, and S. R. Kushner.** 2000. Analysis of mRNA decay and rRNA processing in Escherichia coli in the absence of RNase E-based degradosome assembly. Mol Microbiol **38:**854-66.

152. **Ow, M. C., T. Perwez, and S. R. Kushner.** 2003. RNase G of Escherichia coli exhibits only limited functional overlap with its essential homologue, RNase E. Mol Microbiol **49:**607-22.

153. **Pace, N. R., and D. Smith.** 1990. Ribonuclease P: function and variation. J Biol Chem **265:**3587-90.

154. **Pachter, J. S., T. J. Yen, and D. W. Cleveland.** 1987. Autoregulation of tubulin expression is achieved through specific degradation of polysomal tubulin mRNAs. Cell **51:**283-92.

155. **Pedersen, K., A. V. Zavialov, M. Y. Pavlov, J. Elf, K. Gerdes, and M. Ehrenberg.** 2003. The bacterial toxin RelE displays codon-specific cleavage of mRNAs in the ribosomal A site. Cell **112:**131-40.

156. **Pedersen, S.** 1984. Escherichia coli ribosomes translate in vivo with variable rate. Embo J **3:**2895-8.

157. **Persing, D. H., L. McGinty, C. W. Adams, and R. G. Fowler.** 1981. Mutational specificity of the base analogue, 2-aminopurine, in Escherichia coli. Mutat Res **83:**25-37.

158. **Pham, T., A. Kaul, A. Hart, P. Goluszko, J. Moulds, S. Nowicki, D. M. Lublin, and B. J. Nowicki.** 1995. dra-related X adhesins of gestational pyelonephritis-associated Escherichia coli recognize SCR-3 and SCR-4 domains of recombinant decay- accelerating factor. Infect Immun **63:**1663-8.

159. **Portier, C., L. Dondon, M. Grunberg-Manago, and P. Regnier.** 1987. The first step in the functional inactivation of the Escherichia coli polynucleotide phosphorylase messenger is a ribonuclease III processing at the 5' end. Embo J **6:**2165-70.

160. **Py, B., H. Causton, E. A. Mudd, and C. F. Higgins.** 1994. A protein complex mediating mRNA degradation in Escherichia coli. Mol Microbiol **14:**717-29.

161. **Py, B., C. F. Higgins, H. M. Krisch, and A. J. Carpousis.** 1996. A DEAD-box RNA helicase in the Escherichia coli RNA degradosome. Nature **381:**169-72.

162. **Ramakrishnan, V.** 2002. Ribosome structure and the mechanism of translation. Cell **108:**557-72.

163. **Rauhut, R., and G. Klug.** 1999. mRNA degradation in bacteria. FEMS Microbiol Rev **23:**353-70.

164. **Ray, B. K., and D. Apirion.** 1981. Transfer RNA precursors are accumulated in Escherichia coli in the absence of RNase E. Eur J Biochem **114:**517-24.

165. **Raymond, C. K., E. H. Sims, A. Kas, D. H. Spencer, T. V. Kutyavin, R. G. Ivey, Y. Zhou, R. Kaul, J. B. Clendenning, and M. V. Olson.** 2002. Genetic variation at the O-antigen biosynthetic locus in Pseudomonas aeruginosa. J Bacteriol **184:**3614-22.

166. **Regnier, P., and C. M. Arraiano.** 2000. Degradation of mRNA in bacteria: emergence of ubiquitous features. Bioessays **22:**235-44.

167. **Regnier, P., and E. Hajnsdorf.** 1991. Decay of mRNA encoding ribosomal protein S15 of Escherichia coli is initiated by an RNase E-dependent endonucleolytic cleavage that removes the 3' stabilizing stem and loop structure. J Mol Biol **217:**283-92.

168. **Reiner, A. M.** 1969. Isolation and mapping of polynucleotide phosphorylase mutants of Escherichia coli. J Bacteriol **97:**1431-6.

169. **Robertson, H. D.** 1982. Escherichia coli ribonuclease III cleavage sites. Cell **30:**669-72.

170. **Robertson, H. D., Webster, R.E., and N.D. Zinder.** 1967. A nuclease specific for double-stranded RNA. Virology **12:**718-719.

171. **Roche, E. D., and R. T. Sauer.** 1999. SsrA-mediated peptide tagging caused by rare codons and tRNA scarcity. Embo J **18:**4579-89.

172. **Ruby, S. W., and J. Abelson.** 1991. Pre-mRNA splicing in yeast. Trends Genet **7:**79-85.

173. **Rudinger-Thirion, J., R. Giege, and B. Felden.** 1999. Aminoacylated tmRNA from Escherichia coli interacts with prokaryotic elongation factor Tu. Rna **5**:989-92.

174. **Saito, H., and C. C. Richardson.** 1981. Processing of mRNA by ribonuclease III regulates expression of gene 1.2 of bacteriophage T7. Cell **27**:533-42.

175. **Sambrook, J., and D. W. Russell.** 2001. Molecular cloning : a laboratory manual, 3rd ed. Cold Spring Harbor Laboratory Press, Cold Spring Harbor, N.Y.

176. **Schagger, H., and G. von Jagow.** 1987. Tricine-sodium dodecyl sulfate-polyacrylamide gel electrophoresis for the separation of proteins in the range from 1 to 100 kDa. Anal Biochem **166**:368-79.

177. **Schmeissner, U., K. McKenney, M. Rosenberg, and D. Court.** 1984. Removal of a terminator structure by RNA processing regulates int gene expression. J Mol Biol **176**:39-53.

178. **Schneider, S., H. R. Hotz, and B. Schwer.** 2002. Characterization of dominant-negative mutants of the DEAH-box splicing factors Prp22 and Prp16. J Biol Chem **277**:15452-8.

179. **Schwer, B.** 2001. A new twist on RNA helicases: DExH/D box proteins as RNPases. Nat Struct Biol **8**:113-6.

180. **Schwer, B., and C. H. Gross.** 1998. Prp22, a DExH-box RNA helicase, plays two distinct roles in yeast pre-mRNA splicing. Embo J **17**:2086-94.

181. **Schwer, B., and C. Guthrie.** 1991. PRP16 is an RNA-dependent ATPase that interacts transiently with the spliceosome. Nature **349**:494-9.

182. **Shimizu, Y., and T. Ueda.** 2002. The role of SmpB protein in trans-translation. FEBS Lett **514**:74-7.

183. **Sikorski, R. S., and P. Hieter.** 1989. A system of shuttle vectors and yeast host strains designed for efficient manipulation of DNA in Saccharomyces cerevisiae. Genetics **122**:19-27.

184. **Silverman, E., G. Edwalds-Gilbert, and R. J. Lin.** 2003. DExD/H-box proteins and their partners: helping RNA helicases unwind. Gene **312**:1-16.

185. **Simon, R., U. Priefer, and A. Puhler.** 1983. A Broad Host Range Mobilization System for Invivo Genetic-Engineering - Transposon Mutagenesis in Gram-Negative Bacteria. Bio-Technology **1**:784-791.

186. **Singer, M., T. A. Baker, G. Schnitzler, S. M. Deischel, M. Goel, W. Dove, K. J. Jaacks, A. D. Grossman, J. W. Erickson, and C. A. Gross.** 1989. A collection of strains containing genetically linked alternating antibiotic resistance elements for genetic mapping of Escherichia coli. Microbiol Rev **53**:1-24.

187. **Singer, R. H., and S. Penman.** 1973. Messenger RNA in HeLa cells: kinetics of formation and decay. J Mol Biol **78**:321-34.

188. **Sokurenko, E. V., V. Tchesnokova, A. T. Yeung, C. A. Oleykowski, E. Trintchina, K. T. Hughes, R. A. Rashid, J. M. Brint, S. L. Moseley, and S. Lory.** 2001. Detection of simple mutations and polymorphisms in large genomic regions. Nucleic Acids Res **29**:E111.

189. **Song, H., P. Mugnier, A. K. Das, H. M. Webb, D. R. Evans, M. F. Tuite, B. A. Hemmings, and D. Barford.** 2000. The crystal structure of human eukaryotic release factor eRF1--mechanism of stop codon recognition and peptidyl-tRNA hydrolysis. Cell **100**:311-21.

190. **Spahr, P. F.** 1964. Purification and Properties of Ribonuclease Ii from Escherichia Coli. J Biol Chem **239**:3716-26.

191. **Staley, J. P., and C. Guthrie.** 1998. Mechanical devices of the spliceosome: motors, clocks, springs, and things. Cell **92**:315-26.

192. **Stapleton, A., S. Moseley, and W. E. Stamm.** 1991. Urovirulence determinants in Escherichia coli isolates causing first-episode and recurrent cystitis in women. J Infect Dis **163**:773-9.

193. **Steege, D. A.** 2000. Emerging features of mRNA decay in bacteria. Rna **6**:1079-90.

194. **Sunohara, T., T. Abo, T. Inada, and H. Aiba.** 2002. The C-terminal amino acid sequence of nascent peptide is a major determinant of SsrA tagging at all three stop codons. Rna **8**:1416-27.

195. **Svard, S. G., and L. A. Kirsebom.** 1993. Determinants of Escherichia coli RNase P cleavage site selection: a detailed in vitro and in vivo analysis. Nucleic Acids Res **21**:427-34.

196. **Tadaki, T., M. Fukushima, C. Ushida, H. Himeno, and A. Muto.** 1996. Interaction of 10Sa RNA with ribosomes in Escherichia coli. FEBS Lett **399**:223-6.

197. **Tanner, N. K., and P. Linder.** 2001. DExD/H box RNA helicases: from generic motors to specific dissociation functions. Mol Cell **8**:251-62.

198. **Taraseviciene, L., G. R. Bjork, and B. E. Uhlin.** 1995. Evidence for an RNA binding region in the Escherichia coli processing endoribonuclease RNase E. J Biol Chem **270**:26391-8.

199. **Taylor, W. E., D. B. Straus, A. D. Grossman, Z. F. Burton, C. A. Gross, and R. R. Burgess.** 1984. Transcription from a heat-inducible promoter causes heat shock regulation of the sigma subunit of E. coli RNA polymerase. Cell **38**:371-81.

200. **Tenson, T., and M. Ehrenberg.** 2002. Regulatory nascent peptides in the ribosomal tunnel. Cell **108**:591-4.

201. **Theodorakis, N. G., and D. W. Cleveland.** 1992. Physical evidence for cotranslational regulation of beta-tubulin mRNA degradation. Mol Cell Biol **12**:791-9.

202. **Thompson, J., D. F. Kim, M. O'Connor, K. R. Lieberman, M. A. Bayfield, S. T. Gregory, R. Green, H. F. Noller, and A. E. Dahlberg.** 2001. Analysis of mutations at residues A2451 and G2447 of 23S rRNA in the peptidyltransferase active site of the 50S ribosomal subunit. Proc Natl Acad Sci U S A **98:**9002-7.

203. **Tock, M. R., A. P. Walsh, G. Carroll, and K. J. McDowall.** 2000. The CafA protein required for the 5'-maturation of 16 S rRNA is a 5'-end-dependent ribonuclease that has context-dependent broad sequence specificity. J Biol Chem **275:**8726-32.

204. **Tomcsanyi, T., and D. Apirion.** 1985. Processing enzyme ribonuclease E specifically cleaves RNA I. An inhibitor of primer formation in plasmid DNA synthesis. J Mol Biol **185:**713-20.

205. **Vanzo, N. F., Y. S. Li, B. Py, E. Blum, C. F. Higgins, L. C. Raynal, H. M. Krisch, and A. J. Carpousis.** 1998. Ribonuclease E organizes the protein interactions in the Escherichia coli RNA degradosome. Genes Dev **12:**2770-81.

206. **Vestergaard, B., L. B. Van, G. R. Andersen, J. Nyborg, R. H. Buckingham, and M. Kjeldgaard.** 2001. Bacterial polypeptide release factor RF2 is structurally distinct from eukaryotic eRF1. Mol Cell **8:**1375-82.

207. **Wachi, M., N. Kaga, G. Umitsuki, D. P. Clark, and K. Nagai.** 2001. A novel RNase G mutant that is defective in degradation of adhE mRNA but proficient in the processing of 16S rRNA precursor. Biochem Biophys Res Commun **289:**1301-6.

208. **Wachi, M., G. Umitsuki, and K. Nagai.** 1997. Functional relationship between Escherichia coli RNase E and the CafA protein. Mol Gen Genet **253:**515-9.

209. **Wachi, M., G. Umitsuki, M. Shimizu, A. Takada, and K. Nagai.** 1999. Escherichia coli cafA gene encodes a novel RNase, designated as RNase G, involved in processing of the 5' end of 16S rRNA. Biochem Biophys Res Commun **259:**483-8.

210. **Wagner, J. D., E. Jankowsky, M. Company, A. M. Pyle, and J. N. Abelson.** 1998. The DEAH-box protein PRP22 is an ATPase that mediates ATP-dependent

mRNA release from the spliceosome and unwinds RNA duplexes. Embo J **17**:2926-37.

211. **Walker, J. E., M. Saraste, M. J. Runswick, and N. J. Gay.** 1982. Distantly related sequences in the alpha- and beta-subunits of ATP synthase, myosin, kinases and other ATP-requiring enzymes and a common nucleotide binding fold. Embo J **1**:945-51.

212. **Wang, Y., J. D. Wagner, and C. Guthrie.** 1998. The DEAH-box splicing factor Prp16 unwinds RNA duplexes in vitro. Curr Biol **8**:441-51.

213. **Warner, J. R., and C. Gorenstein.** 1978. Yeast has a true stringent response. Nature **275**:338-9.

214. **Williams, K. P.** 2002. The tmRNA Website: invasion by an intron. Nucleic Acids Res **30**:179-82.

215. **Wimberly, B. T., D. E. Brodersen, W. M. Clemons, Jr., R. J. Morgan-Warren, A. P. Carter, C. Vonrhein, T. Hartsch, and V. Ramakrishnan.** 2000. Structure of the 30S ribosomal subunit. Nature **407**:327-39.

216. **Withey, J., and D. Friedman.** 1999. Analysis of the role of trans-translation in the requirement of tmRNA for lambdaimmP22 growth in Escherichia coli. J Bacteriol **181**:2148-57.

217. **Withey, J. H., and D. I. Friedman.** 2002. The biological roles of trans-translation. Curr Opin Microbiol **5**:154-9.

218. **Withey, J. H., and D. I. Friedman.** 2003. A salvage pathway for protein structures: tmRNA and trans-translation. Annu Rev Microbiol **57**:101-23.

219. **Wower, J., C. W. Zwieb, D. W. Hoffman, and I. K. Wower.** 2002. SmpB: a protein that binds to double-stranded segments in tmRNA and tRNA. Biochemistry **41**:8826-36.

220. **Xu, F., S. Lin-Chao, and S. N. Cohen.** 1993. The Escherichia coli pcnB gene promotes adenylylation of antisense RNAI of ColE1-type plasmids in vivo and degradation of RNAI decay intermediates. Proc Natl Acad Sci U S A **90**:6756-60.

221. **Yajnik, V., and G. N. Godson.** 1993. Selective decay of Escherichia coli dnaG messenger RNA is initiated by RNase E. J Biol Chem **268**:13253-60.

222. **Yen, T. J., D. A. Gay, J. S. Pachter, and D. W. Cleveland.** 1988. Autoregulated changes in stability of polyribosome-bound beta-tubulin mRNAs are specified by the first 13 translated nucleotides. Mol Cell Biol **8**:1224-35.

223. **Yen, T. J., P. S. Machlin, and D. W. Cleveland.** 1988. Autoregulated instability of beta-tubulin mRNAs by recognition of the nascent amino terminus of beta-tubulin. Nature **334**:580-5.

224. **Yonath, A., K. R. Leonard, and H. G. Wittmann.** 1987. A tunnel in the large ribosomal subunit revealed by three-dimensional image reconstruction. Science **236**:813-6.

225. **Yusupova, G. Z., M. M. Yusupov, J. H. Cate, and H. F. Noller.** 2001. The path of messenger RNA through the ribosome. Cell **106**:233-41.

226. **Zamore, P. D.** 2001. RNA interference: listening to the sound of silence. Nat Struct Biol **8**:746-50.

227. **Zhao, X., E. G. Muller, and R. Rothstein.** 1998. A suppressor of two essential checkpoint genes identifies a novel protein that negatively affects dNTP pools. Mol Cell **2**:329-40.

228. **Zhu, L. Q., T. Gangopadhyay, K. P. Padmanabha, and M. P. Deutscher.** 1990. Escherichia coli rna gene encoding RNase I: cloning, overexpression, subcellular distribution of the enzyme, and use of an rna deletion to identify additional RNases. J Bacteriol **172**:3146-51.

229. **Zubay, G.** 1973. In vitro synthesis of protein in microbial systems. Annu Rev Genet **7**:267-87.

VITA

Jovanka Tepavcevic Koo

University of Washington

2004

EDUCATION

University of Washington, Seattle, WA
    Department of Microbiology
    Degree: Ph.D. in Microbiology 2004

Swarthmore College, Swarthmore, PA
    Degree: B.A. in Biology (minor in Chemistry) 1997

HONORS AND AWARDS

2003-2004   Helen Whiteley Fellowship, Department of Microbiology, University of
             Washington

1999-2002   Molecular and Cellular Biology Training Grant, University of Washington

1997   High Honors in Biology (major) and Chemistry (minor), Swarthmore
             College

1996-1997   Edward Martin Scholarship from Swarthmore College Biology
             Department

1996   Howard Hughes Undergraduate Fellowship

PUBLICATIONS

Koo, J.T., Choe, J., and Moseley, S.L. (2004) HrpA, a DEAH-box RNA helicase, is involved in processing of mRNA in a fimbrial operon in *Escherichia coli. Mol Microbiol* (in press)

Koo, J.T., Tabata, T.A., Withey, J.H., and Moseley, S.L. (2004) The role of ribosome-associated factor *ssrA* in mRNA processing in *Escherichia coli*. *J. Bacteriology* (submitted)

Loomis, W. P., Koo, J. T., Cheung, T. P., and Moseley, S. L. (2000) A tripeptide sequence within the nascent DaaP protein is required for mRNA processing of a fimbrial operon in *Escherichia coli*. *Mol Microbiol* **39**: 693-707

Milosavljevic, A., Savkovic, S., Crkvenjakov, R., Salbego, D., Serrato, H., Kreuzer, H., Gemmel, A., Batus, S., Grujuic, D., Carnahan, S., Paunesku, T., Tepavcevic, J. (1996) DNA Sequence Recognition by Hybridization to Short Oligomers: Experimental Verification of the Method on the *E coli* Genome. *Genomics* **37**: 77-86

ABSTRACTS PRESENTED AT MEETINGS

Koo, J.T. and Moseley, S.L. Regulation of mRNA Processing in *Escherichia coli* by the Ribosome. In Abstracts of the Molecular Genetics of Bacteria and Phages Meeting. 2002. Cold Springs Harbor Laboratories, Cold Springs Harbor, NY.

Koo, J.T., Loomis, W.P., Tabata, T. and Moseley, S.L. Regulation of mRNA Processing in *Escherichia coli* by the Ribosome. In Abstracts of EMBO Workshop on mRNA Enigmas: Transport, Silencing, Decay, and their Interplay with Translation. 2001. CNRS, Aussois, France.

Tepavcevic, J., Loomis, W.P., Cheung, T.P. and Moseley, S.L. Characterization of the Role of the Nascent DaaP Peptide in the Translational Control of mRNA Processing in the F1845 Fimbrial Operon of *Escherichia coli*, H-108. In Abstracts of the 99th General Meeting of the American Society for Microbiology. 1999. American Society for Microbiology, Washington, D.C.

Loomis, W.P., Tepavcevic, J. and Moseley, S.L. Translational Control of mRNA Processing in the F1845 Fimbrial Operon of *Escherichia coli*. In Abstracts of the Translational Control Meeting. 1998. Cold Springs Harbor Laboratories, Cold Springs Harbor, NY.

Tepavcevic, J. and Vollmer, A.C. Transcriptional Activation of the *recA* promoters from *Escherichia coli* and *Deinococcus radiodurans* as Measured by Bioluminescence, I-008, p.323. In Abstracts of the 97th General Meeting of the American Society for Microbiology. 1997. American Society for Microbiology, Washington, D.C.

Milosavljevic, A., Savkovic, S., Crkvenjakov, R., Salbego, D., Serrato, H., Kreuzer, H., Gemmell, A., Batus, S., Grujic, D., Caranahan, S, Tepavcevic, J. (1996) Genome-scale DNA sequence recognition by hybridization to short oligomers. *Proceedings of the 4th Conference on Intelligent Systems for Molecular Biology*, AAAI Press